LV-2014-138

Landsvirkjun

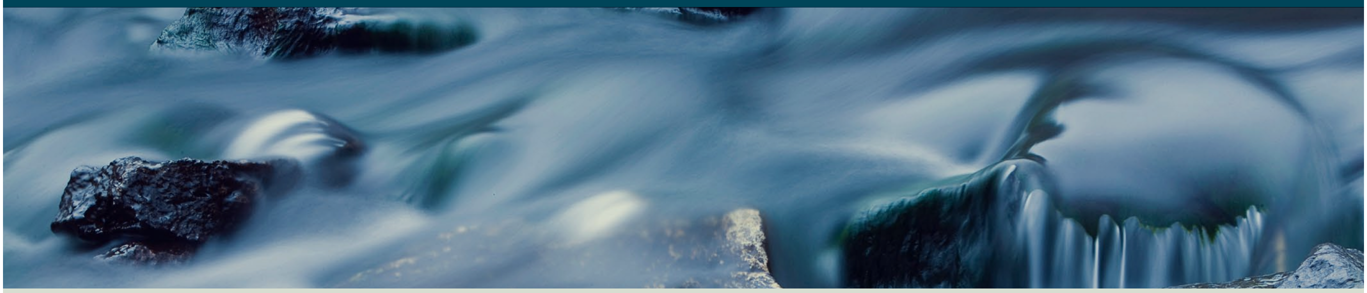

Vatnajökull

Mass balance, meltwater drainage and surface velocity of the glacial year 2013–14

Key Page

Landsvirkjun

LV report no: LV-2014-138 **Date:** 23.12.14

Number of pages: 57 **Copies:** **Distribution:** ☒ On www.lv.is ☒ Open ☐ Limited until

Title: VATNAJÖKULL: Mass balance, meltwater drainage and surface velocity of the glacial year 2013-14

Authors/Company: Finnur Pálsson, Institute of Earth Sciences, University of Iceland

Project manager: Andri Gunnarsson

Prepared for: Landsvirkjun

Co operators:

Abstract: The winter balance was 10% higher than average (average since 1991-92). The summer mass balance (ablation) was ~20% greater than average. The net balance was negative; the mass loss was close to average since 1995-96 (the years of negative balance). The glacial year of 2013-14 was the 20th in a row with negative mass balance for Vatnajökull (since 1994-95) contributing to a total loss of 14,4 m_{we}, 0,76 m_{we} a^{-1} or an average surface lowering of 0,84 ma^{-1}. This is equivalent to ice volume of ~129 km^3, or just over 4% off the total ice volume. Meltwater runoff to Tungnaá was close to average, 6 % over average to Kaldakvísl, 87% of average to Jökulsá á Fjöllum, 5% over average to Jökulsá á Brú (Hálslón), 96% to Jökulsá í Fljótsdal and 30% over average to Jökulsá á Breiðamerkursandi (summer rain and snow that falls and melts during summer is not included).

Keywords:

ISBN no:

Approved by Landsvirkjun's project manager

Andri Gunnarsson

VATNAJÖKULL:
Mass balance, meltwater drainage and surface velocity of the glacial year 2013_14

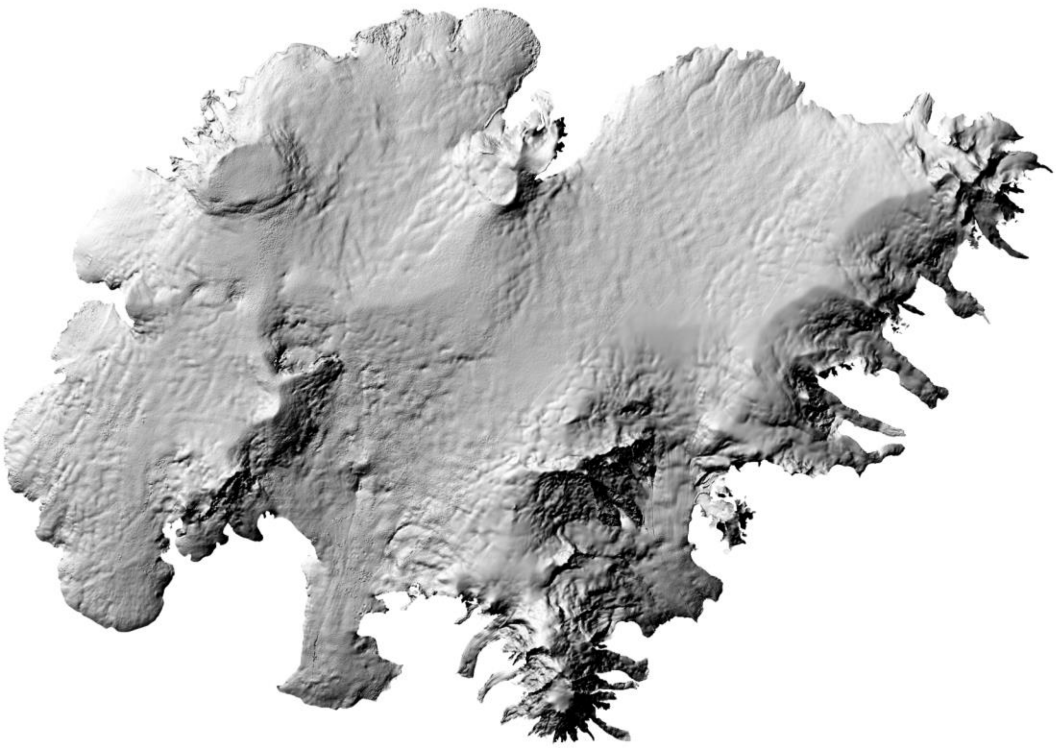

Institute of Earth Sciences
University of Iceland
and
National Power Company

Finnur Pálsson
Andri Gunnarsson
Guðfinna Aðalgeirsdóttir
Þorsteinn Jónsson
Sveinbjörn Steinþórsson
Hlynur Skagfjörð Pálsson

RH-09-2014

Contents:

Figures:

Tables:

Appendixes:

1. INTRODUCTION

In 1992 (glacial year 1991_1992) a program of mass balance measurements was started for Vatnajökull by the Science Institute University of Iceland (now Institute of Earth Sciences, IES) in collaboration with the National Power Company (NPC). For the first year the program was limited to the western part of the glacier, but then expanded to include the northern outlets as well. In 1996 this study was further expanded to include southern outlets, with support from The European Union (Framework IV - Environment and Climate, TEMBA project 1996-1997). This program was extended 1998–2000 with further support from EU (Framework IV - Environment and Climate, ICEMASS project, 1998-2000). In 2000-2002 NPC and IES continued the program. In 2003-2005 IES participated in a multinational research project, which was financially supported by The European Union (EVK2-CT-2002-00152 SPICE). IES was responsible for obtaining data sets for calibration of models of the mass balance and dynamics of Vatnajökull. This work was also supported by The National Power Company of Iceland and The National Road Authority, and is a continuation of the TEMBA-project of 1996-97 and ICEMASS project 1998-2001.

In 2013-2014 IES and NPC continued a similar program. Mass balance measurements on the southeast outlets Breiðamerkurjökull and Hoffellsjökull is financially supported by the National Road Authority.

The aim of the collaborative work of NPC and IES is to improve our understanding of the mass balance and melt water runoff from glaciers. This work in combination with energy balance measurements by NPC and IES on Vatnajökull will be used for calibration of models of the energy and mass balance of Vatnajökull.

This report describes the field measurements, GPS survey, the mass balance and melt water runoff for the glacial year 2013_14.

2. DIARY

May 3 - 8: measurements of the winter balance
June 1 - 7: measurements of the winter balance.
September 6; summer balance measurements, maintenance of AWSs on Breiðamerkurjökull
September 11; summer balance measurement and removal of AWS on Bárðarbunga
(with Iceland coast guard helicopter)
October 11-17: summer balance measurements.

In all expeditions and short visits to the glacier the locations of mass balance stakes were measured with Kinematic GPS (or fast static GPS and a few with DGPS) for surface velocity calculation.

The following members of staff of the Institute of Earth Sciences, University of Iceland, carried out the fieldwork on Vatnajökull: Finnur Pálsson, Þorsteinn Jónsson, Sveinbjörn Steinþórsson and Guðfinna Aðalgeirsdóttir. Also Andri Gunnarsson (National Power Company) and Hlynur Skagfjörð Pálsson (Reykjavík Rescue Team).
Members of the Iceland Glaciological Society assisted in the June fieldwork.

3. MASS BALANCE MEASUREMENTS

The purpose of the mass balance measurements is to describe the temporal and spatial distribution of the components of the mass balance. The mean annual values of the components and their variation from year to year are analyzed and related to meteorological conditions and climatic variability. The results will be used in studies of changes in the glacier volume, estimates of meltwater contribution to glacial rivers, mass balance modeling, evaluation of altitudinal and regional variations of mass balance in response to climatic variations, and to assess the hydrometeorological and dynamic response of the ice cap to climate change.

The mass balance was determined by a stratigraphic method, measuring changes in thickness and density relative to the summer surface. The winter balance was estimated by drilling ice cores through the winter layer in the spring. Ablation was monitored from markers; snow stakes were put up on the glacier and wires were drilled down in the ablation area. The summer balance was measured in the autumn.

3.1 Methods

Measurements of the surface mass balance on a large ice cap like Vatnajökull are impractical in terms of cost with conventional techniques and sampling density that are typically used on small glaciers. The spatial variability of the mass balance may, however, be predictable on the flat large outlets of such an ice cap given data on several profiles extending over the elevation range of the glacier. The precipitation generally increases with elevation and decreases with the distance from the coast, but both the distribution of snowfall and redistribution of snow by drift depend on the prevailing wind direction during the winter. The summer melting depends mainly on the altitude and the albedo of the glacier surface. Therefore, we have used observations along a limited number of flowlines, which span the elevation range of the outlets to assess aerial estimates of surface mass balance. Each profile describes the variation with elevation, but together they also describe the lateral variation of the mass balance. Recently, modern over-snow vehicles and helicopters have allowed fast traverses to ensure successful fieldwork in spite of frequently poor weather conditions. The error for individual point measurement is estimate ~30 cm_{we} for both summer and winter balance. The error for the area integral of mass balance is however considered smaller, since the error for individual survey sites is independent.

The winter mass balance (b_w) is defined as the mass of snow accumulated during the winter months, the summer balance (b_s) is the mass balance during the summer, and the net balance (b_n) is defined as their sum. The specific mass balance is expressed in terms of the equivalent thickness of water. All mass balance components apply to a time interval between given measurement dates, which are not fixed from one year to another. The dates in the autumn are separated by approximately one calendar year, which roughly coincides with the glaciological year defined as October 1st to September 30th. Snow cores are drilled in April-May through the winter layer and profiles of the density are measured. The summer balance is derived in the autumn from measurements of the changes in the snow core density during the summer in the accumulation area and from readings at stakes and wires drilled into the ice in the ablation areas.

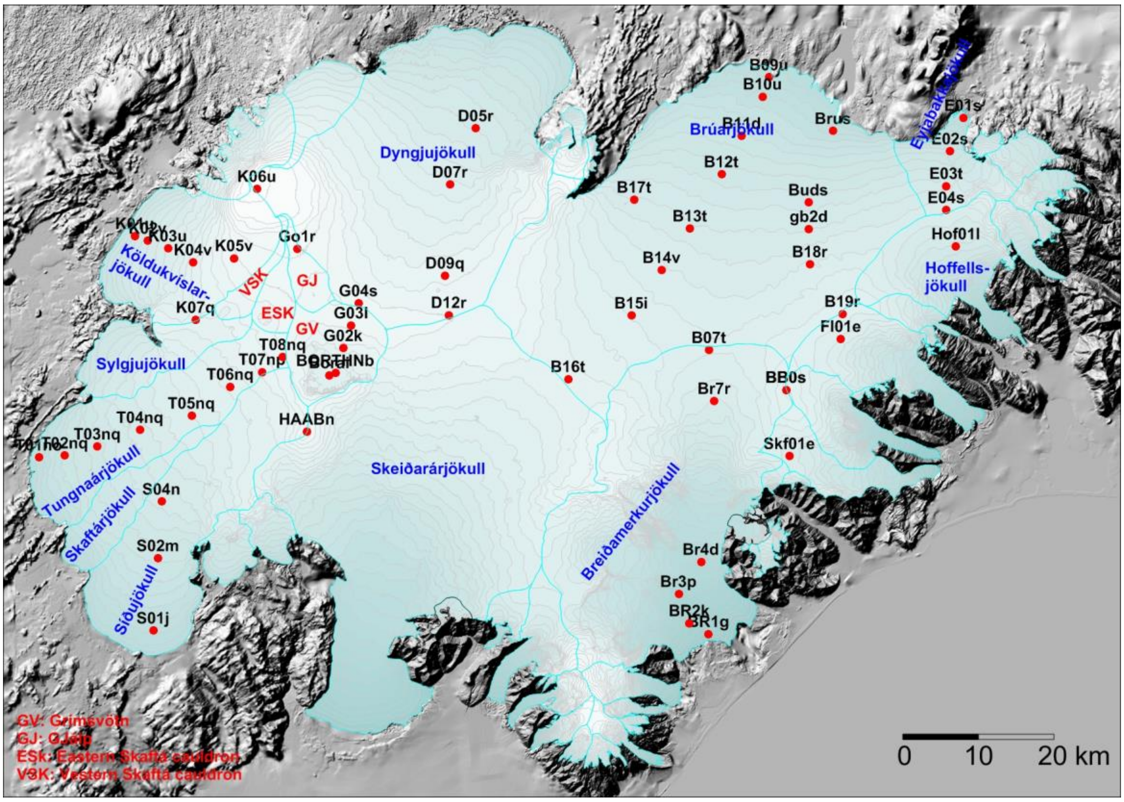

Figure 1. Outlets of Vatnajökull and location of mass balance survey sites 2013_14.

Digital maps are created for winter, summer and net balance for the whole ice cap based on site measurements. The mass balance is calculated over both the ice and water drainage basins. The summer balance over the water basin is an estimate of meltwater contribution to rivers and groundwater storage. This estimate, however, does not include precipitation that falls as rain on the glacier or snow, which falls and melts during the summer. The meltwater contribution is compared with river runoff at stream flow gauges closest to the glacier. For this comparison, we define the glaciological year from the start of October to the end of September and the period draining meltwater from the glacier during the summer from June through September. It would be misleading to include May in the summer period because runoff from the glacier melt in May is delayed due to refreezing during elimination of the cold wave.

3. 2 Results of mass balance measurements.

Mass balance measurements were done at 58 sites in spring 2014 (Fig. 1). The specific mass balance at individual sites is shown in Fig. 2. Most sites are on central flow lines at individual outlets. The specific mass balance along approximate flow lines is given in Fig 3. for the glacier outlets: Síðujökull, Tungnaárjökull, Köldu-kvíslarjökull, Dyngjujökull, Brúar-jökull (west and east), Eyjabakka-jökull, Hoffellsjökull and Breiða-merkurjökull.
Digital maps for winter, summer and net balance are shown in Figure 4. Although no balance measurements are available for Skeiðarárjökull, the balance has been estimated by interpolating the balance values from the neighboring outlets, based on our experience from previous years. The mass balance of individual outlet is discussed in the following subsections.

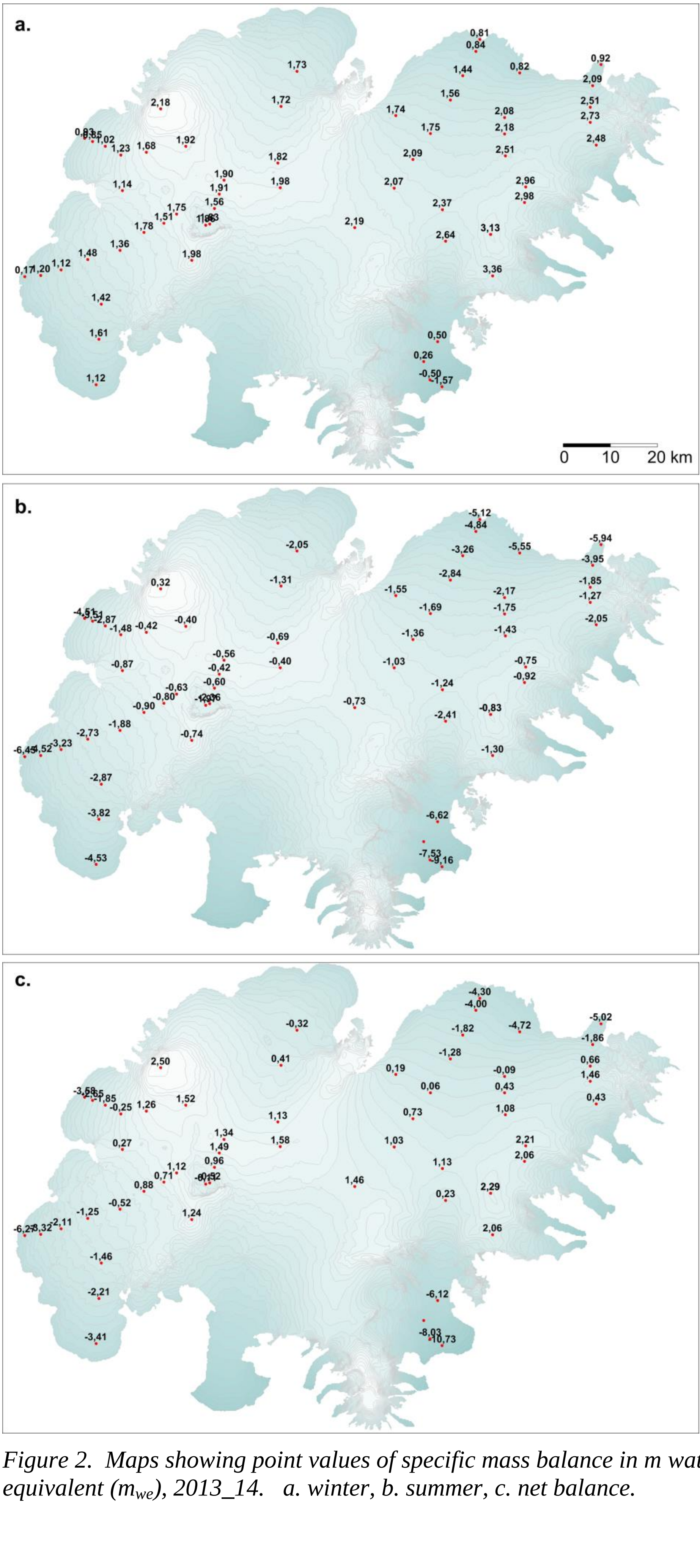

Figure 2. Maps showing point values of specific mass balance in m water equivalent (m_{we}), 2013_14. a. winter, b. summer, c. net balance.

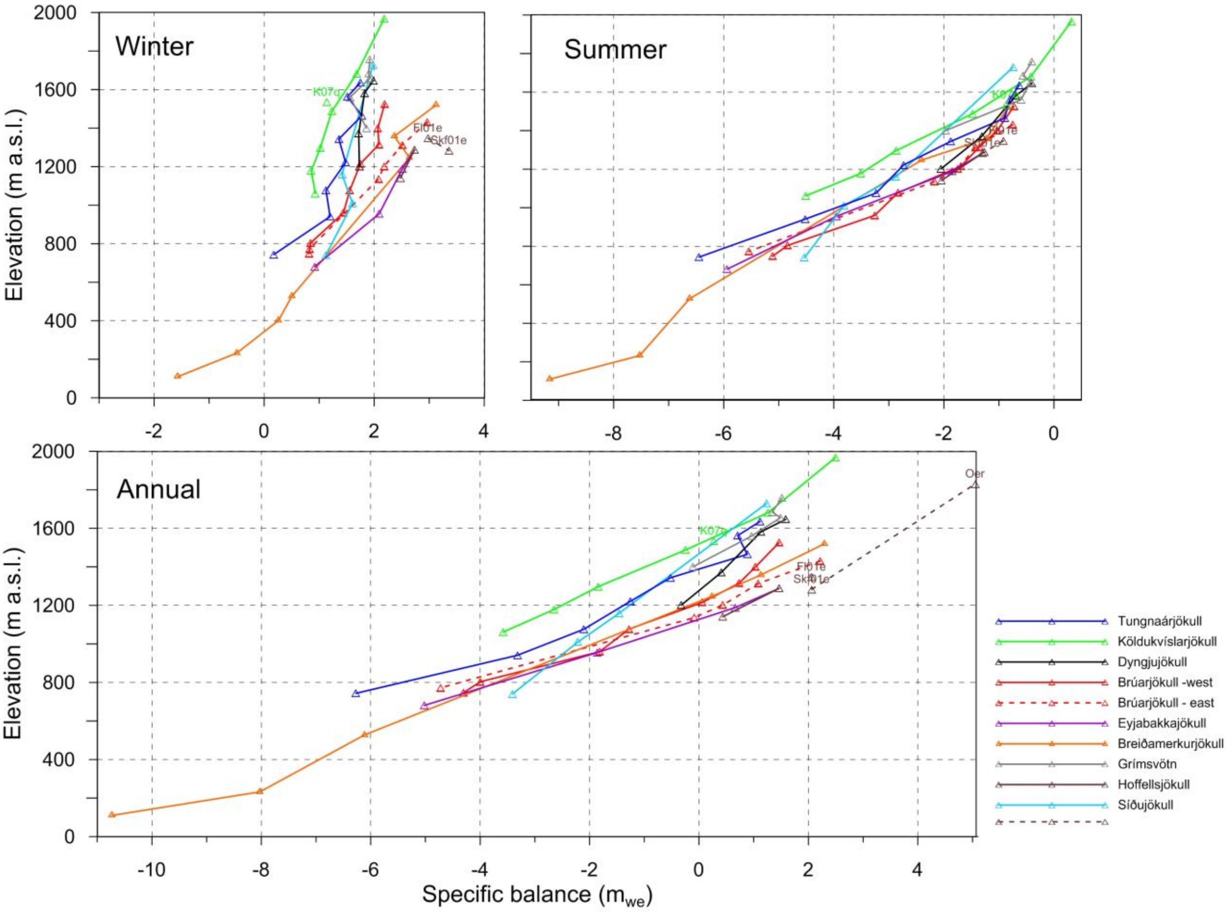

Figure 3a. Specific mass balance (m_{we}), along all mass balance profiles 2013_14.

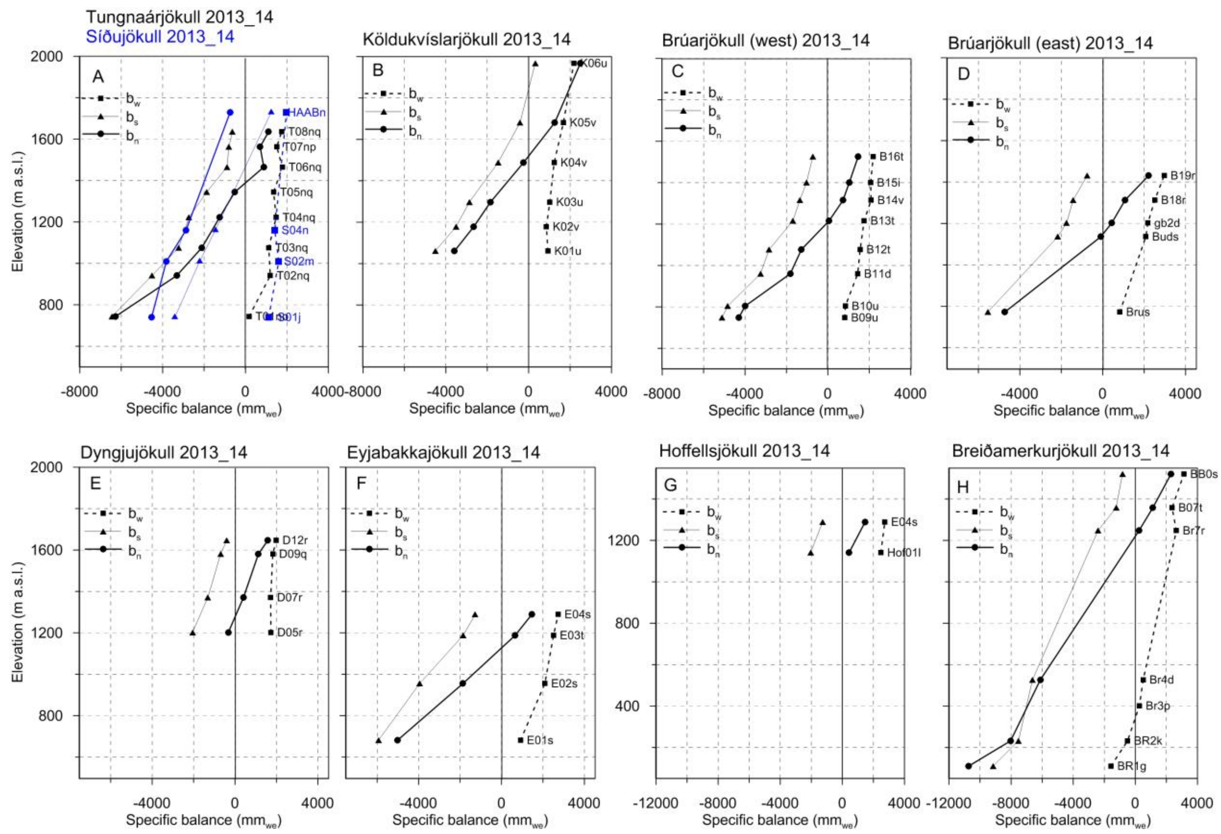

Figure 3b. Specific mass balance (mm_{we}) 2013_14 as a function of elevation on central flow lines on Vatnajökull outlets.

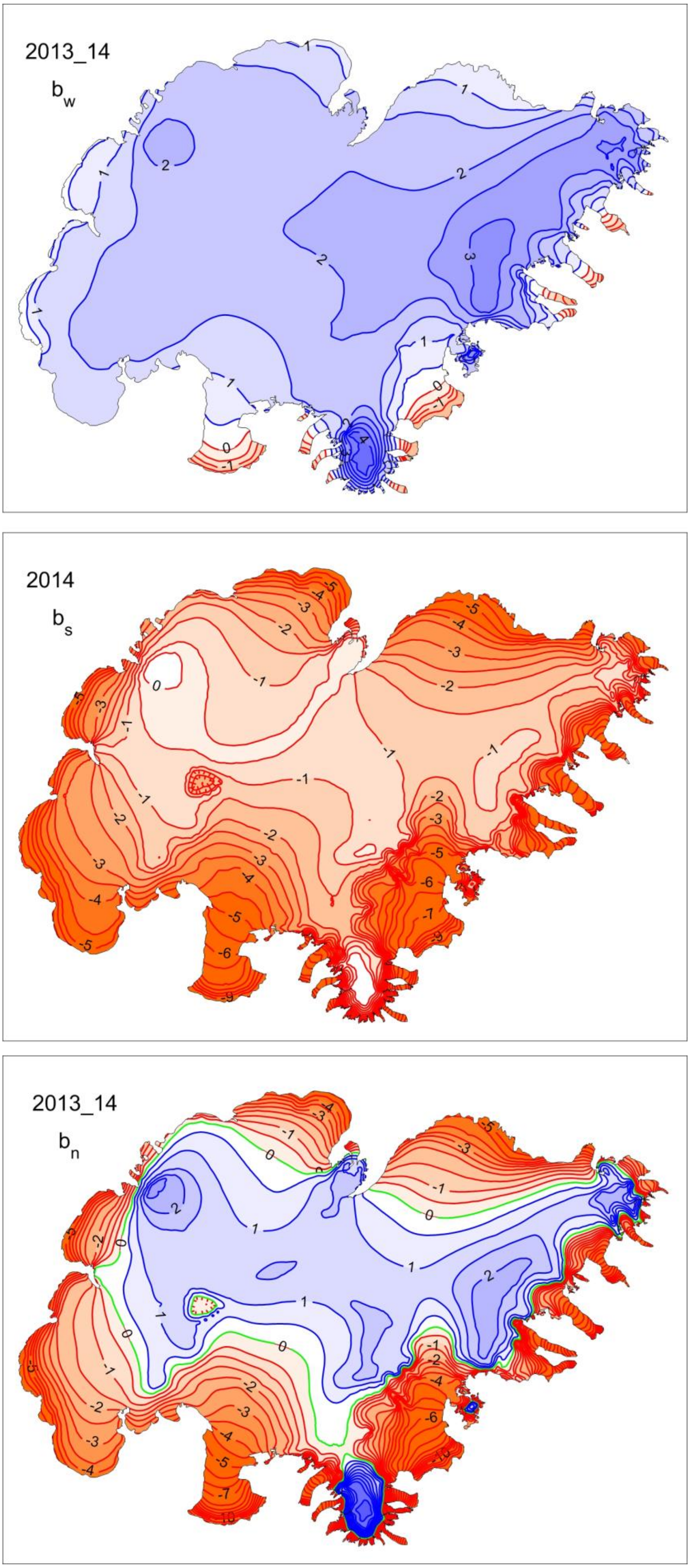

Figure 4. Specific mass balance (m_{we}) maps of Vatnajökull 2013_14. Top: winter, Centre: summer, Bottom: net balance.

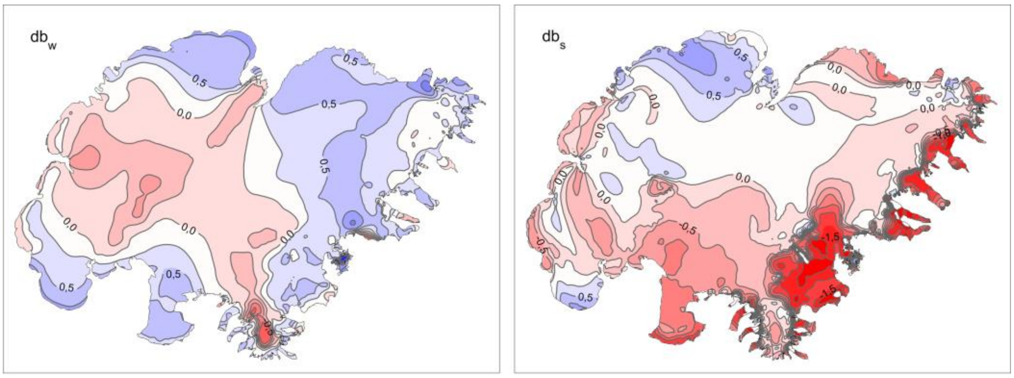

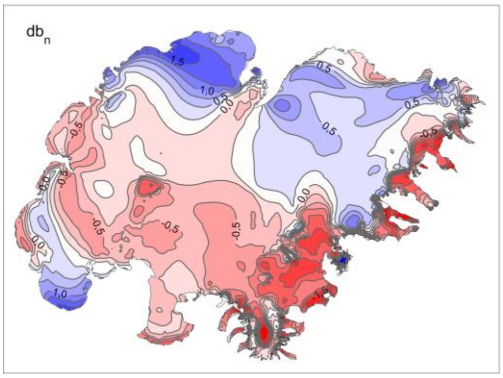

Figure 5. Top left: The difference between winter balance in 2013_14 and the average winter balance 1995_96 to 2012_13. (Blue is higher than average balance). Top right: The difference between summer balance in 2014 and the average summer balance 1996 to 2012. (Red is higher than average ablation). Lower left: The difference between net balance in 2013_14 and the average net balance 1995_96 to 2012_13. (Red is higher than average mass loss).

A DEM of Vatnajökull mostly based on SPOT5 satellite images in 2010, and partly from LiDAR survey 2010, is used for surface area distribution and delineation of ice divides for individual outlets and catchments.

The autumn weather was slightly colder than average the past decade; October rather dry but precipitation in November over the average. The winter months December to March were warmer than average, exceptionally dry in in the SW but very high precipitation in the North and East (the NA-lows frequently passing south and east of Iceland). In these conditions snow collection is high on SE, E, and N Vatnajökull. The spring months were warm, but precipitation in the SE over average. In May the winter snow was already melting in the fore fields of W and N Vatnajökull. In the lower lying south fore fields no snow had collected during the relatively worm winter (see the MODIS images in Appendix F) Figure 5, left, shows the much thicker than average snow cover in N, E and S Vatnajökull. The red central area in the figure shows that snow collection is extremely low in the west and central accumulation areas, especially in the vicinity of Bárðarbunga and Grímsvötn. This can maybe be explained by snow drift, rather few events of very high wind during the winter. The exceptionally high accumulation at the accumulation areas of Brúarjökull; Eyjabakkajökull and SE outlets reflects snowfall in SE, E, and NE wind directions.

The summer of 2014 was unusually warm in Iceland, but also very wet and cloudy in the south and west in June and July. Inspection of the MODIS monthly overview of the summer months in Appendix F shows that days with clear skies over Vatnajökull were ~6 in June, none in the first half of July, but ~3 days in the latter half of the month. In august clear sky was more frequent, ~10 days, in warm weather. September was warm and rather dry in the east, ablation was significant until late September.

This resulted in higher than average ablation on most of Vatnajökull. The exceptions are the center part of Dyngjujökull and snout of Síðujökull where unusually thick snow cover has reduced ablation rates.

(Information about weather is from the web site of the Iceland Met Office).

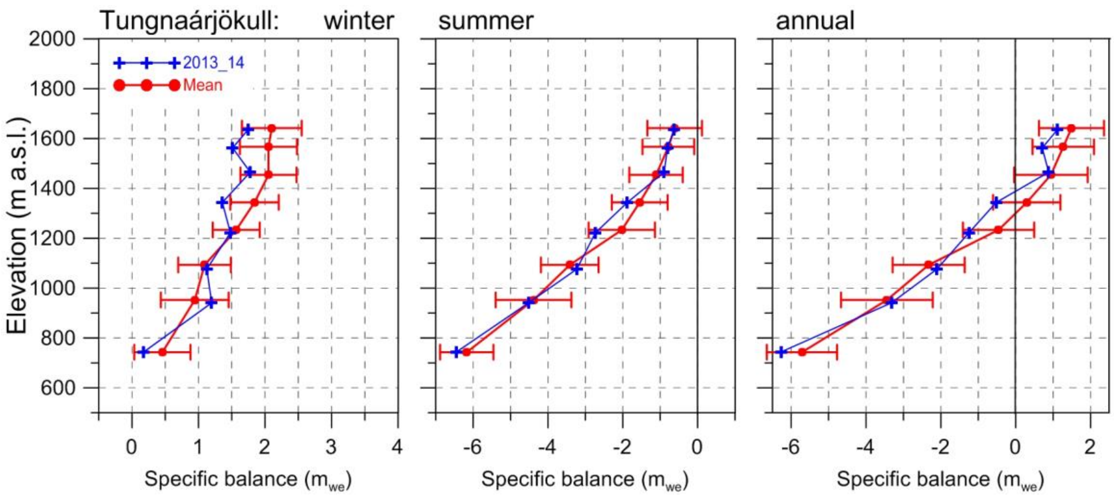

Figure 6. Mass balance at a central flow line of Tungnaárjökull 2013_14, and average mass balance 1991_92 to 2012_13.

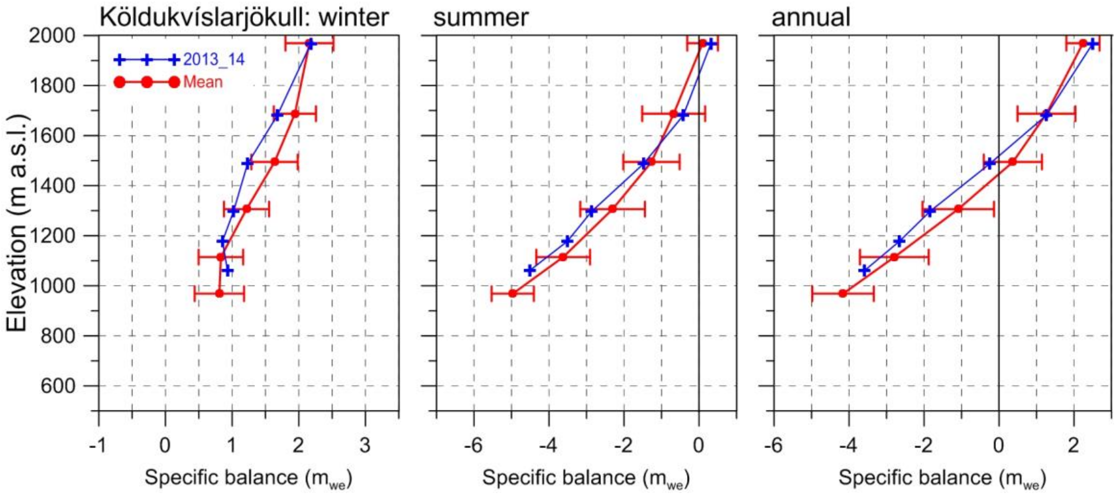

Figure 7. Mass balance at a central flow line of Köldukvíslarjökull 2013_14, and average mass balance 1991_92 to 2012_13.

3.2.1 Tungnaárjökull.

Area = 345 km^2
B_w= 0,47 km$^3_{we}$; b_w = 1,37 m$_{we}$
B_s = -1,00 km$^3_{we}$; $b_{s=}$ -2,90 m$_{we}$
B_n = -0,53 km$^3_{we}$; b_n = -1,53 m$_{we}$
ELA = 1415 m a.s.l. (at profile)
AAR = 28 %
(The terms are defined at the foot of this page)

Variation of mass balance along a central flow line on Tungnaárjökull is shown in Fig. 6. The winter balance was ~1 st. dev. lower than average at the upper survey sites, close to average at the lower. Winter balance was 95% of the average, the prevailing precipitation direction was from SE to NE, western Vatnajökull was somewhat shadowed by the topography. Summer melting was close to average at all survey sites, the total ablation was 10% more than average during the survey period. The net balance was negative the 20th year in a row; the loss was 0,7 m$_{we}$ higher than average during the survey period (30% over the average).

3.2.2 Köldukvíslarjökull

Area = 301 km^2
B_w = 0,37 km$^3_{we}$; b_w = 1,22 m$_{we}$
B_s = -0,63 km$^3_{we}$; b_s = -2,10 m$_{we}$
B_n = -0,26 km$^3_{we}$; b_n = -0,88 m$_{we}$
ELA = 1520 m a.s.l. (at profile)
AAR = 43 %

B_w,B_s and B_n are water equivalent volumes of winter, summer and net balance, ELA the equilibrium line altitude, and AAR is the accumulation area ratio.

Variation of mass balance along a central flow line on Köldukvíslarjökull is shown in Fig. 7. Accumulation was about one st. dev. less than average except the highest and lowest survey sites, where it was close to average. The winter balance was about 85% of the average since 1991_92. The summer melt was less than average at the upper sites, but higher than average in the ablation zone. In total the summer ablation was ~10% over the average. The net balance was negative the 20th year in a row, mass loss was 60% greater than average during the survey period (by 0.23 m_{we}).

3.2.3 Dyngjujökull

Area = 1064 km^2
B_w= 1,81 $km^3{}_{we}$; b_w= 1,71 m_{we}
B_s = -1,63 $km^3{}_{we}$; b_s = -1,54 m_{we}
B_n = 0,18 $km^3{}_{we}$; b_n = 0,17 m_{we}
ELA = 1280 m a.s.l. (at profile)
AAR = 70 %

Variation of mass balance along a flow line on Dyngjujökull is shown on Fig. 8. Mass balance is not measured at the lowest elevations, but assumed to be correlated (as a function of elevation) to that of Brúarjökull and Köldukvíslarjökull. The winter balance in 2013_14 was lower than average at the upper survey sites, but more than 1.5 st. dev. over average at 1200 m. Inspection of the winter Modis images shown in appendix F suggest that at the glacier snout snow cover was very thin, In total the winter balance was ~10% over average.
The summer ablation was close to average in the accumulation zone, but at mid elevation the snow cover reduced total ablation (lowest survey site). The net balance was slightly positive. The high AAR of 70% reflects this.
Dyngjujökull is the outlet of Vatnajökull that during the survey period has often had mass balance close to zero, and the net balance has been slightly positive in some years of the two decade period of continuous mass loss for Vatnajökull as a whole.

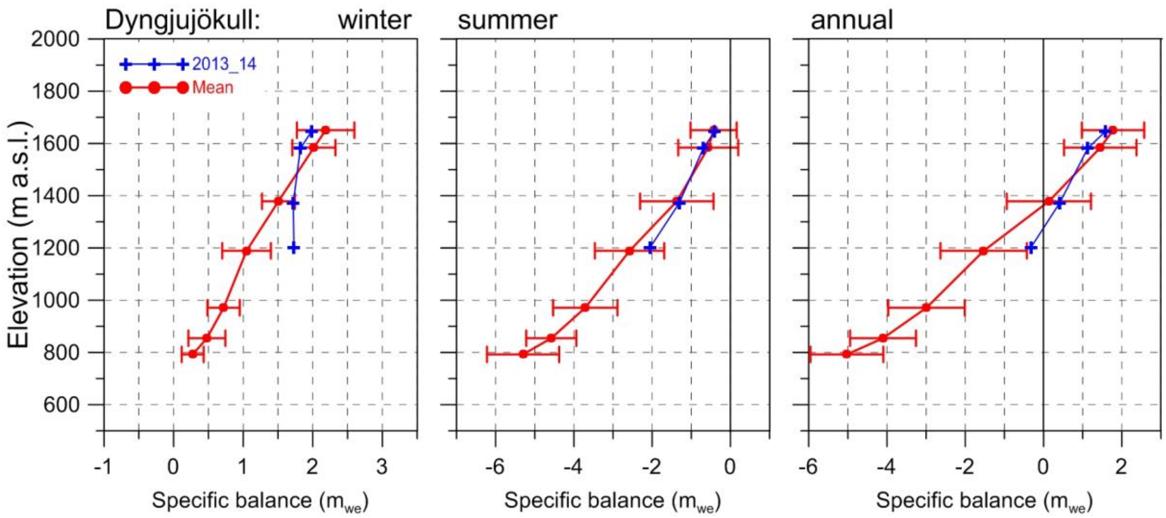

Figure 8. Mass balance at a central flow line on Dyngjujökull 2013_14, and average mass balance 1991_92 to 2012_13 (except 1998_99 – 2003_04 at all but the top elevation).

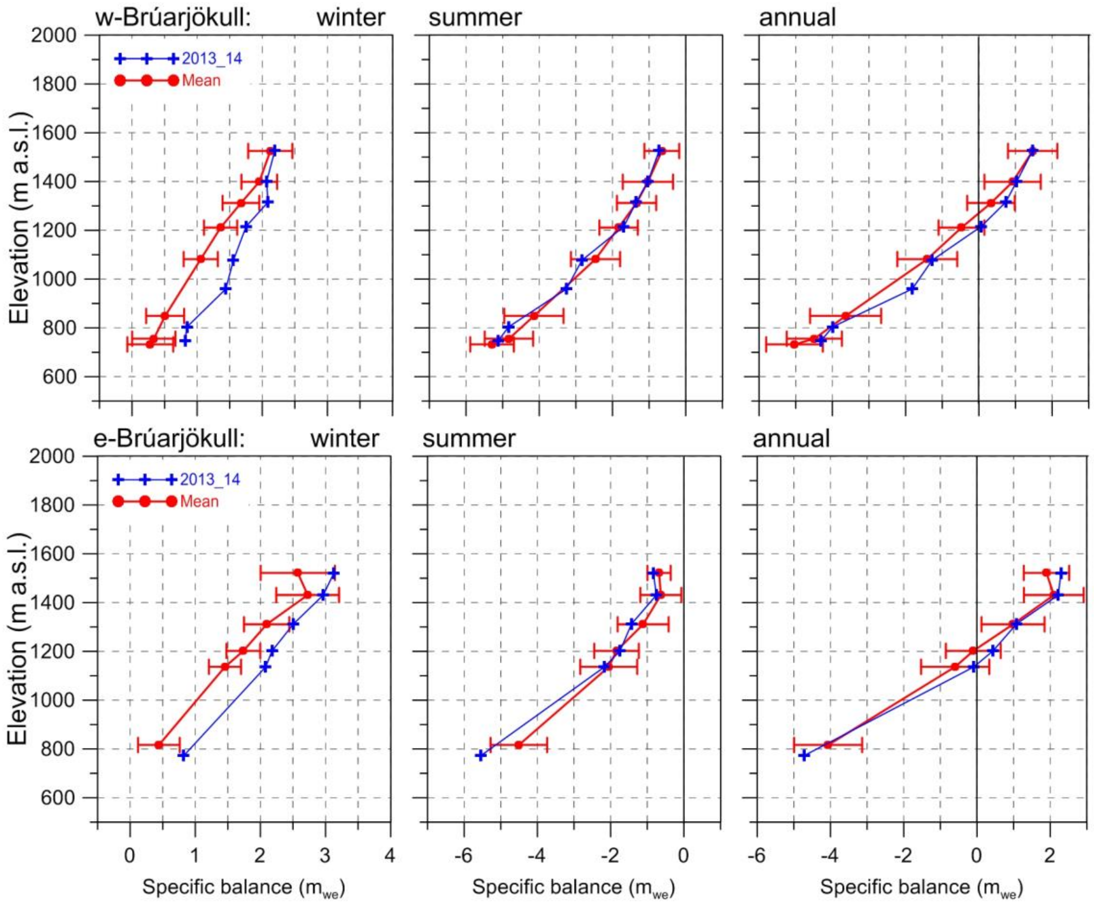

Figure 9. Mass balance at two flow lines on Brúarjökull 2013_14, and average mass balance 1992_93 to 2012_13.

3.2.4 Brúarjökull

Area = 1526 km^2
B_w= 2,92 km$^3_{we}$;b_w = 1,92 m_{we}
B_s = -2,98 km$^3_{we}$; b_s = -1,95 m_{we}
B_n = -0,06 km$^3_{we}$; b_n = -0.03 m_{we}
ELA = 1210 m a.s.l. (western flow line)
ELA = 1150 m a.s.l. (eastern flow line)
AAR = 63 %

Variation of mass balance along two flow lines on Brúarjökull is shown on Fig. 9. At all survey sites on the east survey profile and all sites below 1400 m on the western line accumulation was significantly (more than 1 std. dev.) higher than average. This reflects the prevailing eastern and northern wind direction in precipitation events. The total winter balance was 25% higher than average. The thick snow cover in the ablation zone, delayed ablation in the ablation zone, but this effect was to a large extent compensated by favorable weather in August and September. The resulting summer ablation was just over average. The net mass loss was only slightly negative; but only by 10% of the average. During the survey period, there have been 5 years of positive balance, 17 years with negative balance.

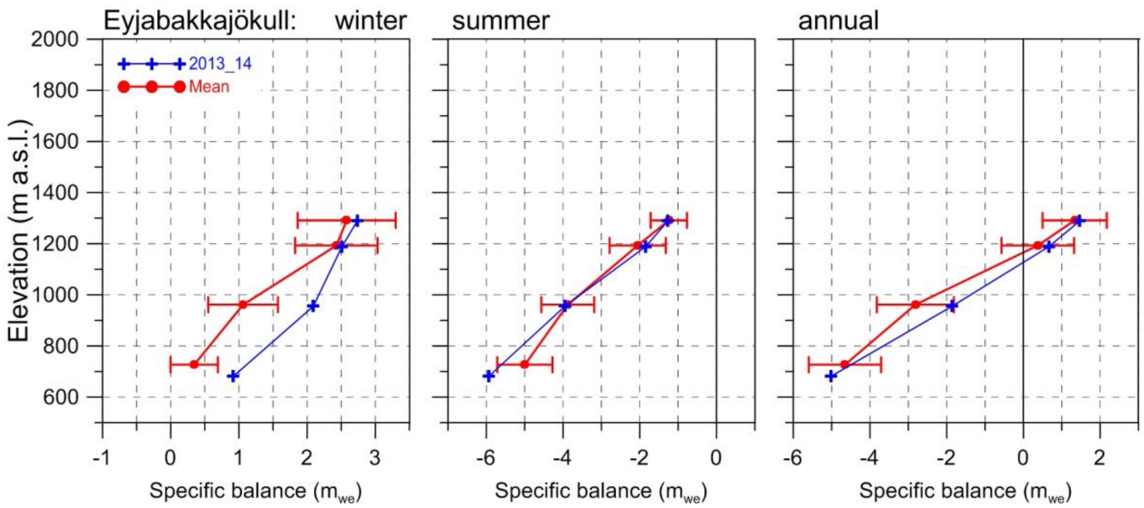

Figure 10. Mass balance at a central flow line of Eyjabakkajökull 2013_14 and average mass balance 1995_96 to 2012_13.

3.2.5 Eyjabakkajökull

Area = 112 km^2
B_w= 0,26 $km^3{}_{we}$; b_w = 2,29 m_{we}
B_s = -0,30 $km^3{}_{we}$; b_s = -2,64 m_{we}
B_n = -0,04 $km^3{}_{we}$; b_n = -0,35 m_{we}
ELA = 1125 m a.s.l. (at profile)
AAR = 52 %

Variation of mass balance along a central flow line on Eyjabakkajökull is shown on Fig. 10. The winter balance was more than 1 std. var. higher than average at lower survey sites but close to 0 at the upper sites. In total the winter balance was 30% over the average. Summer ablation was close to average, in spite of late start of the ablation season, favorable weather in late July, most of August and September (see. Appenix F). The total ablation was 96% of the average. The annual balance was negative, but only 40% of the average since 1995_96.

3.2.6 Breiðamerkurjökull

Area = 938 km^2
B_w= 1,55 $km^3{}_{we}$; b_w = 1,65 m_{we}
B_s = -3,15 $km^3{}_{we}$; b_s = -3,36 m_{we}
B_n = -1,60 $km^3{}_{we}$; b_n= -1,71 m_{we}
ELA = 1215 m a.s.l. (at profile)
AAR = 44 %

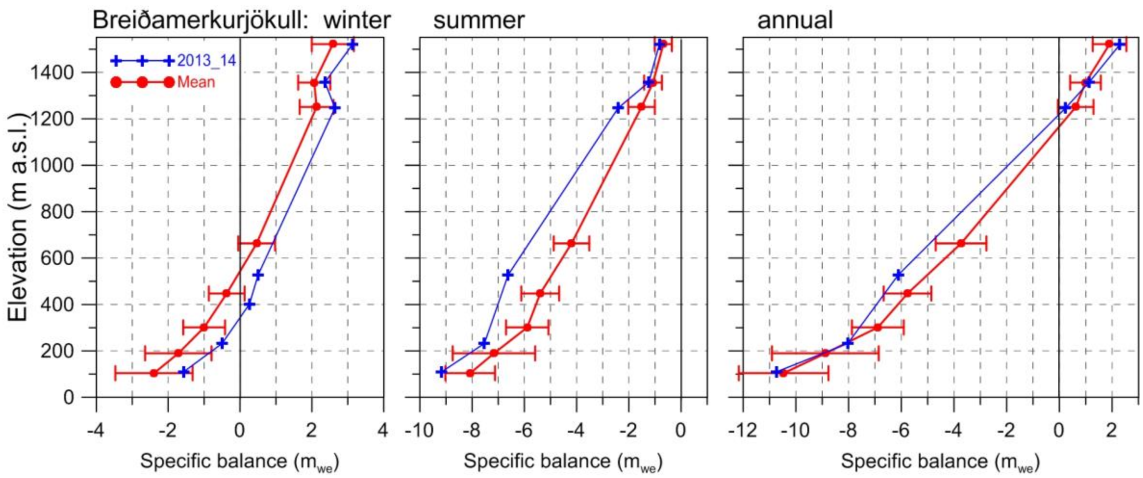

Figure 11. Mass balance at a central flow line of Breiðamerkurjökull 2013_14, and average mass balance 1995_96 to 2012_13.

Variation of mass balance along a central flow line on Breiðamerkur-jökull is shown on Fig. 11. Snow accumulation was about 1 std. dev. over the average in the upper area. In the lower region (below ~400 m) the winter mass loss was close to 1 std. dev. less than average. The winter balance was 20% above average. The latter half of summer was warm and sunny in the region, total ablation was extreme all survey sites except the highest, resulting in summer ablation 30% more than average. The resulting net balance was negative by 40% over the average.

3.2.7 Síðujökull

Area = 430 km^2
B_w= 0,66 km^3_{we}; b_w = 1,52 m_{we}
B_s = -1,29 km^3_{we}; b_s = -2,99 m_{we}
B_n = -0,63 km^3_{we}; b_n= -1,47 m_{we}
ELA = 1470 m a.s.l. (at profile)
AAR = 29 %

Variation of mass balance along a central flow line on Síðujökull is shown on Fig. 12. Snow accumulation much less than average in the upper area, but much higher than average in the lowest area, the precipitation in SE wind directions did reach there. The

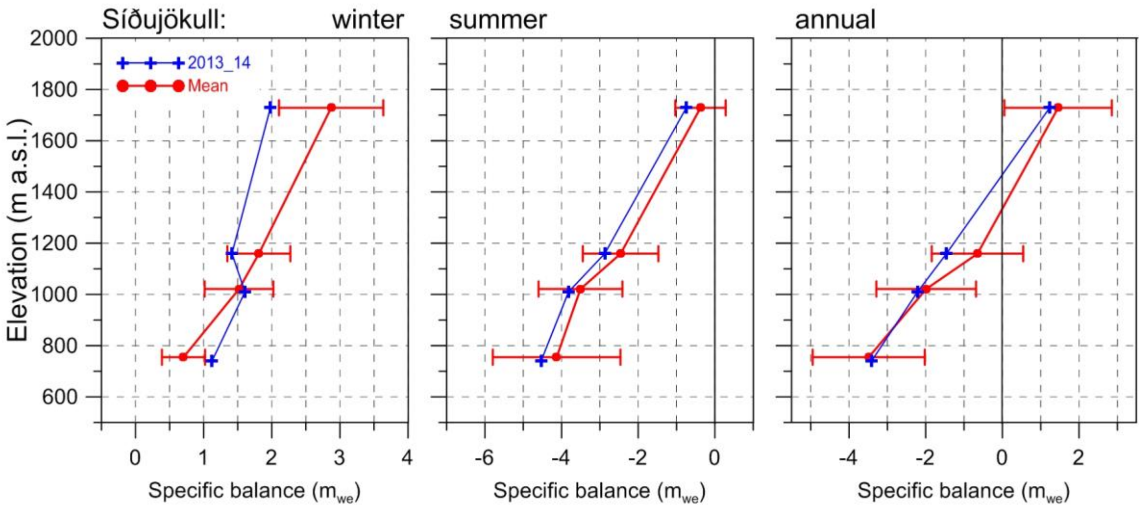

Figure 12. Mass balance at a central flow line of Síðujökull 2013_14, and average mass balance 2004_05 to 2012_13.

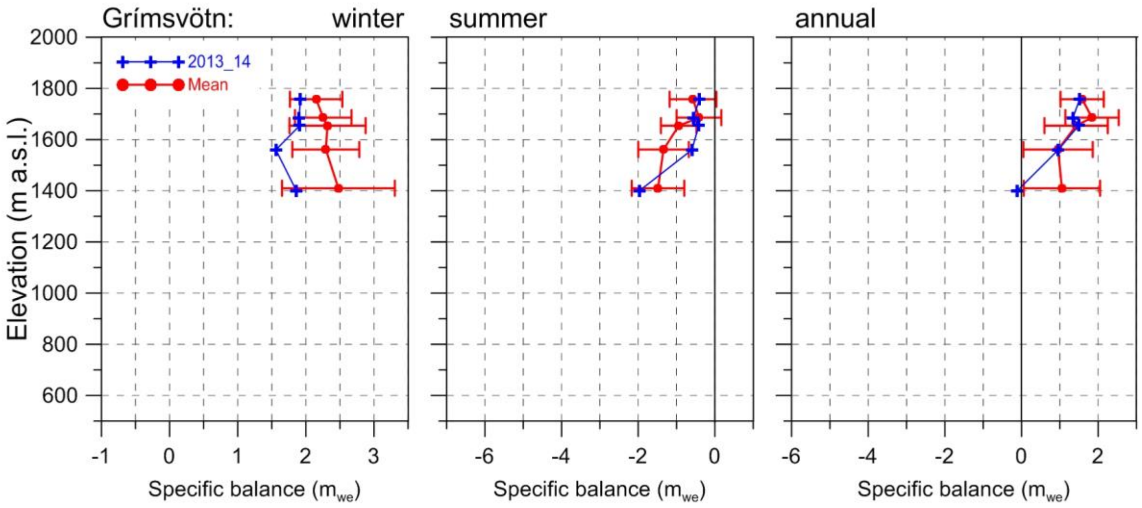

Figure 13. Mass balance at a central flow line towards Grímsvötn 2013_14, and average mass balance 1991_92 to 2012_13.

total winter balance was close to average. The summer ablation was slightly over average at all survey sites. The net balance was negative also close to the average during the survey period.

3.2.6 Grímsvötn-Gjálp

Area = 174 km^2
B_w= 0,25 km^3_{we}; b_w = 1,88 m_{we}
B_s = -0,12 km^3_{we}; b_s = -0,93 m_{we}
B_n = 0,13 km^3_{we}; b_n= 0,95 m_{we}

Variation of mass balance close to a central flow line from Bárðarbunga towards Grímsvötn center is shown in

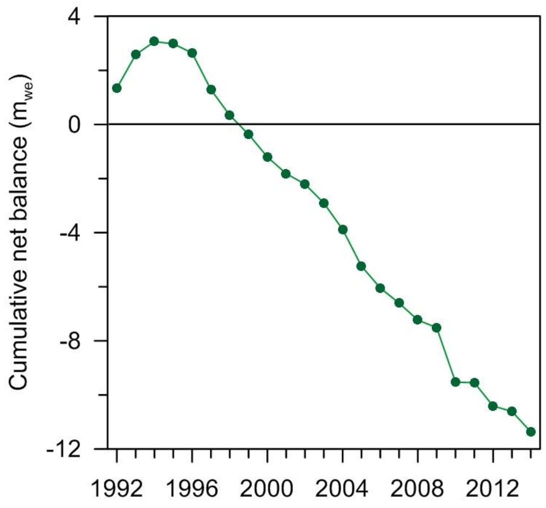

Figure 15. Cumulative specific mass balance of Vatnajökull 1991_92 – 2013_14.

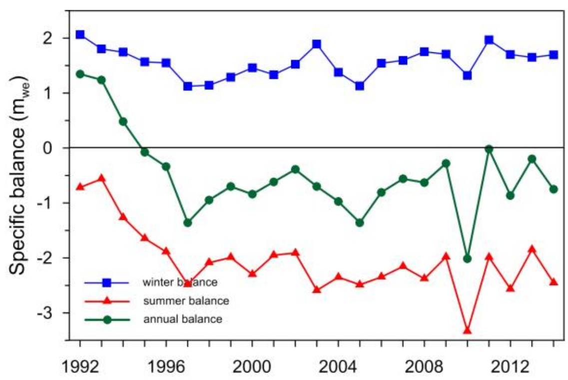

Figure 14. Specific mass balance record for Vatnajökull 1991_92 – 2013_14.

Fig. 13. Snow accumulation was about 1std. dev. less than average at all survey sites. The winter balance was only 84% of the average. Ablation was less than average at all survey sites except on the Grímsvötn ice shelf where ablation was enhanced by tephra blown over from the 2011 eruption site; the summer ablation was 20% over the average. The net balance was positive, by 64% of the average of the survey period.

3.3 The mass balance record for Vatnajökull.

From the digital maps the total volumes of winter, summer and net balance for Vatnajökull have been calculated by integration (appendix D, gives balance values as a function of elevation) and are as follows:

B_w = 13,52 km^3_{we} ; b_w = 1,70 m_{we}
B_s = -19,53 km^3_{we} ; b_s = -2,45 m_{we}
B_n = -6,01 km^3_{we} ; b_n = -0,75 m_{we}
AAR = 52%

Most of the winter was wet, with prevailing SE-E and NE winds. This lead to much higher than average snow accumulation on E- and N-Vatnajökull, but less than average on W-Vatnajökull especially in accumulation area from Grímsvötn to Bárðarbunga. The total winter balance was 10% higher than average (over the observation period from 1991_92, Fig. 14). The 0 mass balance turnover for Vatnajökull (current topography) is close to 13,4 km^3_{we} (1,64 m_{we}) and the winter balance 2013_14 is slightly higher. On W-Vatnajökull there first half of summer was cloudy and wet, the latter half and September were more favorable for ablation; resulting in close to average summer balance there. The relatively long periods of clear skies and warm weather in the east, especially in late summer, resulted in total summer balance (ablation) ~20% over average during the survey period.

As mentioned above, 0 mass balance turnover for Vatnajökull (current topography) is close to 13,4 km^3_{we} (1,64 m_{we}), the summer balance 2014 was 19,53 km^3_{we} or ~45% higher than for zero balance turnover. The net balance was negative, the mass loss was 30% greater than average of the survey period since 1991_92 (-0,58 m); but almost the same as the average loss (-0,72 m) of the past 19 consecutive years of negative balance.

The glacial year of 2013_14 was the 20th in a row with negative mass balance for Vatnajökull (Fig. 14, Fig. 15), contributing to a total loss of 14,4 m_{we} (ice volume of ~129 km^3) since 1994_95.

The temporal variability of mass balance for different outlets is shown in Fig. 16. The greatest variability of the winter balance is for Eyjabakkajökull the eastern most of the studied outlets. This part of the glacier is receives precipitation from all south- and east- and north-easterly wind directions, and thus has high snow accumulation in winters when the paths of the North Atlantic lows are just east of Iceland. This is also the case for the eastern part of Brúarjökull.

Breiðamerkurjökull shows lowest variability in mass balance. It is a maritime glacier with climate controlled by the stable sea temperature and humid air mass. The longest winter balance records seem to reveal periodic behavior, with peaks in ~1991_92 and 2002_03 and a low in ~1998. During the period of net mass loss since 1994_95, the northern outlets have had several years of close to zero and positive mass balance.

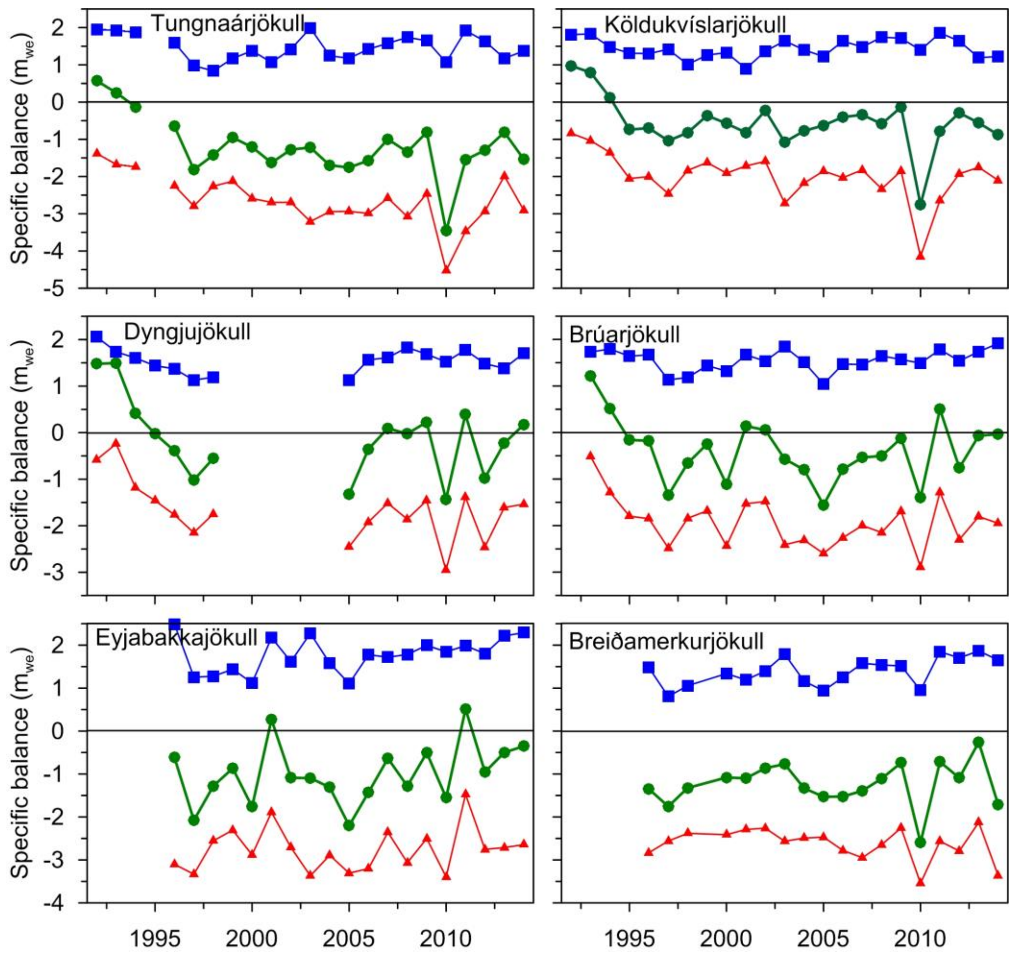

Figure 16. Specific mass balance record for Vatnajökull outlets 1991_92-2013_14.

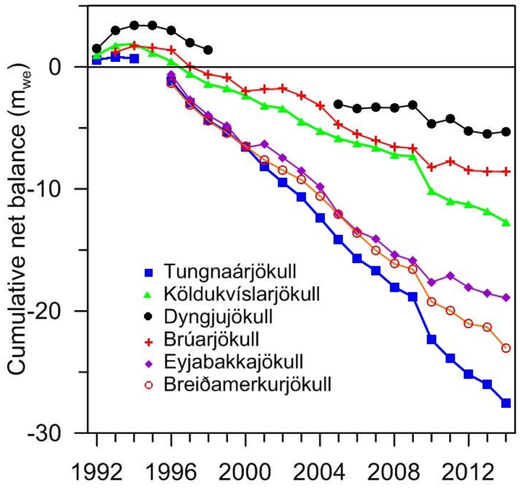

Figure 17. Cumulative specific mass balance for several of Vatnajökull outlets 1991_92 – 2013_14.

The cumulative net balance curves for the outlets of Vatnajökull in Fig. 17 show that all outlets have been losing mass since 1994_95. The slope for mass loss is about 0,7 $m_{we}a^{-1}$ for the northern outlets but 1,5 $m_{we}a^{-1}$ for the south and western outlets.

In Fig. 18 the relation of the annual net balance to the accumulation area ratio (AAR) and equilibrium line altitude (ELA) is shown for different outlets over the survey period. The b_n-AAR gradient is similar for all outlets, about 0,5 m_{we} for 10% change in AAR. The zero-balance AAR varies for different outlets from about 60-65%, similar for all outlets except for the southern outlet Breiðamerkurjökull.

Breiðamerkurjökull is far from equilibrium, the ablation area is too large. A large part of the glacier has carved 200-300 m through the former sediment bed, and the surface elevation has lowered accordingly. Breiða-merkurjökull is now retreating at a high rate.

Similarly the zero-balance ELA varies from about 1000-1100 m a.s.l. for the southern outlets to 1400 m a.s.l. for the NW outlets. The b_n-ELA slope is similar for all outlets -0,7 m_{we} per 100 m.

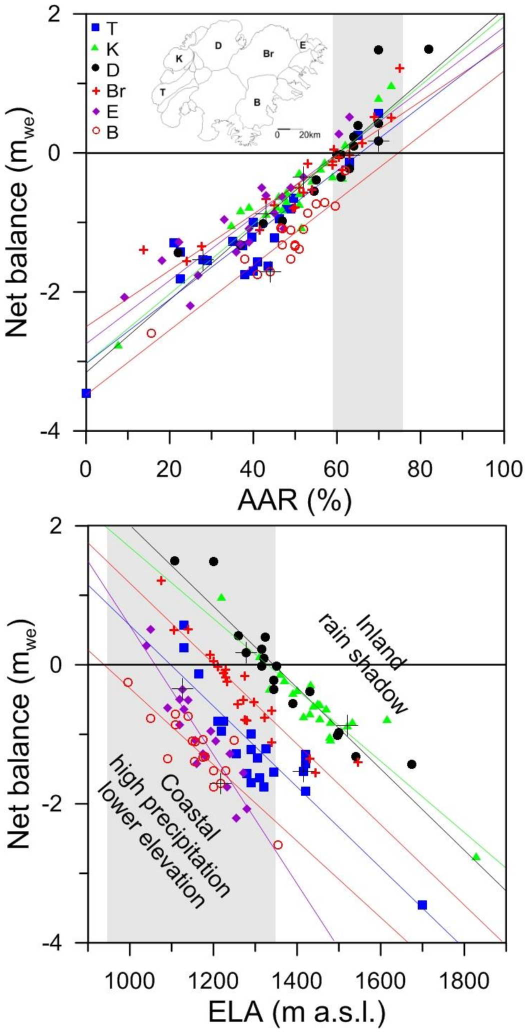

Figure 18. The relation between net annual balance (b_n) and accumulation area ratio (AAR)(upper) and b_n and equilibrium line altitude (ELA), for Vatnajökull outlets during the survey period. (This years points are marked with a black +).

4. SURFACE VELOCITY MEASUREMENTS

The surface velocity of the glacier was calculated from DGPS (accuracy within 1 m), fast static (accuracy about 1 cm) and kinematic GPS (accuracy about 3 cm) positioning of the ablation stakes. All sites were surveyed in spring and autumn (most kinematic, some DGPS), and many also in June (kinematic), August (fast static) and October (kinematic). At a few sites stakes from previous years were found and resurveyed, making it possible to calculate surface velocity over a year or longer time span. The average summer surface velocity is shown on Figure 19.

The use of more accurate instruments and setup, allows estimation of vertical as well as horizontal velocities. Two 6 metre long 4 inch metal poles where set up in the accumulation zone of the western outlet Tungnaárjökull and one on east Brúarjökul to directly measure the vertical displacement. Small GPS units are also attached to the poles and run continuously. At sites close to the glacier edge very small horizontal movement is measured. This indicates that the glacier snouts are almost stagnant. In the centre areas of some of the outlets especially close to the equilibrium line, there is an increase in velocity during summer compared to winter. The summer velocity is of the order of two-fold the winter velocity. This suggests that basal sliding is increased in the melting season, and is of the same magnitude as the deformation velocity.

From previous velocity measurements, surging of outlets has been predicted. No signs of a starting surge are seen from this year's survey.

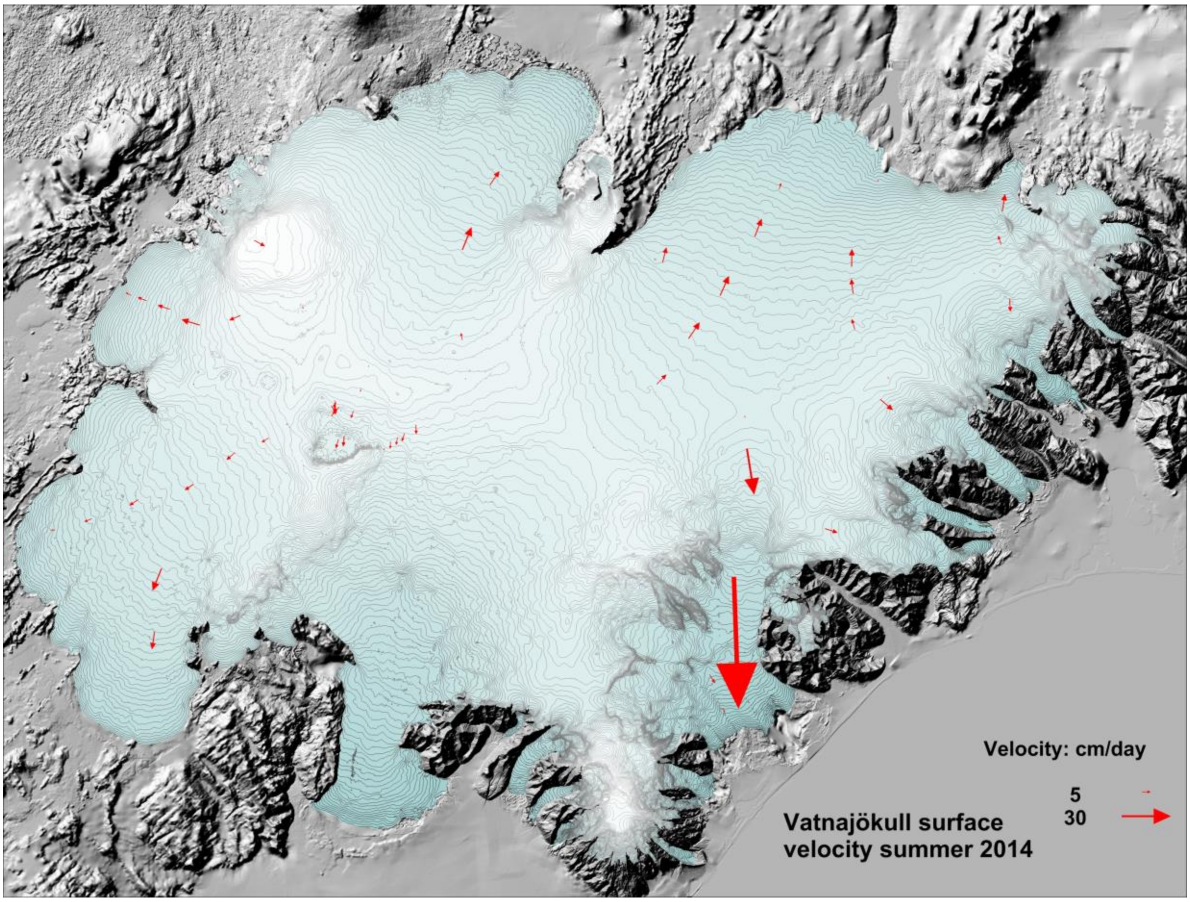

Figure 19. Average surface velocity at survey sites in 2013_14.

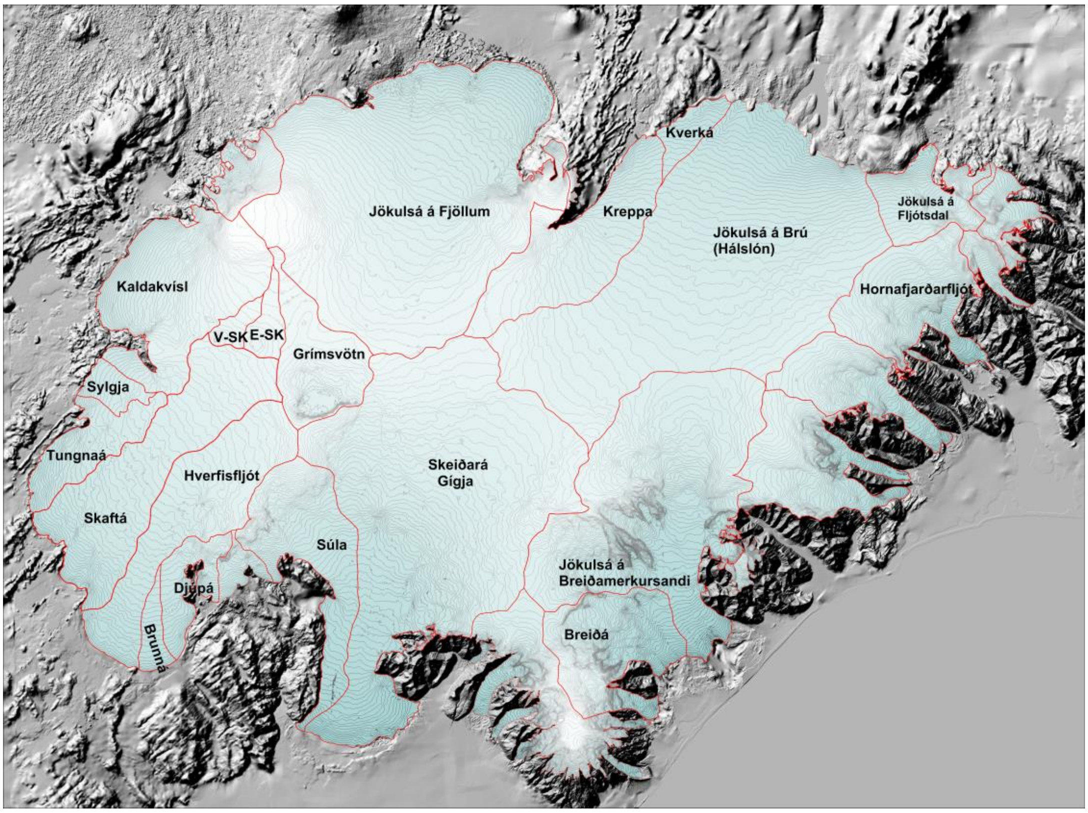

Figure 20. Water divides and drainage basins of selected rivers draining water from Vatnajökull.

5. Melt water runoff.

Water divides and drainage basins for rivers draining water from Vatnajökull have been defined from water pressure potential maps. The potential maps were produced from existing surface (year 2010) and bedrock digital elevation models.

Figure 20 shows the water divides and drainage areas for selected rivers draining melt water from Vatnajökull. The summer balance over the water basin is an estimate of meltwater contribution to rivers and groundwater storage. This estimate, however, does not include precipitation that falls as rain on the glacier, nor snow which falls and melts during the summer. The meltwater contribution can be compared with river runoff at stream flow gauges closest to the glacier. For this comparison, we define the glaciological year from the start of October to the end of September and the period draining meltwater from the glacier during the summer from June through September. It would be misleading to include May in the summer period because runoff from

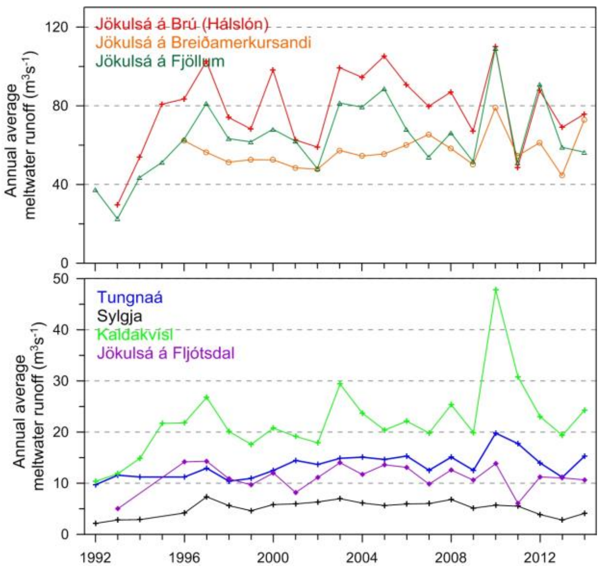

Figure 21. The temporal variation of average annual meltwater runoff to selected river catchments.

Table I. Melt water drainage to selected rivers.

Water Catchment:	Area (km^2)	ΣQ_s ($10^6 m^3$)	Q_s (m^3s^{-1})	Q_a (m^3s^{-1})	q_s ($ls^{-1}km^{-2}$)
Vatnajökull	7968,0	19545,3	1854,3	619,8	77,8
Tungnaá	121,8	482,5	45,8	15,3	125,6
Sylgja	39,7	129,9	12,3	4,1	103,8
Kaldakvísl	367,9	766,1	72,7	24,3	66,0
Jokulsa a Fjöllum	1188,3	1779,0	168,8	56,4	47,5
Kreppa	291,2	409,4	38,8	13,0	44,6
Kverka	47,0	199,1	18,9	6,3	134,3
Jokulsa a Brú	1214,8	2388,5	226,6	75,7	62,3
Jökulsá á Fljótsdal	130,6	336,2	31,9	10,7	81,6
Jökulsá í Lóni	101,3	307,1	29,1	9,7	96,1
Hornafjarðarfljót	239,1	697,9	66,2	22,1	92,6
Jökulsá á Breiðamerkursandi	739,5	2294,2	217,6	72,7	98,4
Breiðá-Fjallsá	234,6	1071,5	101,7	34,0	144,8
Skeiðará-Gígja	1165,2	2938,6	278,8	93,2	80,0
Súla	255,8	925,5	87,8	29,3	114,7
Brunná	35,8	162,4	15,4	5,1	143,8
Djúpá	83,7	318,5	30,2	10,1	120,7
Hverfisfljót	317,7	786,9	74,7	25,0	78,5
Skaftá	394,9	1112,0	105,5	35,3	89,3
Grímsvötn	173,3	141,5	13,4	4,5	25,9
Eystri Skaftárketill	39,4	18,0	1,7	0,6	14,5
Vestari Skaftárketill	25,1	13,5	1,3	0,4	17,1
Hólmsá	164,9	504,7	47,9	16,0	97,1
Heinabergsvötn	229,6	750,7	71,2	23,8	103,7
Skjálfandafljót	71,9	89,6	8,5	2,8	39,5

ΣQ_s: total summer melt water; Q_s : average runoff (averaged over summer, 4 months, June – September)
Q_a : average runoff (averaged over a whole year); q_s : average runoff per km^2 (averaged over a whole year)

the glacier melt in May is delayed due to refreezing during elimination of the cold wave and because of the contribution of the spring melt from the highlands to the runoff. Some melting also occurs during winter, especially in the low snouts of the southern outlets.

Average melt water runoff to different rivers is given in Table I, and temporal variation of the average meltwater runoff in Fig. 21. The average specific runoff (q_s) differs from basin to basin from 14 to 145 $ls^{-1}km^{-2}$. This is mainly due to different elevation distributions, for example, the water drainage basins for Tungnaá and Kverká are within the ablation area, while that of Grímsvötn and Skaftárkatlar are high in the accumulation zone.

6. Conclusions

The autumn weather was slightly colder than average the past decade; October was rather dry but precipitation in November over the average. The winter months December to March were warmer than average, exceptionally dry in in the SW but very high precipitation in the North and East (the NA-low pressure systems frequently passing south and east of Iceland). In these conditions snow collection is high on SE, E, and N Vatnajökull.
The spring months were warm, but precipitation in the SE over average. In a warm May the winter snow was already melting on the low lying snouts of SE-Vatnajökull and the glacier fore fields in west and north. The exceptionally high accumulation on Brúarjökull, Eyjabakkajökull and SE outlets reflects frequent snowfall in SE, E, and NE wind directions.
The summer of 2014 was unusually warm, but also very wet and cloudy in the south and west in June and July. The latter half of summer was warm and sunny, with high melt rates especially in the north and SE. September was warm and rather dry in the east, ablation was significant until late September.
This resulted in higher than average ablation on most of Vatnajökull. The exceptions are the center part of Dyngjujökull and snout of Síðujökull where unusually thick snow cover reduced ablation rates.
The winter balance was 10% higher than average (average since 1991_92). The summer mass balance (ablation) was ~20% greater than average. The net balance was negative; the mass loss was close to average since 1995_96 (the years of negative balance).
The glacial year of 2013_14 was the 20th in a row with negative mass balance for Vatnajökull (since 1994_95) contributing to a total loss of 14,4 m_{we}, 0,76 $m_{we}a^{-1}$ or an average surface lowering of 0,84 ma^{-1}. This is equivalent to ice volume of ~129 km^3, or just over 4% off the total ice volume.
Meltwater runoff to Tungnaá was close to average, 6 % over average to Kaldakvísl, 87% of average to Jökulsá á Fjöllum, 5% over average to Jökulsá á Brú (Hálslón), 96% to Jökulsá í Fljótsdal and 30% over average to Jökulsá á Breiðamerkursandi (summer rain and snow that falls and melts during summer is not included).

Summary:

B_w : 13,52 km^3_{we}
B_s : -19,53 km^3_{we}
B_n : -6,01 km^3_{we}
AAR = 52%

Specific Values:

b_w= 1,70 m_{we}
b_s= -2,45 m_{we}
b_n= -0,75 m_{we}

Appendix A: Mass balance at measurement sites 2013_14.

b_w: specific winter balance, **b_s**: specific summer balance, **b_n**: specific net balance, **l_a**: new snow in autumn (all in water equivalent).

Site	Position				Elevation	Date	Date	b_w	b_s	b_n	la
	Latitude		Longitude		(m a.s.l.)	in spring	in autumn	(mm)	(mm)	(mm)	(mm)
B09u	64	45,040	16	5,474	748	140506	141012	815	-5117	-4302	0
B10u	64	43,687	16	6,699	804	140506	141012	843	-4839	-3996	35
B11d	64	40,958	16	10,468	960	140506	141012	1440	-3258	-1818	35
B12t	64	38,276	16	14,132	1077	140506	141012	1557	-2835	-1278	140
B13t	64	34,518	16	19,732	1216	140506	141012	1751	-1691	60	133
B14v	64	31,640	16	24,705	1315	140505	141012	2087	-1355	732	252
B15i	64	28,487	16	30,016	1400	140505	141012	2066	-1034	1032	298
B16t	64	24,125	16	40,853	1526	140505	141016	2192	-728	1464	371
B17t	64	36,734	16	28,792	1213	140506	141012	1740	-1548	192	133
BR1g	64	5,558	16	19,503	110	140501	140931	-1570	-9162	-10732	0
BR2k	64	6,391	16	22,543	232	140507	140931	-500	-7530	-8030	0
Br3p	64	8,509	16	24,104	401	140507		260			0
Br4d	64	10,733	16	20,238	527	140507	140931	504	-6620	-6116	0
Br7r	64	22,147	16	16,939	1247	140507	141011	2642	-2408	234	210
B07t	64	25,793	16	17,452	1358	140507	141011	2365	-1237	1128	252
BB0s	64	22,718	16	5,051	1520	140507	141011	3125	-833	2292	476
Brus	64	41,000	15	55,223	772	140506	141011	822	-5547	-4725	0
Buds	64	35,991	15	59,890	1136	140506	141011	2080	-2170	-90	56
gb2d	64	34,109	16	0,026	1202	140506	141011	2178	-1746	432	133
B18r	64	31,587	16	0,124	1313	140506	141011	2509	-1429	1080	182
B19r	64	27,933	15	55,164	1431	140507	141011	2965	-751	2214	326
BB0s	64	22,718	16	5,051	1520	140507	141011	3125	-833	2292	476
D05r	64	42,235	16	54,662	1202	140505	141013	1730	-2054	-324	210
D07r	64	38,285	16	59,256	1371	140505	141013	1719	-1311	408	193
D09q	64	31,798	17	0,553	1581	140505	141013	1822	-694	1128	340
D12r	64	28,984	17	0,140	1647	140505	141013	1983	-399	1584	385
E01s	64	41,455	15	33,503	681	140507	141011	917	-5939	-5022	0
E02s	64	39,130	15	35,977	955	140507	141011	2090	-3953	-1863	42
E03t	64	36,667	15	36,909	1188	140507	141011	2510	-1850	660	123
E04s	64	34,952	15	37,106	1289	140506	141011	2734	-1270	1464	249
K01u	64	35,165	17	51,797	1061	140505	141015	930	-4512	-3582	0
K02v	64	34,817	17	49,685	1178	140505	141015	855	-3510	-2655	140
K03u	64	34,247	17	46,382	1297	140505	141015	1020	-2865	-1845	147
K04v	64	33,209	17	42,251	1488	140505	141015	1231	-1479	-248	256
K05v	64	33,451	17	35,428	1681	140505	141016	1678	-418	1260	375
K06u	64	38,358	17	31,364	1968	140602	140911	2180	316	2496	161
K07q	64	29,113	17	42,014	1534	140505	141016	1141	-871	270	266
S01j	64	7,012	17	49,989	740	140504	141014	1123	-4534	-3411	18
S02m	64	12,164	17	48,966	1010	140504	141014	1606	-3820	-2214	175
S04n	64	16,198	17	48,217	1160	140504	141014	1415	-2873	-1458	175
HAABn	64	20,952	17	24,083	1729	140609	141014	1980	-744	1236	560

T01no	64	19,486	18	8,234	744	140504	141014	175	-6448	-6273	42
T02nq	64	19,600	18	3,968	941	140504	141014	1198	-4519	-3321	105
T03nq	64	20,210	17	58,600	1076	140504	141014	1124	-3230	-2106	175
T04nq	64	21,339	17	51,527	1222	140504	141014	1480	-2731	-1251	224
T05nq	64	22,287	17	43,012	1344	140504	141014	1358	-1880	-522	263
T06nq	64	24,281	17	36,538	1465	140504	141014	1778	-896	882	333
T07np	64	25,291	17	31,200	1563	140504	141014	1512	-804	708	357
T08nq	64	26,313	17	27,779	1636	140504	141014	1747	-631	1116	396
BORTHNb	64	25,087	17	19,154	1401	140604	141015	1830	-2355	-525	403
Borai	64	24,938	17	20,158	1400	140604	141015	1860	-1973	-113	389
G02k	64	26,845	17	17,748	1560	140602	141015	1560	-600	960	385
G03l	64	28,445	17	16,347	1655	140602	141015	1910	-420	1490	403
G04s	64	30,016	17	15,025	1685	140602	141015	1900	-562	1338	340
Go1r	64	34,014	17	24,920	1758	140602	141015	1920	-402	1518	413
Hof01l	64	32,327	15	35,844	1141	140506	141011	2478	-2046	432	210
Fl01e	64	26,161	15	55,628	1347	140507	141011	2979	-920	2059	298
Skf01e	64	17,989	16	5,003	1283	140507	141011	3360	-1297	2063	326

Appendix B: Balance distribution by elevation in 2013_14.

ΔS : area in elevation range, ∑ΔS: cumulative area above given elevation, b_w: specific winter balance, b_s: specific summer balance. b_n: specific winter balance, ΔB_w : winter balance at a given elevation range, $\sum\Delta B_w$: cumulative winter balance above given elevation, ΔB_s summer balance at a given elevation range, $\sum\Delta B_s$: cumulative summer balance above given elevation, ΔB_n: net annual balance in a given elevation range, $\sum B_n$: cumulative net annual balance above given elevation.

Vatnajökull

Elevation (m a.s.l.)			ΔS (km^2)	∑ΔS (km^2)	b_w (mm)	b_s (mm)	b_n (mm)	ΔB_w (10^6m^3)	$\sum\Delta B_w$ (10^6m^3)	ΔB_s (10^6m^3)	$\sum\Delta B_s$ (10^6m^3)	ΔB_n (10^6m^3)	$\sum B_n$ (10^6m^3)
2000	2050	2025	0,5	0,5	3729	358	4088	1,8	2	0,2	0	2,0	2
1950	2000	1975	16,3	16,8	2372	359	2732	38,7	41	5,9	6	44,6	47
1900	1950	1925	44,6	61,4	2229	117	2346	99,5	140	5,2	11	104,8	151
1850	1900	1875	35,8	97,2	2364	-72	2292	84,9	225	-2,6	9	82,3	234
1800	1850	1825	40,4	137,6	2533	-70	2463	102,5	327	-2,8	6	99,6	333
1750	1800	1775	55,5	193,1	2247	-258	1989	125,2	453	-14,4	-9	110,8	444
1700	1750	1725	102,5	295,6	2011	-395	1616	206,7	659	-40,6	-49	166,1	610
1650	1700	1675	223,9	519,5	1934	-496	1438	433,6	1093	-111,2	-160	322,4	933
1600	1650	1625	355,2	874,7	1942	-570	1372	690,4	1783	-202,6	-363	487,8	1420
1550	1600	1575	355,7	1230,4	1921	-716	1205	683,7	2467	-254,9	-618	428,8	1849
1500	1550	1525	418,4	1648,8	1912	-870	1042	800,6	3268	-364,2	-982	436,4	2286
1450	1500	1475	450,3	2099,1	1960	-1018	942	883,5	4151	-458,9	-1441	424,6	2710
1400	1450	1425	502,0	2601,1	2086	-1164	921	1048,2	5200	-585,2	-2026	463,0	3173
1350	1400	1375	537,1	3138,2	2147	-1335	812	1154,6	6354	-717,6	-2744	437,0	3610
1300	1350	1325	549,0	3687,2	2099	-1571	528	1154,3	7508	-863,8	-3608	290,5	3901
1250	1300	1275	518,8	4206,0	2067	-1787	280	1074,5	8583	-929,0	-4537	145,6	4046
1200	1250	1225	463,8	4669,8	1926	-2081	-154	895,4	9478	-967,4	-5504	-71,9	3974
1150	1200	1175	411,2	5081,0	1816	-2398	-581	749,4	10228	-989,4	-6493	-239,9	3734
1100	1150	1125	367,9	5448,9	1735	-2723	-988	640,4	10868	-1005,0	-7498	-364,6	3370
1050	1100	1075	331,3	5780,2	1635	-3115	-1480	543,8	11412	-1036,1	-8534	-492,3	2878
1000	1050	1025	306,2	6086,4	1540	-3492	-1951	473,8	11886	-1074,1	-9609	-600,3	2277
950	1000	975	278,9	6365,3	1452	-3858	-2405	406,5	12292	-1080,0	-10689	-673,4	1604
900	950	925	239,7	6605,0	1368	-4166	-2797	329,8	12622	-1003,9	-11692	-674,0	930
850	900	875	216,1	6821,1	1268	-4482	-3213	275,7	12898	-974,1	-12667	-698,4	231
800	850	825	197,8	7018,9	1155	-4833	-3678	230,3	13128	-963,8	-13630	-733,5	-502
750	800	775	170,7	7189,6	1056	-5159	-4102	180,9	13309	-882,9	-14513	-702,1	-1204
700	750	725	135,1	7324,7	998	-5365	-4366	135,4	13444	-727,6	-15241	-592,1	-1796
650	700	675	101,6	7426,3	951	-5604	-4652	97,1	13542	-571,8	-15813	-474,6	-2271
600	650	625	70,3	7496,6	853	-5768	-4915	60,3	13602	-407,7	-16220	-347,4	-2618
550	600	575	63,4	7560,0	686	-6061	-5375	43,9	13646	-387,5	-16608	-343,7	-2962
500	550	525	44,7	7604,7	563	-6255	-5691	25,5	13671	-282,8	-16891	-257,3	-3219
450	500	475	41,4	7646,1	431	-6547	-6115	18,0	13689	-273,7	-17164	-255,6	-3475
400	450	425	44,4	7690,5	304	-6771	-6467	13,7	13703	-304,0	-17468	-290,4	-3765
350	400	375	40,6	7731,1	105	-6932	-6826	4,4	13707	-285,7	-17754	-281,3	-4047
300	350	325	41,1	7772,2	-132	-7137	-7269	-5,5	13702	-297,6	-18052	-303,1	-4350
250	300	275	40,4	7812,6	-391	-7452	-7844	-16,0	13686	-304,1	-18356	-320,1	-4670
200	250	225	37,9	7850,5	-751	-7946	-8698	-28,7	13657	-303,7	-18659	-332,4	-5002
150	200	175	31,6	7882,1	-1101	-8488	-9589	-35,1	13622	-270,4	-18930	-305,5	-5308
100	150	125	32,4	7914,5	-1427	-8998	-10425	-46,9	13575	-295,8	-19226	-342,7	-5651
50	100	75	24,7	7939,2	-1688	-9338	-11027	-42,8	13532	-236,7	-19462	-279,5	-5930
0	50	25	6,1	7945,3	-1857	-9693	-11551	-12,1	13520	-63,0	-19525	-75,1	-6005

Tungnaárjökull

Elevation (m a.s.l.)			ΔS (km^2)	$\sum\Delta S$ (km^2)	b_w (mm)	b_s (mm)	b_n (mm)	ΔB_w ($10^6 m^3$)	$\sum\Delta B_w$ ($10^6 m^3$)	ΔB_s ($10^6 m^3$)	$\sum\Delta B_s$ ($10^6 m^3$)	ΔB_n ($10^6 m^3$)	$\sum B_n$ ($10^6 m^3$)
1650	1700	1675	2,4	2,4	1844	-590	1254	4,4	4	-1,4	-1	3,0	3
1600	1650	1625	13,2	15,6	1821	-635	1185	24,0	28	-8,4	-10	15,6	19
1550	1600	1575	15,3	30,9	1775	-735	1039	27,1	56	-11,2	-21	15,9	34
1500	1550	1525	15,3	46,2	1727	-813	913	26,4	82	-12,4	-33	14,0	48
1450	1500	1475	18,5	64,7	1698	-910	788	31,4	113	-16,8	-50	14,6	63
1400	1450	1425	23,3	88,0	1666	-1216	449	38,8	152	-28,4	-79	10,5	74
1350	1400	1375	21,7	109,7	1595	-1654	-58	34,6	187	-35,8	-114	-1,3	72
1300	1350	1325	28,1	137,8	1534	-2121	-586	43,1	230	-59,5	-174	-16,4	56
1250	1300	1275	21,8	159,6	1514	-2488	-974	33,0	263	-54,3	-228	-21,3	35
1200	1250	1225	24,0	183,6	1475	-2751	-1276	35,5	298	-66,2	-294	-30,7	4
1150	1200	1175	21,0	204,6	1440	-2938	-1498	30,2	328	-61,6	-356	-31,4	-28
1100	1150	1125	19,2	223,8	1394	-3074	-1679	26,8	355	-59,1	-415	-32,3	-60
1050	1100	1075	20,0	243,8	1377	-3396	-2019	27,6	383	-67,9	-483	-40,4	-100
1000	1050	1025	18,2	262,0	1332	-3924	-2591	24,2	407	-71,4	-554	-47,1	-147
950	1000	975	18,9	280,9	1212	-4449	-3236	22,9	430	-84,0	-639	-61,1	-209
900	950	925	15,2	296,1	1030	-4943	-3913	15,6	446	-75,0	-714	-59,4	-268
850	900	875	15,1	311,2	809	-5427	-4617	12,2	458	-81,8	-795	-69,6	-338
800	850	825	14,1	325,3	579	-5921	-5342	8,2	466	-83,4	-879	-75,2	-413
750	800	775	10,3	335,6	399	-6292	-5893	4,1	470	-64,6	-943	-60,5	-473
700	750	725	7,1	342,7	290	-6496	-6206	2,1	472	-46,5	-990	-44,4	-518
650	700	675	1,6	344,3	264	-6553	-6289	0,4	473	-11,0	-1001	-10,6	-528
600	650	625	0,0	344,3	263	-6586	-6322	0,0	473	-0,4	-1001	-0,4	-529

Sylgjujökull

Elevation (m a.s.l.)			ΔS (km^2)	$\sum\Delta S$ (km^2)	b_w (mm)	b_s (mm)	b_n (mm)	ΔB_w ($10^6 m^3$)	$\sum\Delta B_w$ ($10^6 m^3$)	ΔB_s ($10^6 m^3$)	$\sum\Delta B_s$ ($10^6 m^3$)	ΔB_n ($10^6 m^3$)	$\sum B_n$ ($10^6 m^3$)
1600	1650	1625	2,0	2,0	1721	-593	1127	3,5	4	-1,2	-1	2,3	2
1550	1600	1575	6,8	8,8	1599	-722	876	10,8	14	-4,9	-6	5,9	8
1500	1550	1525	18,9	27,7	1381	-876	505	26,1	40	-16,5	-23	9,5	18
1450	1500	1475	12,3	40,0	1376	-1072	303	16,9	57	-13,2	-36	3,7	22
1400	1450	1425	8,2	48,2	1444	-1313	131	11,9	69	-10,8	-47	1,1	23
1350	1400	1375	5,1	53,3	1470	-1697	-226	7,5	77	-8,6	-55	-1,1	21
1300	1350	1325	5,3	58,6	1458	-2229	-771	7,7	84	-11,7	-67	-4,1	17
1250	1300	1275	10,4	69,0	1429	-2580	-1150	14,8	99	-26,7	-94	-11,9	5
1200	1250	1225	12,6	81,6	1383	-2819	-1436	17,4	117	-35,4	-129	-18,1	-13
1150	1200	1175	14,4	96,0	1332	-2969	-1636	19,2	136	-42,7	-172	-23,5	-36
1100	1150	1125	13,2	109,2	1262	-3117	-1854	16,6	152	-41,1	-213	-24,4	-61
1050	1100	1075	13,4	122,6	1073	-3675	-2601	14,4	167	-49,2	-262	-34,9	-96
1000	1050	1025	9,3	131,9	774	-4307	-3532	7,2	174	-40,0	-302	-32,8	-128
950	1000	975	3,1	135,0	659	-4598	-3939	2,0	176	-14,1	-316	-12,1	-140
900	950	925	1,6	136,6	486	-4856	-4370	0,8	177	-7,8	-324	-7,0	-147
850	900	875	0,2	136,8	379	-4995	-4616	0,0	177	-0,9	-325	-0,8	-148

Köldukvíslarjökul

Elevation (m a.s.l.)			ΔS (km^2)	$\sum\Delta S$ (km^2)	b_w (mm)	b_s (mm)	b_n (mm)	ΔB_w ($10^6 m^3$)	$\sum\Delta B_w$ ($10^6 m^3$)	ΔB_s ($10^6 m^3$)	$\sum\Delta B_s$ ($10^6 m^3$)	ΔB_n ($10^6 m^3$)	$\sum B_n$ ($10^6 m^3$)
1950	2000	1975	3,6	3,6	2182	336	2518	7,8	8	1,2	1	9,0	9
1900	1950	1925	12,4	16,0	2097	100	2198	26,0	34	1,2	3	27,2	36
1850	1900	1875	5,9	21,9	2008	-98	1910	11,8	46	-0,6	2	11,2	48
1800	1850	1825	6,0	27,9	1943	-219	1724	11,6	57	-1,3	1	10,3	58
1750	1800	1775	10,5	38,4	1918	-318	1600	20,2	77	-3,4	-3	16,9	75
1700	1750	1725	17,9	56,3	1803	-413	1390	32,2	110	-7,4	-10	24,8	100
1650	1700	1675	15,6	71,9	1663	-496	1167	25,9	136	-7,7	-18	18,2	118
1600	1650	1625	13,8	85,7	1552	-698	854	21,4	157	-9,6	-28	11,8	130
1550	1600	1575	19,2	104,9	1421	-948	472	27,3	184	-18,2	-46	9,1	139
1500	1550	1525	20,9	125,8	1252	-1101	150	26,2	211	-23,0	-69	3,2	142
1450	1500	1475	19,3	145,1	1201	-1334	-132	23,2	234	-25,8	-95	-2,6	139
1400	1450	1425	14,2	159,3	1172	-1706	-533	16,7	250	-24,3	-119	-7,6	132
1350	1400	1375	15,3	174,6	1126	-2155	-1028	17,2	268	-32,9	-152	-15,7	116
1300	1350	1325	17,5	192,1	1053	-2595	-1541	18,4	286	-45,4	-197	-27,0	89
1250	1300	1275	18,0	210,1	974	-2988	-2014	17,6	304	-54,1	-251	-36,5	52
1200	1250	1225	18,3	228,4	912	-3246	-2334	16,7	320	-59,3	-311	-42,7	10
1150	1200	1175	16,4	244,8	847	-3550	-2703	13,9	334	-58,3	-369	-44,4	-35
1100	1150	1125	14,9	259,7	773	-4006	-3233	11,6	346	-59,9	-429	-48,3	-83
1050	1100	1075	13,1	272,8	667	-4498	-3830	8,8	355	-59,2	-488	-50,4	-133
1000	1050	1025	11,1	283,9	554	-4919	-4364	6,2	361	-54,7	-543	-48,5	-182
950	1000	975	10,5	294,4	466	-5283	-4816	4,9	366	-55,4	-598	-50,5	-232
900	950	925	5,6	300,0	399	-5515	-5115	2,2	368	-30,9	-629	-28,7	-261
850	900	875	0,5	300,5	329	-5740	-5411	0,2	368	-3,1	-632	-2,9	-264

Dyngjujökull

Elevation (m a.s.l.)			ΔS (km^2)	$\sum\Delta S$ (km^2)	b_w (mm)	b_s (mm)	b_n (mm)	ΔB_w ($10^6 m^3$)	$\sum\Delta B_w$ ($10^6 m^3$)	ΔB_s ($10^6 m^3$)	$\sum\Delta B_s$ ($10^6 m^3$)	ΔB_n ($10^6 m^3$)	$\sum B_n$ ($10^6 m^3$)
1950	2000	1975	7,4	7,4	2191	375	2566	16,2	16	2,8	3	19,0	19
1900	1950	1925	23,2	30,6	2124	126	2251	49,2	66	2,9	6	52,1	71
1850	1900	1875	15,9	46,5	2036	-176	1859	32,4	98	-2,8	3	29,6	101
1800	1850	1825	9,7	56,2	1978	-305	1672	19,3	117	-3,0	0	16,3	117
1750	1800	1775	16,0	72,2	1950	-394	1555	31,2	148	-6,3	-6	24,9	142
1700	1750	1725	27,3	99,5	1915	-444	1471	52,2	201	-12,1	-19	40,1	182
1650	1700	1675	71,6	171,1	1904	-497	1406	136,3	337	-35,6	-54	100,7	283
1600	1650	1625	114,0	285,1	1891	-538	1353	215,7	553	-61,4	-116	154,3	437
1550	1600	1575	94,7	379,8	1823	-665	1157	172,7	725	-63,1	-179	109,6	547
1500	1550	1525	89,7	469,5	1792	-790	1001	160,7	886	-70,9	-249	89,8	637
1450	1500	1475	75,1	544,6	1774	-916	857	133,2	1019	-68,8	-318	64,4	701
1400	1450	1425	61,4	606,0	1763	-1052	711	108,3	1128	-64,6	-383	43,7	745
1350	1400	1375	49,4	655,4	1753	-1206	546	86,6	1214	-59,6	-442	27,0	772
1300	1350	1325	37,9	693,3	1745	-1364	381	66,2	1280	-51,7	-494	14,5	786
1250	1300	1275	41,3	734,6	1739	-1549	189	71,9	1352	-64,0	-558	7,8	794
1200	1250	1225	48,8	783,4	1723	-1829	-106	84,2	1436	-89,4	-648	-5,2	789
1150	1200	1175	48,2	831,6	1671	-2217	-545	80,7	1517	-107,0	-755	-26,3	762
1100	1150	1125	44,0	875,6	1586	-2599	-1013	69,9	1587	-114,5	-869	-44,6	718
1050	1100	1075	33,1	908,7	1466	-2930	-1463	48,6	1636	-97,2	-966	-48,5	669
1000	1050	1025	35,5	944,2	1334	-3286	-1951	47,6	1683	-117,3	-1084	-69,6	600
950	1000	975	30,8	975,0	1222	-3751	-2529	37,7	1721	-115,7	-1199	-78,0	522
900	950	925	25,6	1000,6	1142	-4242	-3100	29,5	1750	-109,5	-1309	-80,1	442
850	900	875	24,9	1025,5	1076	-4762	-3686	27,3	1778	-120,9	-1430	-93,6	348
800	850	825	19,7	1045,2	1016	-5270	-4253	20,6	1798	-106,7	-1536	-86,1	262
750	800	775	15,2	1060,4	958	-5707	-4748	14,5	1813	-86,5	-1623	-72,0	190
700	750	725	1,7	1062,1	944	-5896	-4952	1,6	1814	-10,3	-1633	-8,6	181

Brúarjökull

Elevation (m a.s.l.)			ΔS (km^2)	$\sum\Delta S$ (km^2)	b_w (mm)	b_s (mm)	b_n (mm)	ΔB_w (10^6m^3)	$\sum\Delta B_w$ (10^6m^3)	ΔB_s (10^6m^3)	$\sum\Delta B_s$ (10^6m^3)	ΔB_n (10^6m^3)	$\sum B_n$ (10^6m^3)
1850	1900	1875	0,8	0,8	1877	-165	1711	1,6	2	-0,1	0	1,5	2
1800	1850	1825	4,2	5,0	1922	-78	1843	8,0	10	-0,3	-1	7,7	9
1750	1800	1775	3,0	8,0	1943	-203	1739	5,8	15	-0,6	-1	5,1	14
1700	1750	1725	3,7	11,7	1943	-367	1575	7,3	23	-1,4	-3	5,9	20
1650	1700	1675	5,3	17,0	1939	-429	1510	10,2	33	-2,3	-5	8,0	28
1600	1650	1625	44,4	61,4	1987	-514	1472	88,3	121	-22,9	-28	65,4	94
1550	1600	1575	47,6	109,0	2034	-588	1445	96,9	218	-28,0	-56	68,8	162
1500	1550	1525	69,8	178,8	2104	-674	1430	147,0	365	-47,1	-103	99,9	262
1450	1500	1475	73,9	252,7	2141	-761	1379	158,4	523	-56,3	-159	102,0	364
1400	1450	1425	108,1	360,8	2343	-923	1419	253,4	777	-99,9	-259	153,5	518
1350	1400	1375	148,2	509,0	2389	-1107	1281	354,4	1131	-164,3	-423	190,1	708
1300	1350	1325	151,3	660,3	2315	-1256	1058	350,5	1482	-190,2	-614	160,3	868
1250	1300	1275	144,8	805,1	2227	-1432	794	322,6	1804	-207,5	-821	115,1	983
1200	1250	1225	121,8	926,9	2053	-1636	416	250,2	2055	-199,4	-1020	50,8	1034
1150	1200	1175	105,8	1032,7	1888	-1938	-50	199,9	2254	-205,2	-1226	-5,4	1029
1100	1150	1125	86,8	1119,5	1755	-2322	-566	152,3	2407	-201,5	-1427	-49,2	980
1050	1100	1075	73,3	1192,8	1658	-2727	-1069	121,6	2528	-200,1	-1627	-78,4	901
1000	1050	1025	65,6	1258,4	1547	-3016	-1468	101,6	2630	-198,0	-1825	-96,4	805
950	1000	975	59,4	1317,8	1420	-3266	-1846	84,3	2714	-193,9	-2019	-109,6	695
900	950	925	48,9	1366,7	1271	-3664	-2393	62,2	2776	-179,2	-2198	-117,0	578
850	900	875	44,9	1411,6	1106	-4193	-3086	49,7	2826	-188,2	-2386	-138,5	440
800	850	825	41,4	1453,0	954	-4743	-3788	39,5	2866	-196,3	-2583	-156,8	283
750	800	775	36,1	1489,1	843	-5132	-4289	30,4	2896	-185,3	-2768	-154,9	128
700	750	725	23,8	1512,9	767	-5471	-4704	18,2	2914	-129,9	-2898	-111,7	16
650	700	675	12,8	1525,7	691	-5878	-5186	8,8	2923	-75,1	-2973	-66,2	-50
600	650	625	0,3	1526,0	634	-6079	-5444	0,2	2923	-2,0	-2975	-1,8	-52

Eyjabakkajökull

Elevation (m a.s.l.)			ΔS (km^2)	$\sum\Delta S$ (km^2)	b_w (mm)	b_s (mm)	b_n (mm)	ΔB_w (10^6m^3)	$\sum\Delta B_w$ (10^6m^3)	ΔB_s (10^6m^3)	$\sum\Delta B_s$ (10^6m^3)	ΔB_n (10^6m^3)	$\sum B_n$ (10^6m^3)
1550	1600	1575	0,0	0,0	3004	-860	2144	0,0	0	0,0	0	0,0	0
1500	1550	1525	0,0	0,0	3008	-845	2162	0,3	0	0,0	0	0,2	0
1450	1500	1475	1,0	1,0	2992	-875	2116	2,9	3	-0,8	-1	2,1	2
1400	1450	1425	1,8	2,8	2977	-913	2064	5,5	9	-1,7	-3	3,8	6
1350	1400	1375	2,5	5,3	2940	-993	1946	7,4	16	-2,5	-5	4,9	11
1300	1350	1325	3,9	9,2	2892	-1068	1824	11,3	27	-4,2	-9	7,1	18
1250	1300	1275	13,4	22,6	2742	-1341	1401	36,6	64	-17,9	-27	18,7	37
1200	1250	1225	13,3	35,9	2618	-1613	1005	34,9	99	-21,5	-49	13,4	50
1150	1200	1175	14,7	50,6	2498	-1919	578	36,7	136	-28,2	-77	8,5	59
1100	1150	1125	12,3	62,9	2398	-2287	111	29,4	165	-28,0	-105	1,4	60
1050	1100	1075	10,6	73,5	2262	-2782	-519	24,0	189	-29,5	-134	-5,5	55
1000	1050	1025	10,1	83,6	2127	-3251	-1124	21,5	211	-32,9	-167	-11,4	43
950	1000	975	7,7	91,3	1967	-3694	-1727	15,2	226	-28,6	-196	-13,4	30
900	950	925	5,2	96,5	1791	-4116	-2325	9,3	235	-21,4	-217	-12,1	18
850	900	875	3,9	100,4	1694	-4440	-2745	6,6	242	-17,3	-235	-10,7	7
800	850	825	3,2	103,6	1613	-4736	-3123	5,1	247	-15,0	-250	-9,9	-3
750	800	775	3,4	107,0	1424	-5196	-3771	4,8	252	-17,5	-267	-12,7	-16
700	750	725	3,3	110,3	1085	-5751	-4665	3,6	255	-19,0	-286	-15,4	-31
650	700	675	1,7	112,0	908	-5961	-5052	1,5	257	-10,1	-296	-8,6	-40

Hoffellsjökull

Elevation (m a.s.l.)			ΔS (km^2)	$\sum\Delta S$ (km^2)	b_w (mm)	b_s (mm)	b_n (mm)	ΔB_w (10^6m^3)	$\sum\Delta B_w$ (10^6m^3)	ΔB_s (10^6m^3)	$\sum\Delta B_s$ (10^6m^3)	ΔB_n (10^6m^3)	$\sum B_n$ (10^6m^3)
1450	1500	1475	0,9	0,9	3009	-869	2140	2,8	3	-0,8	-1	2,0	2
1400	1450	1425	6,7	7,6	2933	-933	1999	19,7	22	-6,3	-7	13,4	15
1350	1400	1375	10,0	17,6	2898	-1026	1872	28,9	51	-10,2	-17	18,7	34
1300	1350	1325	15,4	33,0	2849	-1184	1664	43,8	95	-18,2	-36	25,6	60
1250	1300	1275	33,6	66,6	2748	-1437	1311	92,2	187	-48,2	-84	44,0	104
1200	1250	1225	26,8	93,4	2657	-1632	1024	71,2	259	-43,8	-128	27,5	131
1150	1200	1175	18,2	111,6	2540	-1852	687	46,3	305	-33,7	-161	12,5	144
1100	1150	1125	17,5	129,1	2421	-2210	210	42,4	347	-38,7	-200	3,7	147
1050	1100	1075	13,6	142,7	2260	-2883	-622	30,7	378	-39,1	-239	-8,4	139
1000	1050	1025	10,0	152,7	2095	-3518	-1422	20,9	399	-35,1	-274	-14,2	125
950	1000	975	9,0	161,7	1927	-4092	-2165	17,4	416	-36,9	-311	-19,5	105
900	950	925	6,4	168,1	1771	-4498	-2726	11,4	428	-29,0	-340	-17,6	88
850	900	875	4,3	172,4	1648	-4746	-3098	7,1	435	-20,6	-361	-13,4	74
800	850	825	3,5	175,9	1515	-4962	-3447	5,4	440	-17,8	-378	-12,4	62
750	800	775	3,8	179,7	1372	-5210	-3837	5,3	445	-20,2	-399	-14,9	47
700	750	725	3,8	183,5	1231	-5462	-4231	4,7	450	-20,9	-420	-16,2	31
650	700	675	3,4	186,9	1065	-5744	-4679	3,6	454	-19,3	-439	-15,7	15
600	650	625	2,5	189,4	890	-6056	-5166	2,2	456	-15,0	-454	-12,8	2
550	600	575	1,8	191,2	747	-6337	-5589	1,4	457	-11,5	-465	-10,2	-8
500	550	525	1,5	192,7	618	-6571	-5952	0,9	458	-9,7	-475	-8,8	-17
450	500	475	0,9	193,6	487	-6772	-6285	0,5	459	-6,3	-481	-5,8	-23
400	450	425	0,9	194,5	322	-6955	-6633	0,3	459	-6,6	-488	-6,3	-29
350	400	375	0,6	195,1	134	-7096	-6961	0,0	459	-4,2	-492	-4,1	-33
300	350	325	0,9	196,0	-71	-7232	-7303	0,0	459	-6,6	-499	-6,6	-40
250	300	275	2,1	198,1	-350	-7436	-7786	-0,8	458	-16,1	-515	-16,9	-57
200	250	225	3,3	201,4	-655	-7742	-8397	-2,1	456	-25,3	-540	-27,5	-84
150	200	175	2,6	204,0	-1001	-8336	-9337	-2,6	454	-21,7	-562	-24,3	-108
100	150	125	2,1	206,1	-1285	-8899	-10185	-2,7	451	-19,0	-581	-21,7	-130
50	100	75	2,8	208,9	-1611	-9597	-11209	-4,5	446	-26,9	-608	-31,4	-162
0	50	25	0,5	209,4	-1793	-9923	-11716	-1,0	445	-5,6	-613	-6,6	-168

Breiðamerkurjökull

Elevation (m a.s.l.)			ΔS (km^2)	$\sum\Delta S$ (km^2)	b_w (mm)	b_s (mm)	b_n (mm)	ΔB_w ($10^6 m^3$)	$\sum\Delta B_w$ ($10^6 m^3$)	ΔB_s ($10^6 m^3$)	$\sum\Delta B_s$ ($10^6 m^3$)	ΔB_n ($10^6 m^3$)	$\sum B_n$ ($10^6 m^3$)
1900	1950	1925	0,0	0,0	4106	341	4447	0,2	0	0,0	0	0,2	0
1850	1900	1875	0,4	0,4	4089	325	4415	1,5	2	0,1	0	1,6	2
1800	1850	1825	0,4	0,8	4009	279	4289	1,8	3	0,1	0	1,9	4
1750	1800	1775	0,8	1,6	3780	206	3986	3,1	7	0,2	0	3,3	7
1700	1750	1725	2,5	4,1	2913	-120	2793	7,2	14	-0,3	0	6,9	14
1650	1700	1675	5,8	9,9	2369	-424	1945	13,6	27	-2,4	-2	11,2	25
1600	1650	1625	15,8	25,7	2222	-542	1680	35,1	63	-8,6	-11	26,6	52
1550	1600	1575	25,7	51,4	2178	-677	1501	56,0	119	-17,4	-28	38,6	90
1500	1550	1525	32,2	83,6	2222	-799	1423	71,5	190	-25,7	-54	45,8	136
1450	1500	1475	44,3	127,9	2370	-908	1461	104,9	295	-40,2	-94	64,7	201
1400	1450	1425	58,3	186,2	2357	-1072	1285	137,6	433	-62,5	-157	75,0	276
1350	1400	1375	88,7	274,9	2398	-1299	1099	212,8	645	-115,3	-272	97,5	373
1300	1350	1325	96,9	371,8	2349	-1616	732	227,7	873	-156,7	-429	71,0	444
1250	1300	1275	59,4	431,2	2299	-1982	317	136,7	1010	-117,8	-547	18,9	463
1200	1250	1225	39,7	470,9	2209	-2419	-210	87,7	1097	-96,0	-643	-8,3	455
1150	1200	1175	32,6	503,5	2081	-2850	-769	67,9	1165	-93,1	-736	-25,1	430
1100	1150	1125	27,7	531,2	1978	-3200	-1221	54,9	1220	-88,7	-824	-33,9	396
1050	1100	1075	24,1	555,3	1883	-3469	-1586	45,3	1265	-83,5	-908	-38,2	358
1000	1050	1025	22,1	577,4	1802	-3693	-1890	39,9	1305	-81,7	-990	-41,8	316
950	1000	975	24,5	601,9	1727	-4012	-2285	42,3	1348	-98,4	-1088	-56,0	260
900	950	925	27,3	629,2	1650	-4247	-2597	45,2	1393	-116,3	-1204	-71,1	189
850	900	875	26,2	655,4	1510	-4547	-3036	39,6	1433	-119,2	-1323	-79,6	109
800	850	825	26,0	681,4	1357	-4868	-3511	35,4	1468	-126,9	-1450	-91,6	18
750	800	775	25,3	706,7	1198	-5244	-4046	30,3	1498	-132,5	-1583	-102,2	-85
700	750	725	23,9	730,6	1073	-5517	-4443	25,7	1524	-132,0	-1715	-106,3	-191
650	700	675	30,8	761,4	968	-5682	-4714	29,9	1554	-175,3	-1890	-145,4	-336
600	650	625	26,2	787,6	815	-6014	-5199	21,4	1575	-157,6	-2048	-136,2	-473
550	600	575	26,8	814,4	654	-6363	-5708	17,7	1593	-171,7	-2219	-154,0	-627
500	550	525	15,6	830,0	510	-6519	-6008	8,0	1601	-102,6	-2322	-94,6	-721
450	500	475	16,2	846,2	344	-6762	-6418	5,6	1606	-109,9	-2432	-104,3	-826
400	450	425	15,8	862,0	223	-6920	-6697	3,5	1610	-109,9	-2542	-106,4	-932
350	400	375	12,9	874,9	62	-7057	-6995	0,8	1611	-92,0	-2634	-91,2	-1023
300	350	325	12,9	887,8	-160	-7227	-7388	-2,1	1609	-94,4	-2728	-96,5	-1120
250	300	275	12,0	899,8	-483	-7590	-8074	-5,8	1603	-91,5	-2820	-97,3	-1217
200	250	225	11,5	911,3	-970	-8284	-9254	-11,1	1592	-95,2	-2915	-106,3	-1323
150	200	175	8,5	919,8	-1410	-8939	-10350	-12,1	1580	-76,7	-2992	-88,8	-1412
100	150	125	7,9	927,7	-1698	-9386	-11085	-13,4	1566	-73,9	-3066	-87,2	-1499
50	100	75	6,0	933,7	-1872	-9698	-11571	-11,4	1555	-58,9	-3124	-70,2	-1570
0	50	25	2,9	936,6	-1960	-9868	-11828	-6,0	1549	-30,2	-3155	-36,2	-1606

Síðujökull

Elevation (m a.s.l.)			ΔS (km^2)	$\sum\Delta S$ (km^2)	b_w (mm)	b_s (mm)	b_n (mm)	ΔB_w ($10^6 m^3$)	$\sum\Delta B_w$ ($10^6 m^3$)	ΔB_s ($10^6 m^3$)	$\sum\Delta B_s$ ($10^6 m^3$)	ΔB_n ($10^6 m^3$)	$\sum B_n$ ($10^6 m^3$)
1700	1750	1725	0,7	0,7	1961	-737	1224	1,5	2	-0,6	-1	0,9	1
1650	1700	1675	5,2	5,9	1928	-726	1202	9,9	11	-3,7	-4	6,2	7
1600	1650	1625	11,1	17,0	1892	-734	1158	21,1	33	-8,2	-13	12,9	20
1550	1600	1575	10,1	27,1	1878	-779	1099	19,0	51	-7,9	-20	11,1	31
1500	1550	1525	20,1	47,2	1865	-837	1028	37,6	89	-16,9	-37	20,7	52
1450	1500	1475	40,1	87,3	1810	-1046	764	72,6	162	-42,0	-79	30,7	83
1400	1450	1425	26,9	114,2	1764	-1279	484	47,4	209	-34,4	-114	13,0	96
1350	1400	1375	21,3	135,5	1722	-1730	-7	36,7	246	-36,9	-151	-0,2	95
1300	1350	1325	17,4	152,9	1692	-2155	-462	29,5	275	-37,6	-188	-8,1	87
1250	1300	1275	16,6	169,5	1664	-2403	-738	27,6	303	-39,8	-228	-12,2	75
1200	1250	1225	21,2	190,7	1647	-2607	-959	34,9	338	-55,2	-283	-20,3	55
1150	1200	1175	18,1	208,8	1615	-2848	-1233	29,2	367	-51,6	-335	-22,3	32
1100	1150	1125	17,0	225,8	1607	-3094	-1487	27,4	394	-52,7	-387	-25,3	7
1050	1100	1075	18,0	243,8	1586	-3406	-1819	28,5	423	-61,3	-449	-32,7	-26
1000	1050	1025	21,8	265,6	1532	-3722	-2189	33,4	456	-81,0	-530	-47,7	-73
950	1000	975	21,8	287,4	1434	-3997	-2562	31,3	488	-87,3	-617	-55,9	-129
900	950	925	22,1	309,5	1333	-4170	-2836	29,5	517	-92,3	-709	-62,8	-192
850	900	875	20,9	330,4	1261	-4354	-3092	26,3	543	-90,9	-800	-64,5	-257
800	850	825	25,0	355,4	1201	-4505	-3304	30,0	573	-112,6	-913	-82,6	-339
750	800	775	25,5	380,9	1146	-4709	-3563	29,2	603	-120,1	-1033	-90,8	-430
700	750	725	26,0	406,9	1098	-4996	-3898	28,5	631	-129,8	-1162	-101,2	-531
650	700	675	15,8	422,7	1063	-5293	-4230	16,8	648	-83,8	-1246	-67,0	-598
600	650	625	7,4	430,1	1035	-5488	-4453	7,7	656	-40,7	-1287	-33,0	-631
550	600	575	0,2	430,3	1025	-5393	-4368	0,2	656	-1,1	-1288	-0,9	-632

Skaftárjökull

Elevation (m a.s.l.)			ΔS (km^2)	$\sum\Delta S$ (km^2)	b_w (mm)	b_s (mm)	b_n (mm)	ΔB_w ($10^6 m^3$)	$\sum\Delta B_w$ ($10^6 m^3$)	ΔB_s ($10^6 m^3$)	$\sum\Delta B_s$ ($10^6 m^3$)	ΔB_n ($10^6 m^3$)	$\sum B_n$ ($10^6 m^3$)
1350	1400	1375	2,4	2,4	1658	-1703	-44	4,0	4	-4,1	-4	-0,1	0
1300	1350	1325	5,5	7,9	1615	-2075	-459	8,8	13	-11,3	-16	-2,5	-3
1250	1300	1275	4,5	12,4	1594	-2444	-850	7,2	20	-11,0	-27	-3,8	-7
1200	1250	1225	6,5	18,9	1575	-2717	-1142	10,2	30	-17,6	-44	-7,4	-14
1150	1200	1175	9,3	28,2	1559	-2952	-1392	14,4	45	-27,3	-71	-12,9	-27
1100	1150	1125	12,3	40,5	1544	-3119	-1575	18,9	64	-38,2	-110	-19,3	-46
1050	1100	1075	14,2	54,7	1513	-3442	-1929	21,4	85	-48,8	-158	-27,3	-73
1000	1050	1025	12,1	66,8	1425	-3949	-2524	17,2	102	-47,8	-206	-30,5	-104
950	1000	975	7,6	74,4	1298	-4455	-3156	9,9	112	-33,9	-240	-24,0	-128
900	950	925	5,3	79,7	1197	-4751	-3554	6,4	119	-25,3	-265	-18,9	-147
850	900	875	5,6	85,3	1121	-5049	-3927	6,2	125	-28,0	-293	-21,8	-169
800	850	825	5,7	91,0	1065	-5508	-4443	6,2	131	-32,2	-326	-26,0	-195
750	800	775	5,1	96,1	1083	-5928	-4844	5,6	137	-30,4	-356	-24,9	-219
700	750	725	3,6	99,7	1063	-6283	-5219	3,8	140	-22,4	-378	-18,6	-238
650	700	675	2,8	102,5	1051	-6317	-5265	3,0	143	-17,8	-396	-14,8	-253
600	650	625	0,8	103,3	1027	-6533	-5505	0,8	144	-5,0	-401	-4,2	-257

Vestari Skaftárketill

Elevation (m a.s.l.)			ΔS (km^2)	$\Sigma\Delta S$ (km^2)	b_w (mm)	b_s (mm)	b_n (mm)	ΔB_w (10^6m^3)	$\Sigma\Delta B_w$ (10^6m^3)	ΔB_s (10^6m^3)	$\Sigma\Delta B_s$ (10^6m^3)	ΔB_n (10^6m^3)	ΣB_n (10^6m^3)
1900	1950	1925	0,7	0,7	2055	26	2082	1,4	1	0,0	0	1,4	1
1850	1900	1875	0,6	1,3	2030	-63	1967	1,2	3	0,0	0	1,1	3
1800	1850	1825	0,7	2,0	2004	-178	1826	1,5	4	-0,1	0	1,4	4
1750	1800	1775	2,7	4,7	1940	-380	1559	5,2	9	-1,0	-1	4,2	8
1700	1750	1725	5,9	10,6	1846	-415	1430	10,8	20	-2,4	-4	8,4	17
1650	1700	1675	6,7	17,3	1741	-440	1300	11,6	32	-2,9	-7	8,6	25
1600	1650	1625	7,4	24,7	1667	-543	1124	12,4	44	-4,0	-11	8,3	34
1550	1600	1575	5,2	29,9	1558	-687	870	8,0	52	-3,5	-14	4,5	38
1500	1550	1525	1,5	31,4	1525	-719	806	2,2	54	-1,1	-15	1,2	39

Eystri Skaftárketill

Elevation (m a.s.l.)			ΔS (km^2)	$\Sigma\Delta S$ (km^2)	b_w (mm)	b_s (mm)	b_n (mm)	ΔB_w (10^6m^3)	$\Sigma\Delta B_w$ (10^6m^3)	ΔB_s (10^6m^3)	$\Sigma\Delta B_s$ (10^6m^3)	ΔB_n (10^6m^3)	ΣB_n (10^6m^3)
1750	1800	1775	1,1	1,1	1924	-412	1511	2,1	2	-0,5	-1	1,7	2
1700	1750	1725	11,1	12,2	1863	-421	1441	20,8	23	-4,7	-5	16,1	18
1650	1700	1675	16,2	28,4	1839	-456	1382	29,8	53	-7,4	-13	22,4	40
1600	1650	1625	9,2	37,6	1802	-501	1301	16,7	69	-4,6	-17	12,0	52
1550	1600	1575	2,2	39,8	1800	-508	1291	4,0	73	-1,1	-18	2,9	55

Gjálp

Elevation (m a.s.l.)			ΔS (km^2)	$\Sigma\Delta S$ (km^2)	b_w (mm)	b_s (mm)	b_n (mm)	ΔB_w (10^6m^3)	$\Sigma\Delta B_w$ (10^6m^3)	ΔB_s (10^6m^3)	$\Sigma\Delta B_s$ (10^6m^3)	ΔB_n (10^6m^3)	ΣB_n (10^6m^3)
1900	1950	1925	0,5	0,5	2060	39	2099	1,1	1	0,0	0	1,2	1
1850	1900	1875	0,6	1,1	2024	-112	1912	1,3	2	0,0	0	1,2	2
1800	1850	1825	1,2	2,3	1991	-276	1714	2,3	5	-0,3	0	2,0	4
1750	1800	1775	4,5	6,8	1934	-403	1531	8,8	14	-1,8	-2	7,0	11
1700	1750	1725	15,9	22,7	1892	-439	1452	30,2	44	-7,0	-9	23,2	34
1650	1700	1675	16,5	39,2	1888	-456	1431	31,2	75	-7,5	-17	23,6	58
1600	1650	1625	0,0	39,2	1887	-452	1435	0,0	75	0,0	-17	0,0	58

Grímsvötn

Elevation (m a.s.l.)			ΔS (km^2)	$\Sigma\Delta S$ (km^2)	b_w (mm)	b_s (mm)	b_n (mm)	ΔB_w (10^6m^3)	$\Sigma\Delta B_w$ (10^6m^3)	ΔB_s (10^6m^3)	$\Sigma\Delta B_s$ (10^6m^3)	ΔB_n (10^6m^3)	ΣB_n (10^6m^3)
1700	1750	1725	0,8	0,8	1893	-510	1382	1,6	2	-0,4	0	1,1	1
1650	1700	1675	40,8	41,6	1898	-520	1377	77,5	79	-21,2	-22	56,3	57
1600	1650	1625	30,6	72,2	1890	-642	1247	57,9	137	-19,7	-41	38,2	96
1550	1600	1575	18,6	90,8	1888	-789	1098	35,2	172	-14,7	-56	20,5	116
1500	1550	1525	16,9	107,7	1874	-1133	741	31,6	204	-19,1	-75	12,5	129
1450	1500	1475	11,6	119,3	1868	-1655	212	21,6	225	-19,2	-94	2,5	131
1400	1450	1425	15,1	134,4	1856	-2009	-153	28,0	253	-30,3	-125	-2,3	129
1350	1400	1375	0,6	135,0	1856	-1797	59	1,2	255	-1,2	-126	0,0	129

Appendix C: Coordinates at velocity measurement stakes in 2014.

Position of velocity measurement stakes determined by GPS sub-metre differential (I), fast static (FS) and kinematic (K).
(Accuracy of horizontal position 0.5 – 1.0 m, and vertical accuracy 1-2 m for DGPS, about 1cm for fast static, and 3 cm for kinematic).
The station Hofn in Höfn í Hornafirði is used as a stationary reference for all measurements, ÍSN93 datum, h_l is elevation above ellipsoid, dL antenna height, N estimated difference between ellipsoid and sea-level, H elevation in metres above sea level (H= h_l+N+dL). X and Y are ÍSN93 Lambert conformal conic projected coordinates. M is a quality marker.

Site	time	Date	#	Calender Day	Year	Latitude		Longitude		h_l (m a. e.)	dL (m)	N (m)	H (m a. s. l.)	X	Y	M
B07t	17,521	7	5	127	2014	64	25,79280	16	17,45220	1424,7	0,0	-67,1	1357,7	630477,42	439239,18	K
B07t	15,155	11	10	284	2014	64	25,79212	16	17,45132	1420,6	0,0	-67,1	1353,5	630478,24	439237,62	K
B09u	15,639	6	5	126	2014	64	45,03960	16	5,47380	814,6	0,0	-66,7	747,9	638441,10	475389,05	Kfl
B09u	16,567	12	10	285	2014	64	45,04006	16	5,47351	810,2	-1,6	-66,7	741,9	638441,35	475389,62	FS
B10u	14,905	6	5	126	2014	64	43,68720	16	6,69900	870,6	0,0	-66,7	803,9	637584,82	472833,65	K
B10u	18,117	12	10	285	2014	64	43,68718	16	6,69861	865,9	-1,6	-66,7	797,6	637585,04	472834,03	FS
B11d	13,193	6	5	126	2014	64	40,95780	16	10,46760	1026,6	0,0	-66,8	959,8	634821,55	467633,01	K
B11d	17,250	12	10	285	2014	64	40,96103	16	10,46496	1023,8	-1,7	-66,8	955,2	634823,25	467638,76	FS
B12t	12,524	6	5	126	2014	64	38,27580	16	14,13180	1144,1	0,0	-66,9	1077,2	632127,27	462525,57	Kfl
B12t	16,500	12	10	285	2014	64	38,28484	16	14,12261	1141,3	-1,1	-66,9	1073,3	632133,75	462542,55	*
B13t	10,897	6	5	126	2014	64	34,51800	16	19,73220	1282,5	0,0	-67,0	1215,5	627963,88	455357,47	K
B13t	12,414	12	10	285	2014	64	34,52768	16	19,72022	1278,9	0,0	-67,0	1211,9	627972,43	455376,27	K
B14v	19,867	5	5	125	2014	64	31,63980	16	24,70500	1382,8	-0,4	-67,1	1315,3	624214,51	449849,52	K
B14v	11,667	12	10	285	2014	64	31,64795	16	24,69063	1381,1	-2,1	-67,1	1311,8	624225,17	449865,14	FS
B15i	18,500	5	5	125	2014	64	28,48738	16	30,01617	1467,4	-0,4	-67,2	1399,8	620199,91	443825,98	K
B15i	10,350	12	10	285	2014	64	28,49211	16	30,00414	1465,1	-2,3	-67,2	1395,7	620209,20	443835,14	FS
B16t	19,275	5	5	125	2014	64	24,12540	16	40,85340	1593,5	0,0	-67,3	1526,2	611816,21	435396,06	K
B16t	16,525	16	10	289	2014	64	24,12575	16	40,85200	1591,8	-2,1	-67,3	1522,4	611817,14	435396,54	FS
B17t	9,533	6	5	126	2014	64	36,73380	16	28,79160	1280,0	0,0	-67,1	1212,8	620570,24	459175,05	K
B17t	13,233	12	10	285	2014	64	36,74155	16	28,78631	1279,3	-1,9	-67,1	1210,3	620573,79	459189,15	FS
B18r	15,333	6	5	126	2014	64	31,58700	16	0,12420	1380,3	-0,4	-66,9	1313,0	643866,52	450620,59	K
B18r	14,926	11	10	284	2014	64	31,59250	16	0,12692	1375,7	0,0	-66,9	1308,7	643863,78	450630,29	K
B19r	11,567	7	5	127	2014	64	27,93300	15	55,16399	1499,3	-1,6	-66,9	1430,8	648161,09	444029,40	K
B19r	13,877	11	10	284	2014	64	27,93226	15	55,16273	1492,9	0,0	-66,9	1426,1	648162,34	444028,53	K
BB0s	14,383	7	5	127	2014	64	22,71840	16	5,05080	1586,4	0,0	-66,9	1519,6	640688,87	433975,41	Kfl
BB0s	13,298	11	10	284	2014	64	22,71830	16	5,05199	1582,0	0,0	-66,9	1515,1	640687,73	433975,33	K
BB-ce	11,596	11	9	254	2014	64	38,41438	17	26,79177	1968,1	-0,5	-67,9	1899,8	574257,61	460805,96	FS
Borai	20,426	4	6	155	2014	64	24,93840	17	20,15760	1467,6	0,0	-67,7	1399,9	580200,60	435910,95	K
Borai	16,484	15	10	288	2014	64	24,93469	17	20,16052	1480,7	0,0	-67,7	1413,0	580198,61	435903,85	K
BORTHNb	18,216	4	5	124	2014	64	25,08660	17	19,15380	1468,4	0,0	-67,7	1400,7	580999,71	436207,75	K
BORTHNb	11,857	15	10	288	2014	64	25,08265	17	19,15470	1487,2	0,0	-67,7	1419,5	580999,06	436200,03	K
Br1j	11,525	6	9	249	2014	64	5,55700	16	19,49969	159,0	-0,4	-65,8	92,8	630425,43	401603,99	FS
BR2k	20,783	7	5	127	2014	64	6,39062	16	22,54260	298,9	-0,9	-66,0	232,0	627889,85	403048,42	K
Br2k	13,537	6	9	249	2014	64	6,38854	16	22,54113	291,2	-0,4	-66,0	224,8	627891,22	403044,12	FS
Br3p	19,617	7	5	127	2014	64	8,50860	16	24,10440	468,5	-0,8	-66,3	401,4	626460,43	406927,68	K
Br4d	19,100	7	5	127	2014	64	10,73322	16	20,23772	593,8	0,0	-66,4	527,5	629421,07	411187,78	K
Br7r	19,226	7	5	127	2014	64	22,14720	16	16,93860	1313,7	0,0	-67,0	1246,7	631180,79	432489,72	K
Br7r	14,115	11	10	284	2014	64	22,12361	16	16,93234	1308,6	0,0	-67,0	1241,6	631187,51	432445,72	K
Brus	16,772	6	5	126	2014	64	41,00040	15	55,22340	838,9	0,0	-66,7	772,2	646931,54	468278,08	K
Brus	18,741	11	10	284	2014	64	41,00124	15	55,22421	832,1	0,0	-66,7	765,4	646930,67	468279,44	K
Buds	18,150	6	5	126	2014	64	35,99100	15	59,89020	1203,0	0,0	-66,9	1136,2	643664,98	458802,64	K
Buds	18,189	11	10	284	2014	64	36,00009	15	59,88879	1198,7	0,0	-66,9	1131,9	643665,36	458819,39	K

D05r	13,848	5	5	125	2014	64	42,23460	16	54,66240	1269,0	0,0	-67,4	1201,7	599612,06	468636,99	K
D05r	16,212	13	10	286	2014	64	42,24137	16	54,65046	1265,8	0,0	-67,4	1198,4	599621,05	468650,33	K
D07r	14,600	5	5	125	2014	64	38,28480	16	59,25600	1438,9	0,0	-67,5	1371,4	596195,96	461184,33	Kfl
D07r	16,711	13	10	286	2014	64	38,29679	16	59,24415	1435,0	0,0	-67,5	1367,5	596204,78	461206,56	K
D09q	15,846	5	5	125	2014	64	31,79820	17	0,55320	1648,7	0,0	-67,6	1581,2	595542,35	449105,71	K
D09q	16,246	13	10	286	2014	64	31,80203	17	0,55457	1645,8	0,0	-67,6	1578,2	595541,07	449112,26	K
D12r	16,725	5	5	125	2014	64	28,98360	17	0,14040	1714,3	0,0	-67,6	1646,8	596037,69	443888,25	K
D12r	20,343	13	10	286	2014	64	28,98386	17	0,14026	1711,3	0,0	-67,6	1643,8	596037,79	443889,17	K
E01s	11,873	7	5	127	2014	64	41,45460	15	33,50280	747,7	0,0	-66,7	681,0	664140,94	470011,48	K
E01s	17,901	11	10	284	2014	64	41,45509	15	33,50381	740,2	0,0	-66,7	673,5	664140,32	470012,24	K
E02s	10,984	7	5	127	2014	64	39,13020	15	35,97720	1022,0	0,0	-66,8	955,3	662408,45	465592,71	K
E02s	17,597	11	10	284	2014	64	39,13902	15	35,97278	1016,3	0,0	-66,8	949,5	662411,05	465609,00	K
E03t	10,251	7	5	127	2014	64	36,66720	15	36,90900	1255,3	0,0	-66,9	1188,4	661912,48	460983,31	K
E03t	17,340	11	10	284	2014	64	36,67198	15	36,91154	1250,0	0,0	-66,9	1183,1	661909,79	460991,72	K
E04s	17,917	6	5	126	2014	64	34,95203	15	37,10630	1355,7	-0,4	-66,8	1288,5	661925,52	457792,32	K
E04s	15,504	11	10	284	2014	64	34,95291	15	37,10597	1351,0	0,0	-66,8	1284,2	661925,71	457793,96	K
Fl01e	12,783	7	5	127	2014	64	26,16060	15	55,62780	1415,4	-1,3	-66,8	1347,3	647949,82	440722,33	K
Fl01e	14,487	11	10	284	2014	64	26,15460	15	55,61375	1408,5	0,0	-66,8	1341,7	647961,59	440711,96	K
G02k	21,723	2	6	153	2014	64	26,84520	17	17,74800	1627,8	0,0	-67,7	1560,1	582040,56	439503,91	K
G02k	15,637	15	10	288	2014	64	26,84220	17	17,75045	1625,5	0,0	-67,7	1557,8	582038,57	439498,29	K
G03l	20,577	2	6	153	2014	64	28,44480	17	16,34700	1723,0	0,0	-67,7	1655,3	583083,02	442505,21	K
G03l	15,369	15	10	288	2014	64	28,44344	17	16,34757	1720,6	0,0	-67,7	1652,8	583082,58	442502,82	K
G04s	12,666	2	6	153	2014	64	30,01560	17	15,02520	1752,5	0,0	-67,7	1684,8	584061,27	445451,41	K
G04s	14,982	15	10	288	2014	64	30,01582	17	15,02524	1750,1	0,0	-67,7	1682,4	584061,38	445452,33	K
gb2d	13,917	6	5	126	2014	64	34,10880	16	0,02568	1268,8	-0,4	-66,9	1201,5	643722,97	455304,21	K
gb2d	17,751	11	10	284	2014	64	34,11637	16	0,02680	1264,2	0,0	-66,9	1197,3	643721,37	455318,15	K
Go1r	19,280	2	6	153	2014	64	34,01400	17	24,92040	1825,9	0,0	-67,8	1758,1	575953,19	452669,25	K
Go1r	14,601	15	10	288	2014	64	34,01311	17	24,91952	1823,1	0,0	-67,8	1755,3	575953,86	452668,00	K
GvK4-1b	11,187	6	6	157	2014	64	27,56340	17	20,40360	1663,3	0,0	-67,8	1595,6	579875,33	440781,56	K
GvK4-1b	16,484	15	10	288	2014	64	27,56082	17	20,40539	1660,1	0,0	-67,8	1592,4	579873,86	440776,35	K
GvK4-2b	11,101	6	6	157	2014	64	27,35880	17	20,31840	1642,3	0,0	-67,8	1574,5	579953,32	440402,63	K
GvK4-2b	16,409	15	10	288	2014	64	27,35459	17	20,31960	1638,5	0,0	-67,8	1570,8	579952,71	440395,11	K
GvK4-3b	11,258	6	6	157	2014	64	27,27780	17	20,34540	1624,7	0,0	-67,8	1556,9	579935,85	440252,14	K
GvK4-3b	16,300	15	10	288	2014	64	27,27310	17	20,34519	1618,4	0,0	-67,8	1550,6	579936,16	440243,21	K
Gvk4-4b	10,957	6	6	157	2014	64	27,18660	17	20,37060	1598,1	0,0	-67,8	1530,3	579919,85	440082,07	K
Gvk4-4b	16,266	15	10	288	2014	64	27,18291	17	20,36995	1591,8	0,0	-67,8	1524,1	579920,71	440075,19	K
Gvk4-5b	10,873	6	6	157	2014	64	27,09780	17	20,49960	1595,3	0,0	-67,8	1527,5	579820,97	439914,20	K
Gvk4-5b	16,187	15	10	288	2014	64	27,09560	17	20,50083	1592,6	0,0	-67,8	1524,8	579820,00	439910,25	K
GvK4-6b	10,801	6	6	157	2014	64	27,01620	17	20,59740	1587,7	0,0	-67,8	1519,9	579746,53	439761,11	K
GvK4-6b	16,123	15	10	288	2014	64	27,01475	17	20,59810	1584,5	0,0	-67,8	1516,7	579745,92	439758,04	K
GvK4-7b	10,729	6	6	157	2014	64	26,86620	17	20,78940	1577,0	0,0	-67,8	1509,3	579599,60	439478,25	K
GvK4-7b	15,983	15	10	288	2014	64	26,86513	17	20,79116	1574,1	0,0	-67,8	1506,3	579598,35	439476,09	K
GvK4-8b	11,340	6	6	157	2014	64	27,20760	17	20,58300	1620,1	0,0	-67,8	1552,3	579748,48	440116,75	K
GvK4-8b	16,657	15	10	288	2014	64	27,20429	17	20,57881	1615,6	0,0	-67,8	1547,9	579752,17	440110,50	K
GvK4-9b	11,014	6	6	157	2014	64	27,16560	17	20,13420	1610,6	0,0	-67,8	1542,8	580110,60	440047,85	K
GvK4-9b	16,579	15	10	288	2014	64	27,16303	17	20,13951	1605,8	0,0	-67,8	1538,0	580106,49	440043,11	K
HAABn	11,351	9	6	160	2014	64	20,95200	17	24,08340	1796,8	0,0	-67,5	1729,3	577235,16	428425,10	K
HAABn	11,880	14	10	287	2014	64	20,95213	17	24,08359	1792,5	0,0	-67,5	1724,9	577235,09	428425,30	K
Hof01l	19,918	6	5	126	2014	64	32,32740	15	35,84400	1207,8	0,0	-66,7	1141,1	663194,30	452977,08	K
Hof01l	15,796	11	10	284	2014	64	32,32096	15	35,84401	1202,9	0,0	-66,7	1136,2	663194,96	452964,93	K
K01u	10,462	5	5	125	2014	64	35,16540	17	51,79740	1128,9	0,0	-67,6	1061,3	554447,06	454346,92	K
K01u	13,352	15	10	288	2014	64	35,16715	17	51,80342	1123,1	0,0	-67,6	1055,6	554442,21	454349,61	K
K02v	10,862	5	5	125	2014	64	34,81740	17	49,68540	1245,7	0,0	-67,6	1178,1	556144,75	453730,95	K
K02v	13,069	15	10	288	2014	64	34,81944	17	49,69619	1240,5	0,0	-67,6	1172,9	556136,22	453734,40	K
K03u	11,339	5	5	125	2014	64	34,24740	17	46,38180	1364,5	0,0	-67,7	1296,9	558803,07	452721,91	K
K03u	12,808	15	10	288	2014	64	34,24972	17	46,39623	1359,9	0,0	-67,7	1292,2	558791,39	452726,03	K
K04v	11,940	5	5	125	2014	64	33,20940	17	42,25080	1555,2	0,0	-67,7	1487,5	562141,54	450859,78	K
K04v	13,762	15	10	288	2014	64	33,21268	17	42,27313	1550,7	0,0	-67,7	1483,0	562123,78	450865,33	K
K05v	12,884	5	5	125	2014	64	33,45060	17	35,42820	1749,0	0,0	-67,8	1681,1	567583,78	451424,35	K
K05v	9,576	16	10	289	2014	64	33,44815	17	35,44223	1746,6	0,0	-67,8	1678,8	567572,80	451419,51	FS
K06u	17,197	2	6	153	2014	64	38,35800	17	31,36440	2035,4	0,0	-67,9	1967,5	570617,59	460613,66	K
K06u	13,226	11	9	254	2014	64	38,35588	17	31,35669	2029,3	-0,5	-67,9	1961,0	570624,03	460610,11	FS
K07q	9,657	5	5	125	2014	64	29,11320	17	42,01380	1601,4	0,0	-67,7	1533,7	562487,46	443254,25	K
K07q	10,776	16	10	289	2014	64	29,11324	17	42,01535	1599,3	0,0	-67,7	1531,6	562486,37	443254,42	FS

Ln1-1b	10,343	9	6	160	2014	64	24,50340	17	12,99780	1565,9	0,0	-67,6	1498,2	585973,23	435259,70	K
Ln1-1b	17,490	15	10	288	2014	64	24,50266	17	12,99921	1563,4	0,0	-67,6	1495,8	585972,28	435258,30	K
Ln1-2b	10,482	9	6	160	2014	64	24,74580	17	12,01260	1590,0	0,0	-67,6	1522,4	586752,07	435732,62	K
Ln1-2b	19,594	13	10	286	2014	64	24,74321	17	12,01283	1587,0	0,0	-67,6	1519,4	586751,87	435727,52	K
Ln1-3b	10,580	9	6	160	2014	64	24,99540	17	10,99920	1596,2	0,0	-67,6	1528,6	587552,71	436219,29	K
Ln1-3b	19,436	13	10	286	2014	64	24,99248	17	11,00038	1593,5	0,0	-67,6	1525,8	587551,70	436213,75	K
Ln1-4b	10,687	9	6	160	2014	64	25,24200	17	10,00380	1622,3	0,0	-67,6	1554,7	588338,65	436700,08	K
Ln1-4b	19,364	13	10	286	2014	64	25,23877	17	10,00623	1619,4	0,0	-67,6	1551,8	588336,74	436694,20	K
Ln1-5b	10,776	9	6	160	2014	64	25,74360	17	7,99260	1662,6	0,0	-67,6	1595,0	589925,75	437679,36	K
Ln1-5b	19,198	13	10	286	2014	64	25,74004	17	7,99259	1659,8	0,0	-67,6	1592,2	589925,94	437672,48	K
S01j	13,222	4	5	124	2014	64	7,01160	17	49,98900	807,2	0,0	-66,8	740,4	556856,18	402071,88	K
S01j	16,526	14	10	287	2014	64	7,01156	17	49,98929	801,4	0,0	-66,8	734,6	556855,82	402071,51	K
S02m	14,164	4	5	124	2014	64	12,16380	17	48,96600	1076,8	0,0	-67,1	1009,8	557507,33	411658,02	K
S02m	15,839	14	10	287	2014	64	12,15444	17	48,96938	1071,2	0,0	-67,0	1004,1	557505,07	411640,90	K
S04n	14,908	4	5	124	2014	64	16,19760	17	48,21720	1226,9	0,0	-67,2	1159,6	557971,91	419163,50	K
S04n	15,355	14	10	287	2014	64	16,18609	17	48,22823	1222,1	0,0	-67,2	1154,9	557963,28	419141,74	K
Skf01e	16,050	7	5	127	2014	64	17,98920	16	5,00280	1349,8	0,0	-66,6	1283,2	641132,43	425199,50	Kfl
Skf01e	12,593	11	10	284	2014	64	17,98672	16	4,98864	1344,5	0,0	-66,6	1277,9	641144,12	425195,74	K
T01no	8,414	4	5	124	2014	64	19,48560	18	8,23440	810,9	0,0	-67,3	743,7	541723,91	425008,12	K
T01no	14,372	14	10	287	2014	64	19,48500	18	8,23393	803,2	0,0	-67,3	735,9	541724,11	425007,48	K
T02nq	9,121	4	5	124	2014	64	19,59960	18	3,96840	1008,2	0,0	-67,3	940,9	545158,58	425268,98	K
T02nq	13,907	14	10	287	2014	64	19,59948	18	3,97362	1001,6	0,0	-67,3	934,3	545154,60	425268,94	K
T03nq	10,365	4	5	124	2014	64	20,21040	17	58,60020	1143,4	0,0	-67,3	1076,1	549466,59	426471,01	K
T03nq	14,957	14	10	287	2014	64	20,20893	17	58,60909	1138,3	0,0	-67,3	1071,0	549459,46	426468,08	K
T04nq	11,537	4	5	124	2014	64	21,33900	17	51,52680	1289,5	0,0	-67,4	1222,1	555126,86	428665,03	K
T04nq	13,290	14	10	287	2014	64	21,33607	17	51,53710	1284,3	0,0	-67,4	1216,9	555118,61	428659,51	K
T05nq	12,350	4	5	124	2014	64	22,28700	17	43,01220	1411,8	-0,8	-67,5	1343,5	561945,00	430557,75	K
T05nq	17,582	14	10	287	2014	64	22,28416	17	43,02259	1406,9	0,0	-67,5	1339,4	561936,90	430552,13	K
T05rorf	12,350	4	5	124	2014	64	22,28700	17	43,01220	1411,8	0,4	-67,5	1343,9	561945,00	430557,75	K
T05rorf	17,582	14	10	287	2014	64	22,28416	17	43,02259	1406,9	4,0	-67,5	1343,4	561936,90	430552,13	K
T06nq	16,162	4	5	124	2014	64	24,28140	17	36,53760	1532,8	0,0	-67,6	1465,2	567072,20	434372,07	K
T06nq	18,591	14	10	287	2014	64	24,27746	17	36,54803	1528,9	0,0	-67,6	1461,3	567064,12	434364,95	K
T07np	16,958	4	5	124	2014	64	25,29060	17	31,20000	1630,3	0,0	-67,7	1562,6	571317,11	436344,43	K
T07np	19,933	14	10	287	2014	64	25,28847	17	31,20834	1626,6	0,0	-67,7	1558,9	571310,50	436340,33	K
T08nq	17,604	4	5	124	2014	64	26,31300	17	27,77940	1703,7	0,0	-67,8	1635,9	574017,31	438309,42	K
T08nq	20,522	14	10	287	2014	64	26,31298	17	27,78163	1700,6	0,0	-67,8	1632,8	574015,76	438308,96	K

Appendix D: Measured surface velocity on Vatnajökull in 2014.

Site	Calendar day date	#	Calendar day date	#	# of days	translation (m)	(°)	velocity (cm/day)	(m/annum)
B07t	140507	127	141011	284	157	1,44	151	0,92	3,36
B09u	140506	126	141012	285	159	0,88	15	0,55	2,03
B10u	140506	126	141012	285	159	0,31	97	0,2	0,72
B11d	140506	126	141012	285	159	6,34	19	3,99	14,55
B12t	140506	126	141012	285	159	18,27	24	11,49	41,95
B13t	140506	126	141012	285	159	20,32	28	12,78	46,64
B14v	140505	125	141012	285	160	18,97	37	11,86	43,28
B15i	140505	125	141012	285	160	13,03	48	8,14	29,71
B16t	140505	125	141016	289	164	1,3	60	0,79	2,89
B17t	140506	126	141012	285	159	14,96	16	9,41	34,34
B18r	140506	126	141011	284	158	10,42	348	6,59	24,06
B19r	140507	127	141011	284	157	1,7	144	1,08	3,96
BB0s	140507	127	141011	284	157	0,97	259	0,62	2,27
Borai	140604	155	141015	288	133	7,26	199	5,46	19,92
BORTHNb	131006	279	140504	124	210	13,47	188	6,42	23,42
BORTHNb	140504	124	141015	288	164	7,35	186	4,48	16,36
BR2k	130131	31	140507	127	461	13,63	164	2,96	10,79
Br3p	130131	31	140507	127	461	26,99	150	5,85	21,37
Br4d	130130	30	140507	127	462	372,71	180	80,67	294,45
Br7r	140507	127	141011	284	157	43,98	173	28,01	102,24
Brus	140506	126	141011	284	158	1,68	338	1,07	3,89
Buds	140506	126	141011	284	158	16,87	4	10,68	38,98
D05r	140505	125	141013	286	161	15,72	37	9,77	35,64
D07r	140505	125	141013	286	161	24,13	23	14,99	54,7
D09q	140505	125	141013	286	161	7,18	351	4,46	16,27
D12r	140505	125	141013	286	161	0,49	13	0,31	1,12
E01s	140507	127	141011	284	157	1,21	318	0,77	2,82
E02s	140507	127	141011	284	157	16,71	12	10,64	38,85
E03t	140507	127	141011	284	157	9,08	347	5,78	21,11
E04s	140506	126	141011	284	158	1,65	9	1,04	3,81
Fl01e	140507	127	141011	284	157	15,83	135	10,08	36,8
G02k	140602	153	141015	288	135	5,89	199	4,37	15,93
G03l	140602	153	141015	288	135	2,56	190	1,9	6,92
G04s	140602	153	141015	288	135	0,41	356	0,3	1,1
gb2d	140506	126	141011	284	158	14,05	356	8,89	32,45
Go1r	140602	153	141015	288	135	1,79	157	1,33	4,84
GvK4-1b	140606	157	141015	288	131	4,99	197	3,81	13,9
GvK4-2b	140606	157	141015	288	131	7,86	187	6	21,89
GvK4-3b	140606	157	141015	288	131	8,71	179	6,65	24,26
Gvk4-4b	140606	157	141015	288	131	6,85	176	5,23	19,1
Gvk4-5b	140606	157	141015	288	131	4,19	194	3,2	11,68
GvK4-6b	140606	157	141015	288	131	2,74	192	2,09	7,64
GvK4-7b	140606	157	141015	288	131	2,43	215	1,86	6,78
GvK4-8b	140606	157	141015	288	131	6,99	151	5,34	19,48
GvK4-9b	140606	157	141015	288	131	6,39	222	4,88	17,79
HAABn	140609	160	141014	287	127	0,29	328	0,22	0,82
Hof01l	140506	126	141011	284	158	11,93	180	7,55	27,55

K01u	140505	125	141015	288	163	5,8	304	3,56	12,98
K02v	140505	125	141015	288	163	9,4	294	5,77	21,06
K03u	140505	125	141015	288	163	12,3	290	7,54	27,54
K04v	140505	125	141015	288	163	18,85	289	11,56	42,2
K05v	140505	125	141016	289	164	12,09	248	7,37	26,91
K06u	140602	153	140911	254	101	7,29	123	7,22	26,34
K07q	140505	125	141016	289	164	1,24	273	0,76	2,77
Ln1-1b	140609	160	141015	288	128	1,78	220	1,39	5,07
Ln1-2b	140609	160	141013	286	126	4,8	182	3,81	13,91
Ln1-3b	140609	160	141013	286	126	5,49	190	4,36	15,9
Ln1-4b	140609	160	141013	286	126	6,29	198	4,99	18,23
Ln1-5b	140609	160	141013	286	126	6,59	180	5,23	19,1
S01j	140504	124	141014	287	163	0,25	253	0,15	0,55
S02m	140504	124	141014	287	163	17,55	189	10,77	39,3
S04n	140504	124	141014	287	163	23,1	203	14,17	51,73
Skf01e	140507	127	141011	284	157	12,31	112	7,84	28,61
T01no	140504	124	141014	287	163	1,17	161	0,72	2,63
T02nq	140504	124	141014	287	163	4,21	267	2,58	9,43
T03nq	140504	124	141014	287	163	7,66	249	4,7	17,15
T04nq	140504	124	141014	287	163	9,91	237	6,08	22,19
T05nq	140504	124	141014	287	163	9,87	238	6,06	22,11
T05rorf	131005	278	140504	124	211	10,31	237	4,89	17,84
T05rorf	140504	124	141014	287	163	9,87	238	6,06	22,11
T06nq	140504	124	141014	287	163	11,11	229	6,82	24,88
T07np	140504	124	141014	287	163	7,77	239	4,77	17,4
T08nq	140504	124	141014	287	163	1,79	269	1,1	4,01

Appendix E: Melt water runoff to selected rivers in summer 2014, derived from summer balance.

ΔS: area in a given elevation range where summer balance is negative, **∑ΔS**: cumulative area above a given elevation, **ΔQ_s**: melt water runoff from a given elevation range, **$\sum\Delta Q_s$** : cumulative melt water runoff from an area above given elevation.

Tungnaá water drainage basin

Elevation (m a. s. l.)		ΔS km^2	∑ΔS km^2	ΔQ_s ($10^6 m^3$)	$\sum\Delta Q_s$ ($10^6 m^3$)
1350	1400	0,6	0,6	1,1	1,1
1300	1350	6,2	6,8	13,8	14,9
1250	1300	10,7	17,4	27,5	42,4
1200	1250	11,4	28,9	31,8	74,3
1150	1200	10,8	39,6	31,8	106,1
1100	1150	12,8	52,4	39,5	145,5
1050	1100	11,9	64,3	41,4	186,9
1000	1050	9,7	74,0	38,2	225,2
950	1000	10,8	84,8	47,6	272,8
900	950	9,0	93,7	44,0	316,8
850	900	8,3	102,0	44,9	361,7
800	850	8,6	110,6	50,4	412,2
750	800	6,3	116,9	39,7	451,9
700	750	4,2	121,0	27,1	478,9
650	700	0,5	121,6	3,6	482,5

Sylgja water drainage basin

Elevation (m a. s. l.)		ΔS km^2	∑ΔS km^2	ΔQ_s ($10^6 m^3$)	$\sum\Delta Q_s$ ($10^6 m^3$)
1300	1350	1,3	1,3	3,2	3,2
1250	1300	3,6	5,0	9,6	12,7
1200	1250	6,4	11,4	18,2	30,9
1150	1200	8,3	19,7	24,6	55,5
1100	1150	6,6	26,3	20,3	75,9
1050	1100	7,6	33,9	27,9	103,8
1000	1050	3,8	37,7	16,4	120,2
950	1000	1,5	39,2	6,9	127,0
900	950	0,6	39,8	2,8	129,8
850	900	0,0	39,8	0,1	129,9

Western Skaftá cauldron water drainage basin

Elevation (m a. s. l.)		ΔS km^2	∑ΔS km^2	ΔQ_s ($10^6 m^3$)	$\sum\Delta Q_s$ ($10^6 m^3$)
1700	1750	3,2	3,2	1,3	1,3
1650	1700	7,0	10,2	3,0	4,4
1600	1650	8,4	18,6	4,6	9,0
1550	1600	5,0	23,6	3,4	12,4
1500	1550	1,5	25,1	1,0	13,5

Eastern Skaftár cauldoron water drainage basin

Elevation (m a. s. l.)		ΔS km^2	∑ΔS km^2	ΔQ_s (10^6m^3)	$\sum\Delta Q_s$ (10^6m^3)
1750	1800	2,5	2,5	1,0	1,0
1700	1750	10,6	13,1	4,5	5,5
1650	1700	14,8	27,8	6,8	12,2
1600	1650	9,3	37,1	4,6	16,9
1550	1600	2,2	39,3	1,1	18,0

Grímsvötn water drainage basin

Elevation (m a. s. l.)		ΔS km^2	∑ΔS km^2	ΔQ_s (10^6m^3)	$\sum\Delta Q_s$ (10^6m^3)
1900	1950	0,1	0,1	0,0	0,0
1850	1900	1,3	1,4	0,1	0,1
1800	1850	1,6	3,1	0,4	0,5
1750	1800	3,9	7,0	1,6	2,0
1700	1750	15,9	22,9	7,0	9,1
1650	1700	56,4	79,2	28,4	37,4
1600	1650	30,9	110,1	19,8	57,3
1550	1600	18,7	128,8	14,7	72,0
1500	1550	16,7	145,5	18,9	90,9
1450	1500	11,6	157,1	19,2	110,1
1400	1450	15,1	172,1	30,3	140,4
1350	1400	0,6	172,8	1,2	141,5

Kaldakvísl water drainage basin

Elevation (m a. s. l.)		ΔS km^2	∑ΔS km^2	ΔQ_s (10^6m^3)	$\sum\Delta Q_s$ (10^6m^3)
1900	1950	1,7	1,7	0,0	0,0
1850	1900	6,3	8,0	0,7	0,8
1800	1850	6,4	14,4	1,5	2,2
1750	1800	11,7	26,1	3,8	6,1
1700	1750	21,1	47,2	8,8	14,9
1650	1700	16,7	63,9	8,3	23,2
1600	1650	14,2	78,1	9,9	33,1
1550	1600	19,4	97,4	18,4	51,5
1500	1550	27,2	124,7	29,6	81,1
1450	1500	28,5	153,2	36,5	117,5
1400	1450	23,1	176,3	36,7	154,2
1350	1400	21,6	197,9	44,3	198,5
1300	1350	21,3	219,2	54,0	252,5
1250	1300	22,6	241,8	65,9	318,4
1200	1250	22,6	264,4	72,0	390,4
1150	1200	20,2	284,6	69,8	460,2
1100	1150	18,3	302,8	70,4	530,6
1050	1100	17,2	320,0	74,0	604,7
1000	1050	14,9	334,9	71,2	675,9
950	1000	10,7	345,6	56,2	732,1
900	950	5,6	351,2	30,9	763,0
850	900	0,5	351,7	3,1	766,1

Jökulsá á Fjöllum water drainage basin

Elevation (m a. s. l.)		ΔS km^2	∑ΔS km^2	ΔQ_s $(10^6 m^3)$	$\sum\Delta Q_s$ $(10^6 m^3)$
1900	1950	2,2	2,2	0,0	0,0
1850	1900	18,4	20,6	3,1	3,2
1800	1850	14,6	35,2	3,6	6,8
1750	1800	22,3	57,5	8,0	14,8
1700	1750	34,2	91,7	14,7	29,5
1650	1700	79,5	171,2	39,2	68,7
1600	1650	116,5	287,7	62,9	131,6
1550	1600	100,9	388,7	67,3	198,9
1500	1550	97,8	486,5	77,4	276,3
1450	1500	85,7	572,1	78,5	354,8
1400	1450	74,3	646,4	78,7	433,4
1350	1400	60,2	706,6	73,4	506,8
1300	1350	49,1	755,7	68,2	575,1
1250	1300	52,5	808,2	83,1	658,2
1200	1250	57,4	865,6	106,1	764,3
1150	1200	54,5	920,1	121,7	886,0
1100	1150	45,9	966,1	119,8	1005,8
1050	1100	34,1	1000,2	100,0	1105,7
1000	1050	36,4	1036,5	119,5	1225,3
950	1000	31,5	1068,0	118,0	1343,2
900	950	26,2	1094,2	111,3	1454,5
850	900	25,4	1119,6	121,0	1575,5
800	850	20,2	1139,9	106,7	1682,2
750	800	15,2	1155,0	86,5	1768,7
700	750	1,7	1156,8	10,3	1779,0

Kreppa and Kverká water drainage basin

Elevation (m a. s. l.)		ΔS km^2	∑ΔS km^2	ΔQ_s ($10^6 m^3$)	$\sum\Delta Q_s$ ($10^6 m^3$)
1900	1950	0,0	0,0	0,0	0,0
1850	1900	1,0	1,1	0,2	0,2
1800	1850	4,3	5,3	0,4	0,6
1750	1800	2,8	8,1	0,6	1,1
1700	1750	3,6	11,8	1,3	2,5
1650	1700	5,0	16,8	2,1	4,6
1600	1650	37,9	54,6	18,9	23,5
1550	1600	22,6	77,3	12,6	36,1
1500	1550	14,3	91,5	9,1	45,2
1450	1500	15,4	107,0	11,6	56,8
1400	1450	19,3	126,3	17,9	74,8
1350	1400	25,2	151,5	27,9	102,6
1300	1350	20,5	172,0	25,8	128,4
1250	1300	16,4	188,4	22,6	151,0
1200	1250	18,1	206,4	28,1	179,1
1150	1200	18,2	224,6	33,4	212,5
1100	1150	17,5	242,1	39,8	252,3
1050	1100	11,6	253,7	31,5	283,9
1000	1050	14,1	267,8	42,2	326,1
950	1000	16,1	283,9	51,4	377,5
900	950	14,4	298,2	50,3	427,8
850	900	14,5	312,7	58,0	485,8
800	850	11,5	324,2	52,4	538,2
750	800	9,3	333,5	46,3	584,5
700	750	4,2	337,7	21,6	606,1
650	700	0,4	338,1	2,3	608,5

Hálslón water drainage basin

Elevation (m a. s. l.)		ΔS km^2	∑ΔS km^2	ΔQ_s ($10^6 m^3$)	$\sum\Delta Q_s$ ($10^6 m^3$)
1600	1650	8,3	8,3	4,6	4,6
1550	1600	30,4	38,7	19,2	23,8
1500	1550	60,6	99,3	41,8	65,6
1450	1500	63,6	162,9	48,7	114,3
1400	1450	95,6	258,5	88,0	202,3
1350	1400	124,5	383,0	138,0	340,4
1300	1350	133,2	516,2	167,3	507,7
1250	1300	128,3	644,5	184,7	692,4
1200	1250	102,8	747,3	169,8	862,2
1150	1200	87,3	834,6	171,0	1033,2
1100	1150	69,3	903,8	161,6	1194,8
1050	1100	61,8	965,7	168,8	1363,6
1000	1050	51,8	1017,4	156,5	1520,1
950	1000	43,4	1060,8	142,9	1663,0
900	950	34,6	1095,5	129,3	1792,3
850	900	30,4	1125,8	130,2	1922,5
800	850	29,9	1155,7	143,9	2066,4
750	800	26,8	1182,5	139,1	2205,4
700	750	19,6	1202,1	108,3	2313,7
650	700	12,3	1214,4	72,7	2386,5
600	650	0,3	1214,8	2,0	2388,5

Jökulsá á Fljótsdal water drainage basin

Elevation (m a. s. l.)		ΔS km^2	∑ΔS km^2	ΔQ_s ($10^6 m^3$)	$\sum \Delta Q_s$ ($10^6 m^3$)
1500	1550	0,0	0,0	0,0	0,0
1450	1500	0,9	1,0	0,8	0,9
1400	1450	1,9	2,9	1,8	2,6
1350	1400	2,8	5,8	2,9	5,6
1300	1350	5,2	11,0	5,8	11,4
1250	1300	15,8	26,8	21,5	32,9
1200	1250	15,9	42,7	25,7	58,5
1150	1200	17,6	60,3	33,4	91,9
1100	1150	15,1	75,4	34,1	126,1
1050	1100	12,7	88,1	34,7	160,7
1000	1050	11,9	100,0	38,4	199,1
950	1000	9,0	109,0	32,9	232,0
900	950	5,8	114,8	23,3	255,2
850	900	4,3	119,1	18,8	274,0
800	850	3,3	122,3	15,5	289,5
750	800	3,4	125,7	17,6	307,1
700	750	3,3	129,0	19,0	326,1
650	700	1,7	130,7	10,1	336,2

Hornafjarðarfljót water drainage basin

Elevation (m a. s. l.)		ΔS km^2	$\sum\Delta S$ km^2	ΔQ_s $(10^6 m^3)$	$\sum\Delta Q_s$ $(10^6 m^3)$
1450	1500	1,0	1,0	0,8	0,8
1400	1450	7,4	8,4	6,9	7,8
1350	1400	12,2	20,6	12,8	20,6
1300	1350	18,3	38,9	22,0	42,6
1250	1300	36,6	75,5	52,6	95,2
1200	1250	30,2	105,7	49,3	144,4
1150	1200	20,8	126,5	39,4	183,8
1100	1150	19,8	146,2	44,7	228,5
1050	1100	15,3	161,5	44,6	273,0
1000	1050	11,7	173,2	41,1	314,1
950	1000	11,1	184,2	45,0	359,2
900	950	8,2	192,4	36,7	395,8
850	900	5,5	198,0	26,2	422,0
800	850	4,4	202,4	21,9	443,9
750	800	4,1	206,5	21,5	465,3
700	750	4,0	210,5	21,7	487,0
650	700	3,5	213,9	19,9	506,9
600	650	2,6	216,5	15,6	522,6
550	600	2,0	218,5	12,8	535,3
500	550	1,8	220,4	11,9	547,3
450	500	1,4	221,8	9,5	556,8
400	450	1,3	223,0	8,8	565,6
350	400	0,8	223,8	5,6	571,2
300	350	1,1	225,0	8,1	579,4
250	300	2,3	227,3	17,5	596,9
200	250	3,5	230,8	27,1	623,9
150	200	2,7	233,5	22,4	646,3
100	150	2,1	235,6	19,1	665,5
50	100	2,8	238,4	26,9	692,3
0	50	0,6	239,0	5,6	697,9

Jökulsá á Breiðamerkursandi water drainage basin

Elevation (m a. s. l.)		ΔS km^2	∑ΔS km^2	$ΔQ_s$ $(10^6 m^3)$	$∑ΔQ_s$ $(10^6 m^3)$
1700	1750	0,8	0,8	0,4	0,4
1650	1700	4,0	4,9	2,2	2,6
1600	1650	12,9	17,8	7,5	10,2
1550	1600	19,1	36,8	13,3	23,5
1500	1550	23,0	59,8	18,6	42,1
1450	1500	35,2	95,0	32,2	74,3
1400	1450	49,6	144,6	53,5	127,8
1350	1400	83,3	227,9	107,2	235,0
1300	1350	85,4	313,2	135,1	370,1
1250	1300	53,1	366,4	105,3	475,4
1200	1250	35,1	401,5	85,6	560,9
1150	1200	28,9	430,3	83,1	644,0
1100	1150	24,6	454,9	79,2	723,2
1050	1100	20,7	475,6	72,6	795,8
1000	1050	17,8	493,4	67,4	863,2
950	1000	19,0	512,4	76,4	939,6
900	950	20,2	532,6	85,5	1025,1
850	900	20,5	553,2	92,8	1117,9
800	850	20,2	573,3	97,1	1215,0
750	800	19,5	592,9	101,7	1316,7
700	750	21,1	614,0	115,7	1432,3
650	700	26,7	640,6	149,9	1582,3
600	650	18,5	659,1	111,0	1693,2
550	600	18,5	677,7	118,0	1811,2
500	550	7,0	684,7	45,7	1856,9
450	500	7,7	692,3	52,4	1909,4
400	450	5,8	698,2	40,6	1950,0
350	400	5,5	703,6	38,7	1988,6
300	350	6,5	710,2	47,1	2035,7
250	300	6,0	716,1	45,5	2081,2
200	250	6,3	722,5	52,8	2134,0
150	200	5,1	727,6	46,1	2180,1
100	150	5,1	732,7	47,9	2228,1
50	100	4,1	736,8	39,7	2267,8
0	50	2,7	739,5	26,4	2294,2

Breiðárlón/Fjallsárlón water drainage basin

Elevation (m a. s. l.)		ΔS km^2	∑ΔS km^2	$ΔQ_s$ ($10^6 m^3$)	$∑ΔQ_s$ ($10^6 m^3$)
1750	1800	0,0	0,0	0,0	0,0
1700	1750	0,2	0,3	0,0	0,0
1650	1700	2,6	2,8	0,3	0,3
1600	1650	4,0	6,8	1,2	1,4
1550	1600	4,2	11,0	2,1	3,5
1500	1550	6,0	17,1	4,4	7,9
1450	1500	5,0	22,1	4,7	12,6
1400	1450	5,3	27,3	6,1	18,7
1350	1400	6,4	33,8	9,4	28,1
1300	1350	12,6	46,4	23,3	51,4
1250	1300	6,7	53,1	13,7	65,1
1200	1250	5,6	58,7	13,1	78,2
1150	1200	5,1	63,7	13,9	92,1
1100	1150	4,5	68,2	14,0	106,1
1050	1100	5,0	73,3	16,6	122,7
1000	1050	6,0	79,3	20,8	143,5
950	1000	7,0	86,2	27,7	171,2
900	950	8,4	94,6	36,0	207,2
850	900	6,7	101,4	31,0	238,3
800	850	8,4	109,8	41,4	279,6
750	800	8,8	118,6	46,8	326,4
700	750	6,1	124,7	34,0	360,4
650	700	7,4	132,1	43,1	403,5
600	650	8,3	140,4	50,5	454,0
550	600	8,8	149,3	56,1	510,0
500	550	9,5	158,7	61,6	571,6
450	500	9,6	168,3	64,4	636,0
400	450	11,1	179,4	76,5	712,5
350	400	8,5	187,9	60,2	772,7
300	350	7,7	195,6	55,5	828,2
250	300	7,4	203,0	56,4	884,6
200	250	6,8	209,8	54,9	939,5
150	200	4,6	214,4	40,2	979,7
100	150	4,3	218,7	39,5	1019,2
50	100	3,7	222,4	34,8	1053,9
0	50	1,8	224,2	17,6	1071,5

Skeiðarársandur water drainage basin (Gígja)

Elevation (m a. s. l.)		ΔS km^2	∑ΔS km^2	ΔQ_s $(10^6 m^3)$	$\sum \Delta Q_s$ $(10^6 m^3)$
1700	1750	1,2	1,2	0,7	0,7
1650	1700	20,5	21,7	12	12,7
1600	1650	76,2	97,9	45,2	57,9
1550	1600	84,6	182,5	67,1	124,9
1500	1550	104	286,7	106,5	231,4
1450	1500	97,6	384,3	118,1	349,5
1400	1450	95,1	479,3	131,9	481,4
1350	1400	83,3	562,6	132,6	614
1300	1350	71,9	634,5	126,8	740,8
1250	1300	62,8	697,3	125	865,9
1200	1250	52,9	750,1	122	987,9
1150	1200	44,9	795,1	118,5	1106,4
1100	1150	36,1	831,2	104,8	1211,3
1050	1100	29,5	860,7	93,8	1305
1000	1050	25	885,7	85,3	1390,4
950	1000	25	910,7	91	1481,3
900	950	24,8	935,5	96,3	1577,6
850	900	27,8	963,3	114,3	1692
800	850	22,5	985,7	97,6	1789,6
750	800	19,6	1005,3	89,6	1879,2
700	750	19,1	1024,4	92,4	1971,6
650	700	11,9	1036,3	60,8	2032,3
600	650	13,1	1049,4	70,6	2102,9
550	600	12,4	1061,8	69,6	2172,5
500	550	8,3	1070,1	48,4	2220,9
450	500	5,5	1075,6	34	2254,9
400	450	6,7	1082,3	43,5	2298,4
350	400	11,1	1093,4	73,7	2372,1
300	350	14,2	1107,6	97,9	2470
250	300	15,3	1122,9	110,6	2580,6
200	250	12,4	1135,3	96,5	2677,1
150	200	11,3	1146,6	94,4	2771,5
100	150	13,5	1160,1	120,6	2892,1
50	100	5	1165,1	46,5	2938,6

Súla water drainage basin

Elevation (m a. s. l.)		ΔS km^2	∑ΔS km^2	$ΔQ_s$ ($10^6 m^3$)	$∑ΔQ_s$ ($10^6 m^3$)
1700	1750	0,5	0,5	0,4	0,4
1650	1700	1,4	2,0	1,1	1,5
1600	1650	2,6	4,5	2,3	3,8
1550	1600	4,1	8,6	4,1	7,9
1500	1550	5,9	14,6	6,6	14,6
1450	1500	11,4	26,0	14,1	28,7
1400	1450	11,1	37,1	15,6	44,3
1350	1400	9,3	46,4	15,5	59,8
1300	1350	8,2	54,6	15,4	75,2
1250	1300	6,7	61,3	13,9	89,1
1200	1250	8,1	69,3	18,5	107,7
1150	1200	9,2	78,5	23,1	130,7
1100	1150	15,6	94,1	43,7	174,4
1050	1100	15,9	110,0	49,9	224,3
1000	1050	16,5	126,5	56,8	281,1
950	1000	18,7	145,2	69,2	350,3
900	950	15,3	160,5	60,1	410,5
850	900	12,1	172,7	50,1	460,6
800	850	11,7	184,4	50,9	511,5
750	800	7,0	191,3	32,3	543,8
700	750	6,0	197,4	29,3	573,1
650	700	4,9	202,3	25,0	598,2
600	650	9,0	211,3	48,3	646,5
550	600	11,7	223,0	65,4	711,9
500	550	8,9	231,9	51,9	763,8
450	500	7,2	239,1	43,9	807,6
400	450	6,3	245,4	40,4	848,1
350	400	4,8	250,2	31,8	879,8
300	350	1,8	252,0	12,4	892,3
250	300	0,9	252,9	6,9	899,2
200	250	0,8	253,7	6,1	905,3
150	200	0,8	254,5	6,7	912,0
100	150	0,8	255,3	7,5	919,5
50	100	0,6	256,0	6,1	925,5

Djúpá water drainage basin

Elevation (m a. s. l.)		ΔS km^2	∑ΔS km^2	ΔQ_s ($10^6 m^3$)	$\sum\Delta Q_s$ ($10^6 m^3$)
1450	1500	0,1	0,1	0,2	0,2
1400	1450	0,3	0,5	0,6	0,8
1350	1400	0,9	1,4	1,8	2,6
1300	1350	3,8	5,1	8,6	11,2
1250	1300	3,3	8,5	7,9	19,1
1200	1250	2,9	11,4	7,6	26,7
1150	1200	3,5	14,9	9,9	36,6
1100	1150	5,3	20,3	16,0	52,5
1050	1100	7,0	27,3	23,4	76,0
1000	1050	9,8	37,1	36,0	112,0
950	1000	8,0	45,1	31,9	143,9
900	950	8,1	53,2	33,3	177,2
850	900	7,5	60,7	32,3	209,5
800	850	9,1	69,8	40,5	250,0
750	800	6,7	76,5	31,2	281,2
700	750	4,0	80,6	19,8	301,0
650	700	3,0	83,5	15,2	316,2
600	650	0,4	84,0	2,2	318,5

Brunná water drainage basin

Elevation (m a. s. l.)		ΔS km^2	∑ΔS km^2	ΔQ_s ($10^6 m^3$)	$\sum\Delta Q_s$ ($10^6 m^3$)
1050	1100	0,0	0,0	0,3	0,3
1000	1050	1,1	1,2	4,3	4,5
950	1000	3,3	4,5	13,2	17,7
900	950	4,2	8,6	17,1	34,9
850	900	4,3	13,0	18,4	53,3
800	850	4,9	17,8	21,3	74,6
750	800	5,4	23,3	24,7	99,3
700	750	6,4	29,6	30,7	130,1
650	700	3,9	33,5	19,8	149,8
600	650	2,3	35,9	12,4	162,2
550	600	0,0	35,9	0,2	162,4

Hverfisfljót water drainage basin

Elevation (m a. s. l.)		ΔS km^2	∑ΔS km^2	ΔQ_s $(10^6 m^3)$	$\sum\Delta Q_s$ $(10^6 m^3)$
1700	1750	0,8	0,8	0,6	0,6
1650	1700	5,1	5,9	3,7	4,3
1600	1650	9,1	15,0	6,7	11,1
1550	1600	9,0	24,0	7,1	18,1
1500	1550	19,7	43,7	16,6	34,7
1450	1500	42,0	85,8	44,6	79,3
1400	1450	28,5	114,3	36,5	115,8
1350	1400	24,5	138,8	42,1	157,9
1300	1350	22,9	161,6	48,6	206,5
1250	1300	18,6	180,2	44,4	250,9
1200	1250	20,2	200,4	52,5	303,4
1150	1200	14,1	214,5	40,1	343,5
1100	1150	10,9	225,4	33,9	377,4
1050	1100	10,2	235,6	34,8	412,2
1000	1050	9,3	244,8	34,5	446,8
950	1000	9,4	254,2	37,6	484,3
900	950	8,9	263,2	37,2	521,5
850	900	7,4	270,5	32,2	553,7
800	850	9,3	279,8	41,9	595,6
750	800	11,5	291,3	54,1	649,8
700	750	13,7	305,0	68,6	718,3
650	700	7,8	312,8	42,0	760,3
600	650	4,6	317,3	25,6	785,9
550	600	0,2	317,5	1,0	786,9

Skaftá water drainage basin

Elevation (m a. s. l.)		ΔS km^2	∑ΔS km^2	ΔQ_s $(10^6 m^3)$	$\sum\Delta Q_s$ $(10^6 m^3)$
1650	1700	2,9	2,9	1,7	1,7
1600	1650	16,1	19,0	10,4	12,1
1550	1600	23,8	42,8	17,5	29,6
1500	1550	29,5	72,2	24,0	53,5
1450	1500	24,1	96,3	22,1	75,6
1400	1450	22,4	118,7	27,3	102,9
1350	1400	20,7	139,4	34,3	137,2
1300	1350	22,9	162,3	48,0	185,2
1250	1300	16,4	178,7	40,5	225,6
1200	1250	21,5	200,2	58,7	284,4
1150	1200	23,9	224,2	70,5	354,8
1100	1150	24,5	248,7	76,1	431,0
1050	1100	26,8	275,5	91,3	522,3
1000	1050	26,3	301,8	102,6	624,9
950	1000	20,3	322,1	89,2	714,1
900	950	15,8	337,9	75,2	789,3
850	900	16,2	354,1	82,9	872,2
800	850	14,7	368,8	81,2	953,4
750	800	11,6	380,4	68,2	1021,6
700	750	8,5	388,9	52,5	1074,1
650	700	5,1	394,0	32,0	1106,1
600	650	0,9	394,9	5,9	1112,0

Appendix F: MODIS satellite images of Vatnajökull and vicinity 2013-2014.

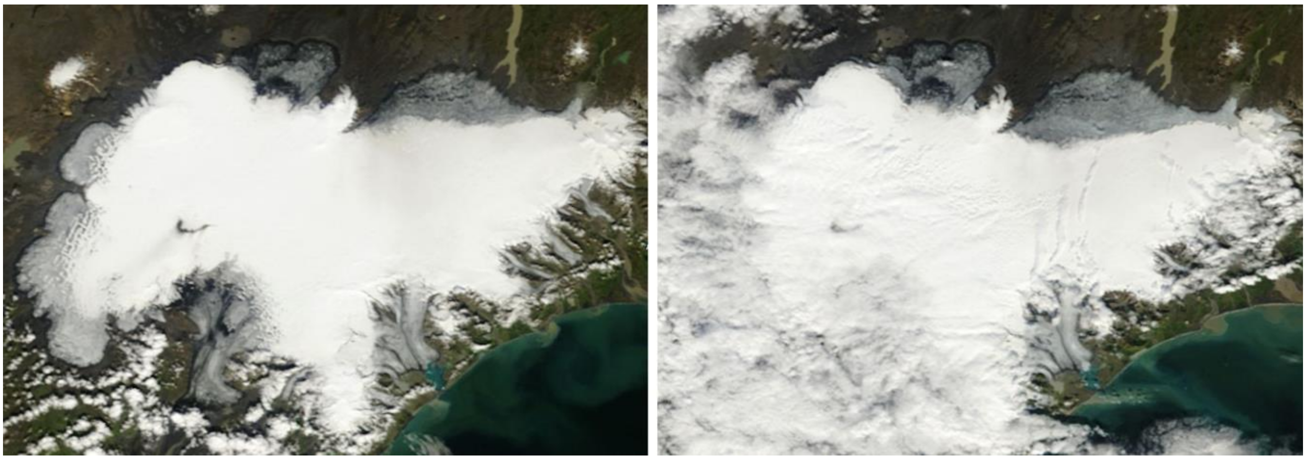

Left: August 12th, the snow line has only migrated slightly over two weeks, fresh snow in the western accumulation zone. Right: August 26th, the snowline of the NE-outlets has risen significantly; a warm and sunny period in NE-Iceland.

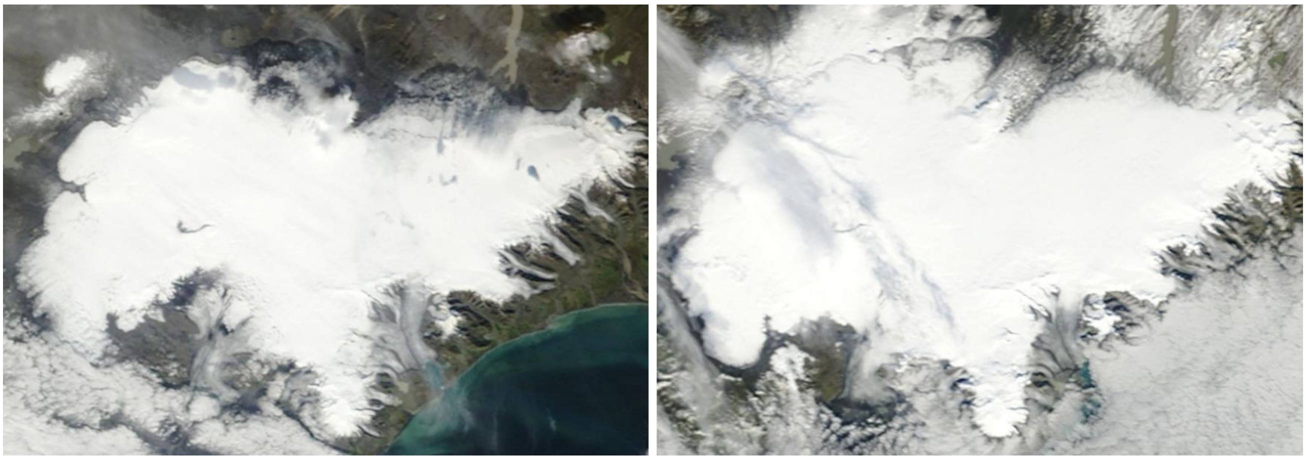

Left: September 7th, fresh snow in most accumulation zones, and even the ablation zones of the western part, frequent low pressure systems pass Iceland; onset of winter. Right: September 24th, clear winter conditions, snow accumulation has started.

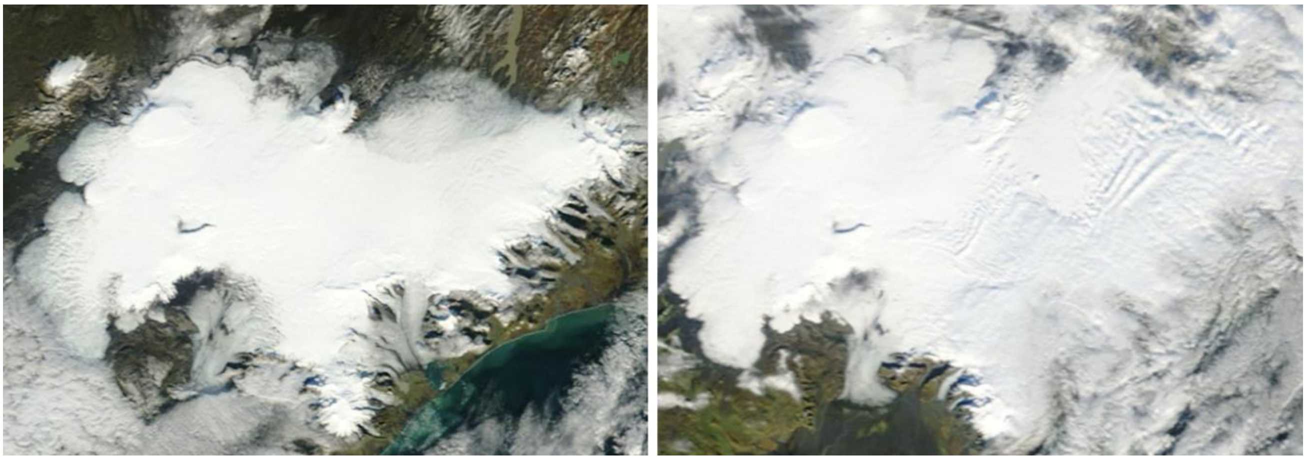

Left: October 14th, the first cloud-free image since September 24th. Some of the fresh snow has melted in the ablation zone; however snow cover up to 1.2 m was measured in the autumn mass balance expedition (October 1-8th) in the upper region. Right October 19th. Winter has settled in.

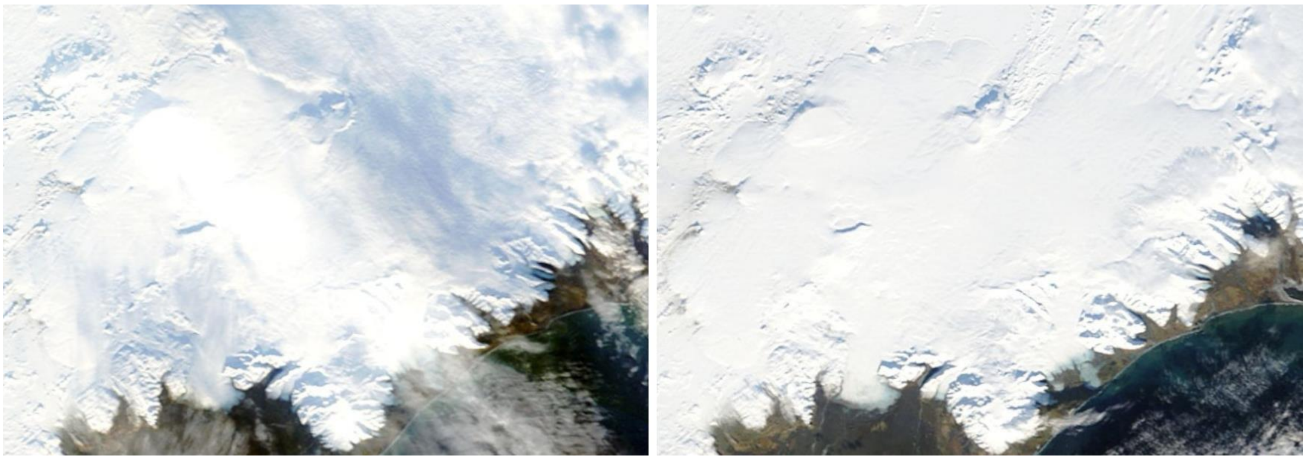

Left: January 29th 2014. Right: February 18th. There is still no snow in the south lowland, and the snow cover west of Vatnajökull is thin and discontinuous.

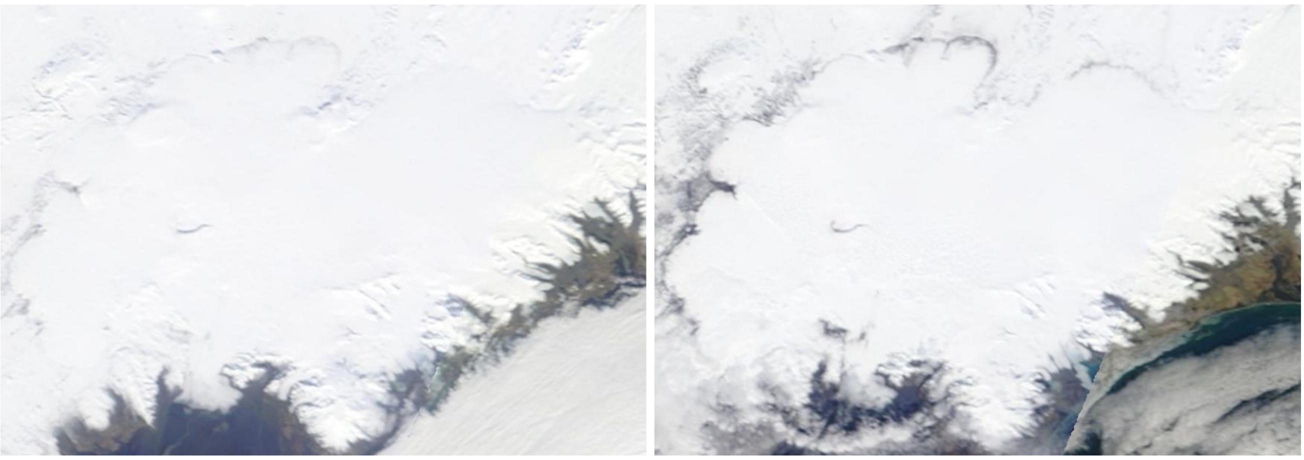

Left: March 31st, the snow cover west of Vatnajökull is still thin, and the lowland is snow free. Right: May 1st, onset of summer conditions, melt season has started, the dark regions on Dyngjujökull snout shows that the thin winter snow has already melted.

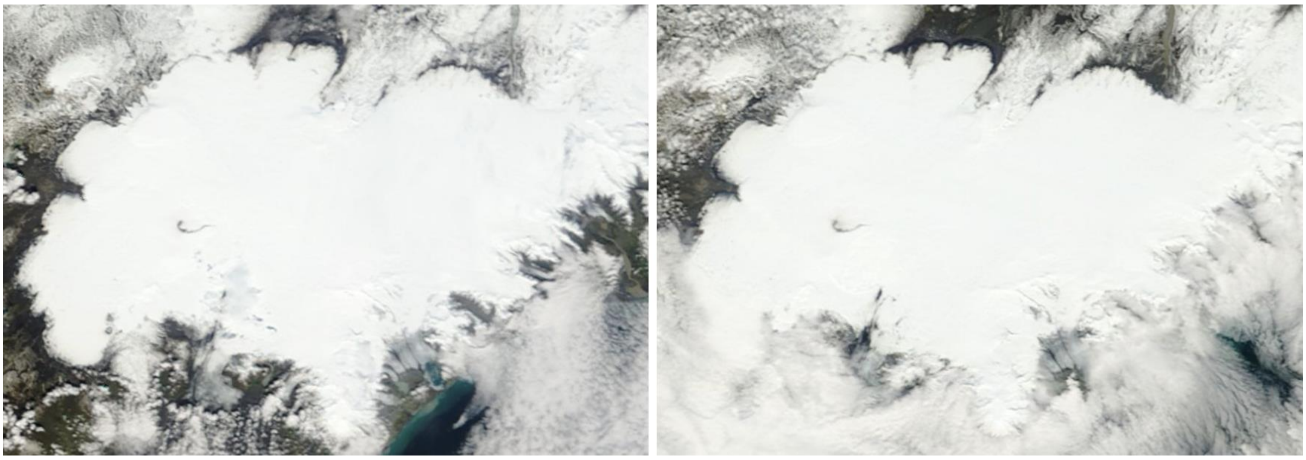

June 6th and June 12th. Visible changes from early May show that snow has melted in the glacier fore-field but little change is visible on the glacier.

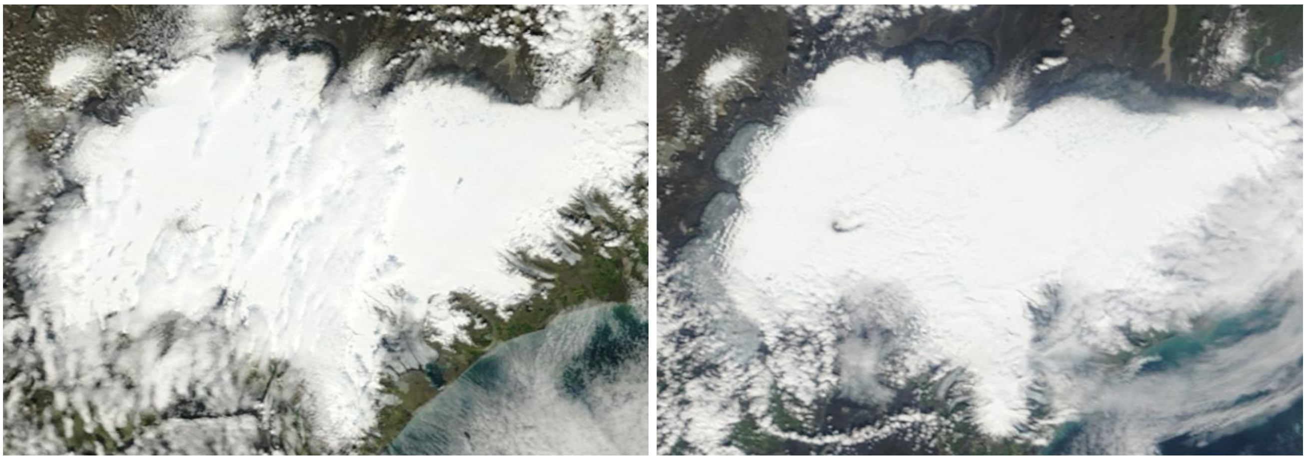

There are no completely cloud-free images in June and July: Left: June 28th, the snowline has only migrated slightly upwards; ablation rates in June are low. Some dirt is nowvisible on the snow surface from Köldukvíslarjökull to Brúarjökull that will lower albedo and enhance melt. Right: July 22nd, the snowline has "jumped" upwards, this is the warmest and sunniest period of summer, high melt rates on all outlets.

August 12th, and 22nd; The snowline of the N and SE outlets has raised significantly; at last a warm and sunny period in E-Iceland. Note how tephra has blown from Grímsvötn and precipitated in the snow to S and SW.

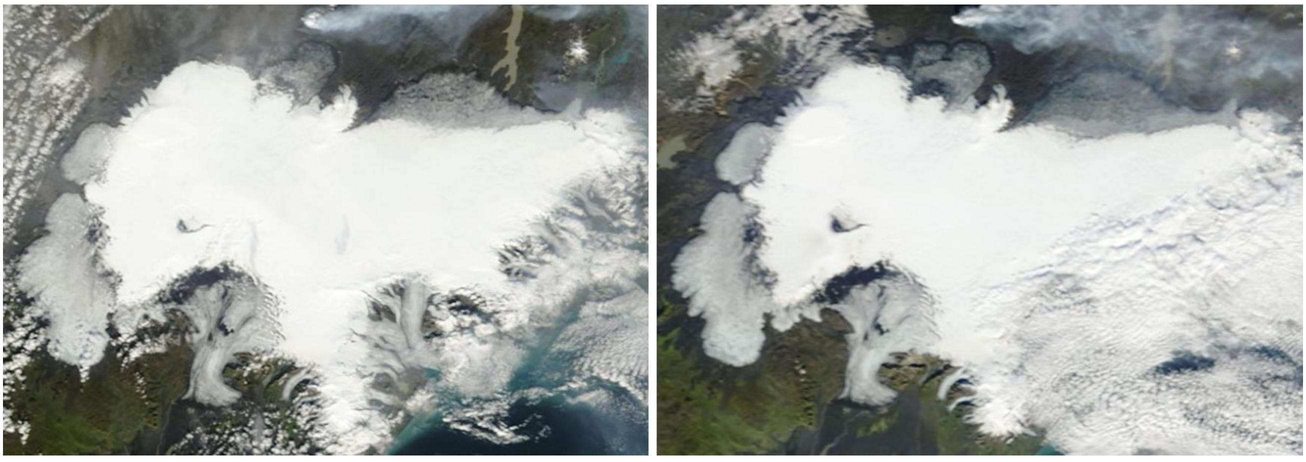

The Holuhraun eruption north of Dyngjujökull is clearly visible.
Left: September 5th, the snowline has moved significantly upwards on the N outlets, less so on the W and S outlets; there may be some fresh snow in the highest regions.
Right: September 20th, still summer conditions on the glacier, the snowline of the N outlets is still migrating upwards in a warm September.

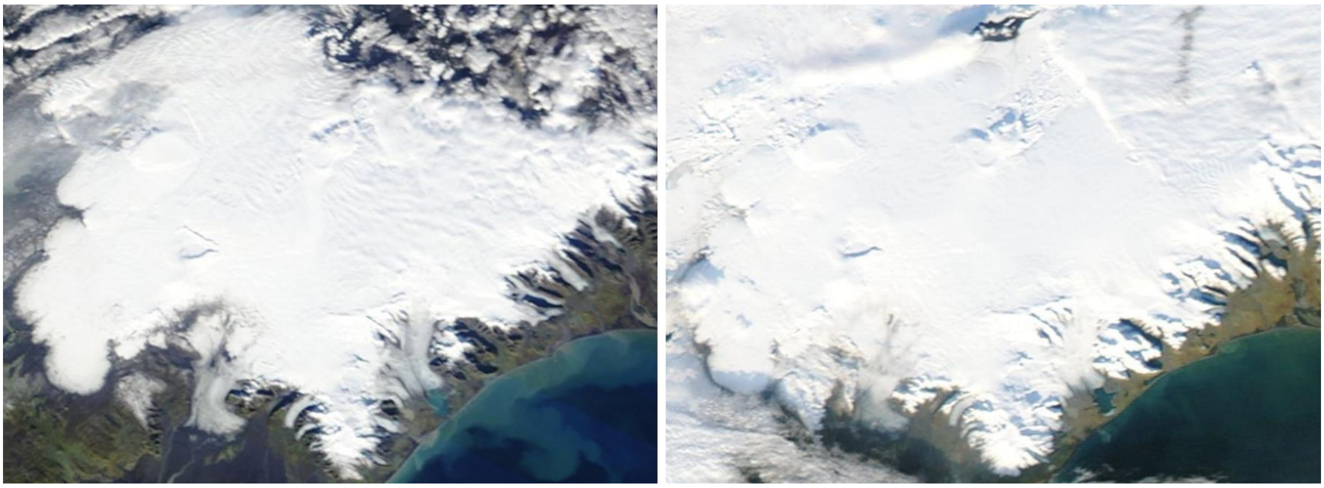

Left: October 10th, winter has arrived; there is now fresh snow on the surface at elevations above ~700m a.s.l..
Right: October 29th; snow cover up to 1.6 m was measured in the autumn mass balance expedition (October 9-17th) in the upper regions, winter has settled in.
The ~ 65 km² fresh lave field in Holuhraun-Flæður is clearly visible. The ice free surface of Hálslón is also visible through thin cloud cover.

The images are either from the MODIS Aqua or MODIS Terra satellites, visible light, 250 m resolution.
http://rapidfire.sci.gsfc.nasa.gov/
The Moderate Resolution Imaging Spectroradiometer (MODIS) flies onboard NASA's Aqua and Terra satellites as part of the NASA-centered international Earth Observing System. Both satellites orbit the Earth from pole to pole, seeing most of the globe every day. Onboard Terra, MODIS sees the Earth during the morning, while Aqua MODIS orbits the Earth in the afternoon.

On the next pages MODIS images for all days of May, June, July, August and September 2014 are shown in 1km resolution.

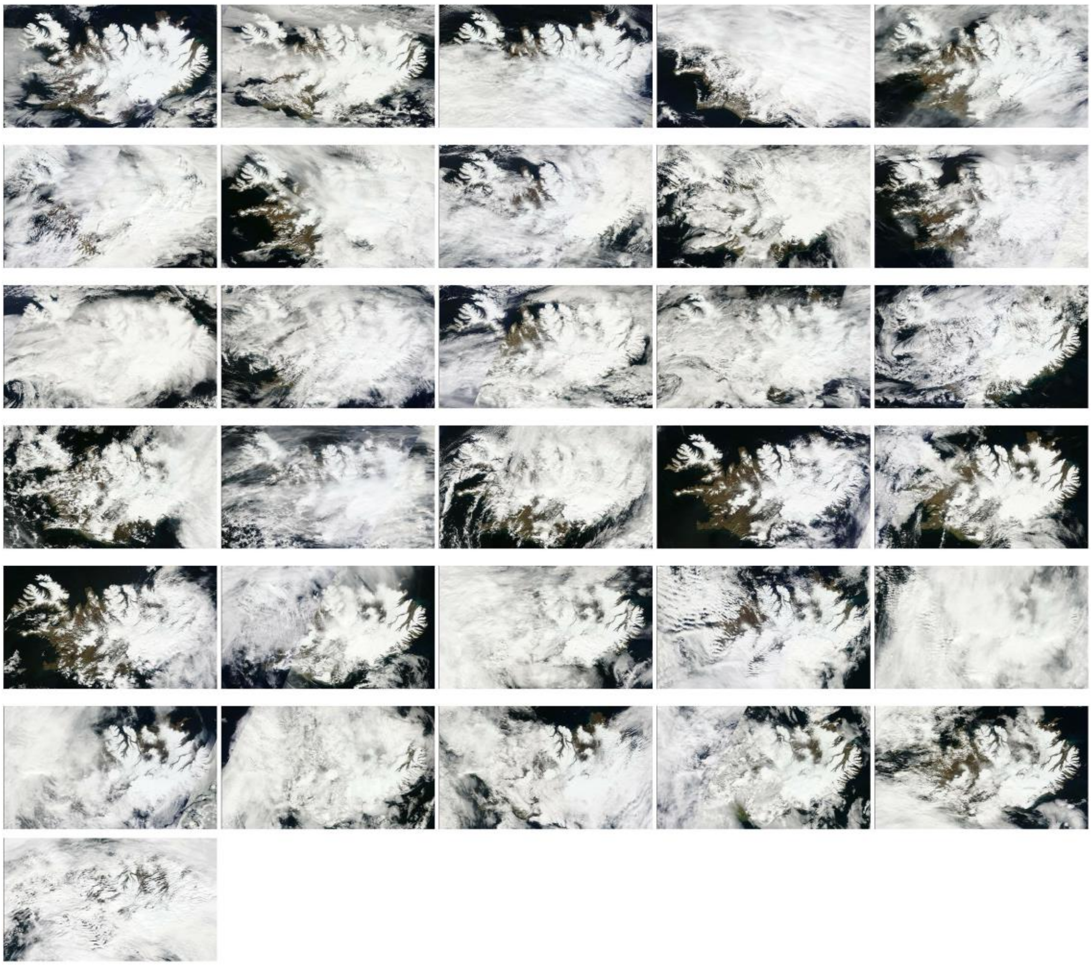

MODIS: May 2014 (read from left to right and downwards).

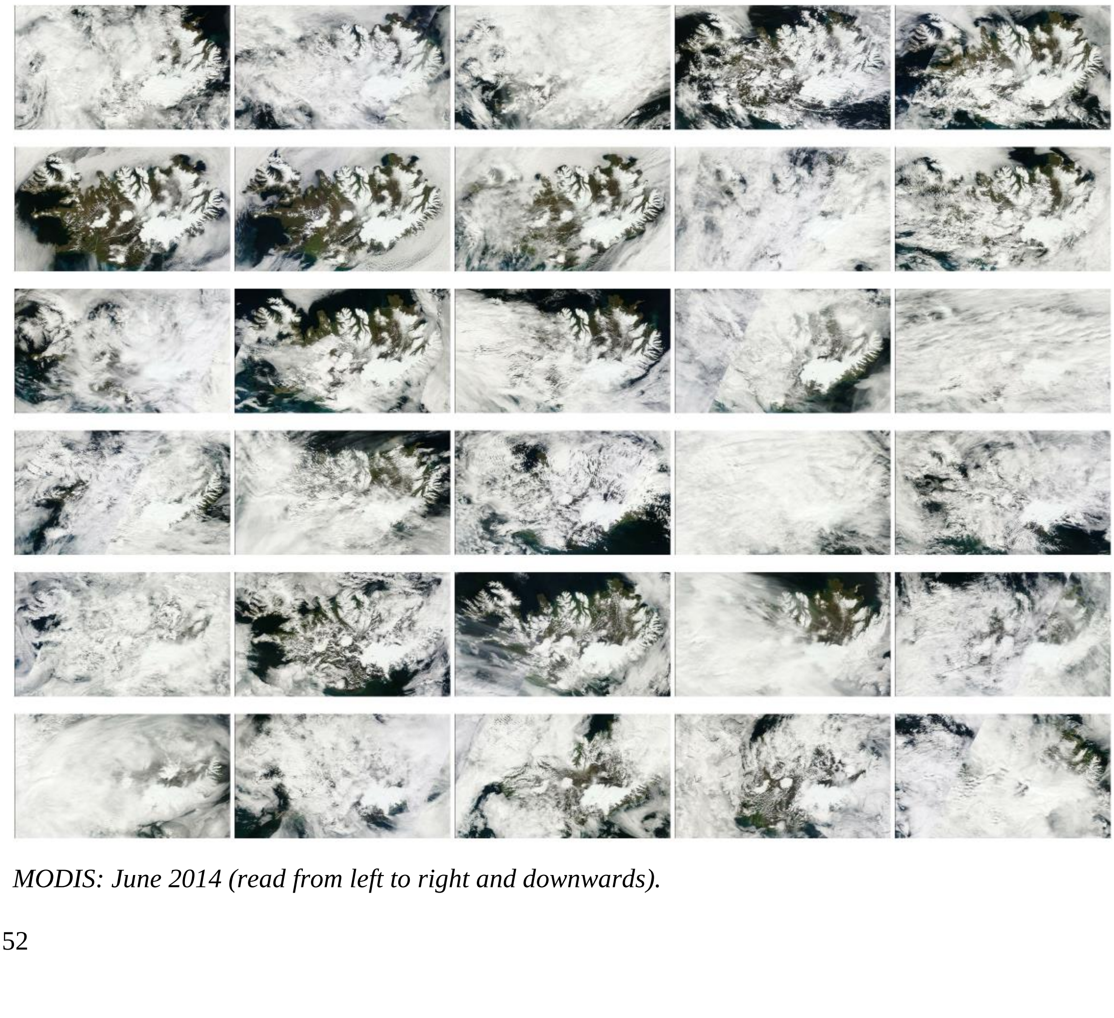

MODIS: June 2014 (read from left to right and downwards).

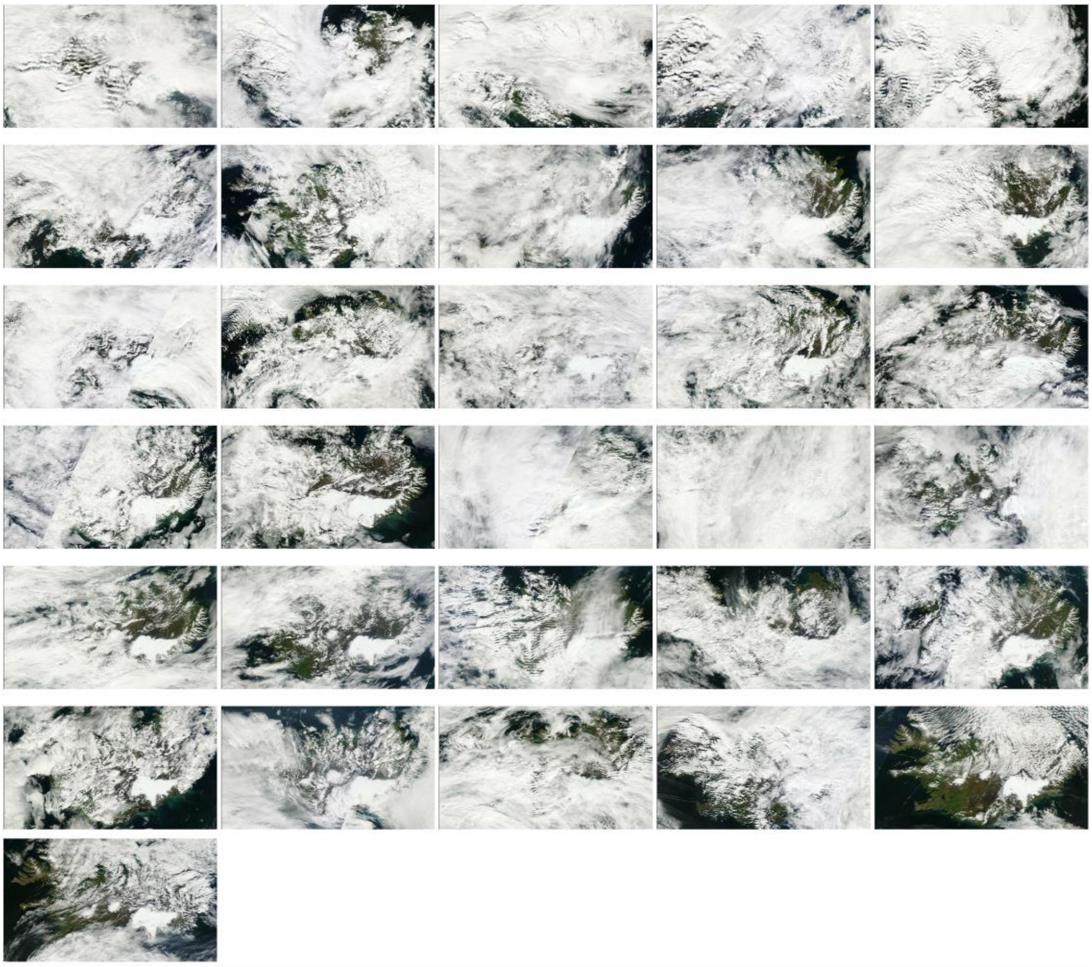

MODIS: July 2014 (read from left to right and downwards).

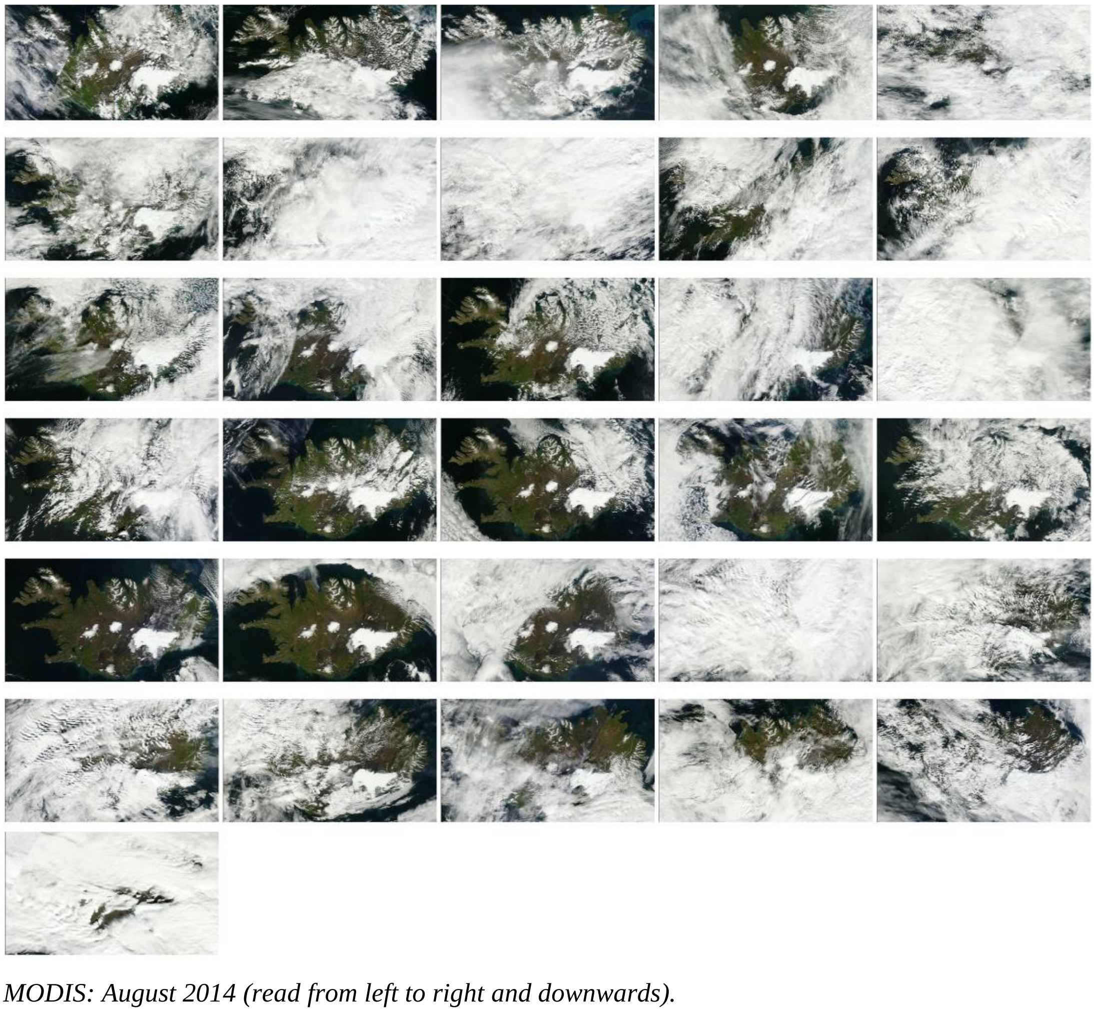

MODIS: August 2014 (read from left to right and downwards).

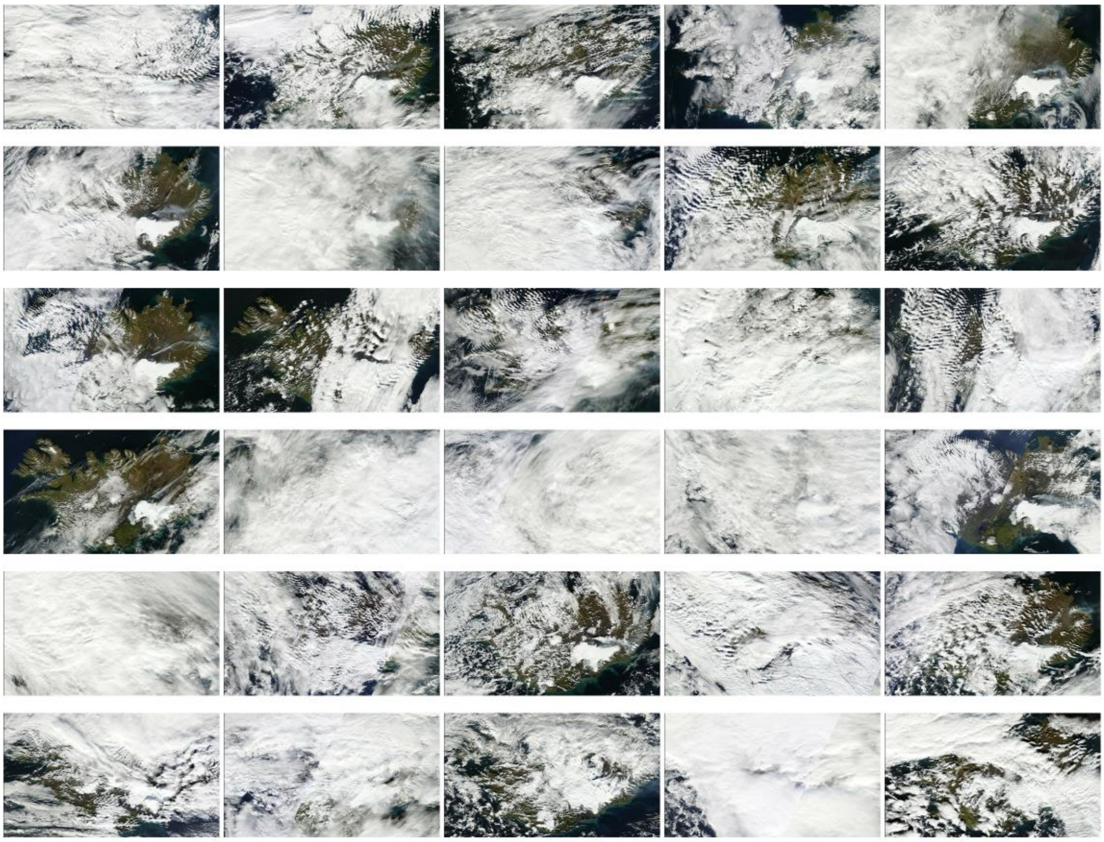

MODIS: September 2014 (read from left to right and downwards).

Landsvirkjun

Háaleitisbraut 68
103 Reykjavik
landsvirkjun.is

landsvirkjun@lv.is
Sími: 515 90 00